FOOTPRINT ESTIMATION FOR FLUX MEASUREMENTS OVER TALL FOREST CANOPIES

by

DEEPTHI ACHUTHAVARIER

(Under the Direction of Monique Y. Leclerc)

ABSTRACT

Analytical footprint models are originally developed for analyzing flux measurements over smooth terrain and their application over tall forest canopies might result in erroneous estimations. A commonly used analytical footprint model is modified to incorporate enhanced turbulence in the roughness sub layer (RSL). The wind speed in the crown space of the canopy is modeled by the exponential wind equation and the integrated stability function evaluated at z_0 is incorporated in the logarithmic wind profile. The influence of the RSL is reflected as an increase in flux maximum for all stability conditions. The modified model is applied to estimate footprint climatologies at the Howland *Ameriflux* site using the wind and CO_2 flux data for a 5-year period. The footprint envelope of the 29 m high eddy-covariance flux tower constitutes 40% of the total 1 km^2 study area in stable conditions and 20% in unstable conditions.

INDEX WORDS: footprint, roughness sub layer, forest canopy, eddy-covariance, CO_2 fluxes

FOOTPRINT ESTIMATION FOR FLUX MEASUREMENTS OVER TALL FOREST CANOPIES

by

DEEPTHI ACHUTHAVARIER

B.S., University of Calicut, India, 1997

M.S., Mahatma Gandhi University, India, 2000

A Thesis Submitted to the Graduate Faculty of The University of Georgia in Partial Fulfillment of the Requirements for the Degree

MASTER OF SCIENCE

ATHENS, GEORGIA

2003

FOOTPRINT ESTIMATION FOR FLUX MEASUREMENTS OVER TALL FOREST CANOPIES

by

DEEPTHI ACHUTHAVARIER

Major Professor: Monique Y. Leclerc

Committee: Anandakumar Karipot
David E. Stooksbury

Electronic Version Approved:

Maureen Grasso
Dean of the Graduate School
The University of Georgia
December 2003

ACKNOWLEDGEMENTS

I would like to express my sincere gratitude to my major professor, Monique Leclerc for her valuable guidance, advice, and kind support throughout the program. This project could not have been materialized without her enthusiasm, inspiration and encouragement. I am extremely grateful to her for having provided me an opportunity to come to the US and work in the Micrometeorology research group at the University of Georgia. A special debt of gratitude is owed to Anandakumar Karipot, who served in my graduate committee, and Thara Prabhakaran, for their immense help, kind encouragement and valuable advice during the last two and a half years. Their experience, knowledge and insight in the subject greatly assisted me in finishing this project. Sincere gratitude is expressed to David Stooksbury who also served in my committee, for teaching me a special course on Micrometeorology and providing valuable advice in the completion of the course work as well as in my thesis. I would also like to thank Gerrit Hoogenboom, for providing valuable guidance and advice in the completion of a course work.

TABLE OF CONTENTS

Page

ACKNOWLEDGEMENTS iv

LIST OF TABLES vi

LIST OF FIGURES vii

CHAPTER

1 INTRODUCTION 1

2 LITERATURE REVIEW 6

3 IMPACT OF ROUGHNESS SUB LAYER ON FLUX FOOTPRINT PREDICTIONS OVER TALL FOREST CANOPIES 39

4 FOOTPRINT CLIMATOLOGY FOR CO_2 FLUXES OVER HOWLAND AMERIFLUX SITE 88

5 CONCLUSION 114

LIST OF TABLES

Page

Table 2.1: Summary of major works in footprint analysis 34

Table 3.1: Tree density and basal area at the Howland site.....68

Table 3.2: Summary of major results.....68

Table 4.1: Percentage occurrence of very unstable and very stable cases in the half hourly mean data observed at Howland forest during the period 1996–2001.....105

LIST OF FIGURES

Page

Figure 2.1: Illustration of flux footprint....36

Figure 2.2: Major steps in the analytical footprint model....37

Figure 2.3: Diagram showing roughness sub layer and flux measurements above forest canopies....38

Figure 3.1: Vertical profile of scalar diffusivity enhancement in unstable conditions....69

Figure 3.2: Vertical profile of scalar diffusivity enhancement in neutral conditions....69

Figure 3.3: Vertical profile of scalar diffusivity enhancement in stable conditions....70

Figure 3.4: Comparison of scalar eddy diffusivity enhancement factors reported in the literature....70

Figure 3.5: Satellite image of the Howland *Ameriflux* site....71

Figure 3.6: Eddy-covariance flux measurement system at Howland, Maine....72

Figure 3.7: Variation of the universal footprint function (Φ) with normalized plume height....73

Figure 3.8: Influence of $\psi(z_0/L)$ on flux footprint over smooth terrain in stable and unstable conditions....73

Figure 3.9: Influence of $\psi(z_0/L)$ on flux footprint over rough terrain (unstable case)....74

Figure 3.10: Influence of $\psi(z_0/L)$ on flux footprint over rough terrain (stable case)....74

Figure 3.11: Mini-SODAR installed at treetop....75

Figure 3.12: Tethered balloon being filled with Helium....75

Figure 3.13: Comparison between the wind profiles obtained from the SODAR, tethersonde and the logarithmic profile 76
Figure 3.14: Comparison between the predicted footprints using wind profiles from the SODAR, tethersonde and logarithmic profile.....76
Figure 3.15: Vertical profiles of mean horizontal wind speed for different stability cases with logarithmic (dotted lines) and exponential relations (solid lines).....77
Figure 3.16: Comparison of flux footprint and cumulative flux with respect to upwind distance between original Horst and Weil (1994) model and modified analytical solution using an exponential wind profile in the crown space 78
Figure 3.17: Variation of mean plume height with downwind distance for unstable (a), near-neutral (b) and stable (c) conditions 79
Figure 3.18: Variation of flux footprint with upwind distance with and without RSL parameterizations.....80
Figure 3.19: Variation of cumulative footprint with upwind distance with and without RSL parameterizations.....81
Figure 3.20: Variation of flux maximum with stability with and without RSL parameterization.....82
Figure 3.21: Variation of flux maximum with measurement height with and without RSL parameterization.....82
Figure 3.22: Comparison of fetch calculated with and without RSL parameterizations.....83
Figure 3.23: Sensitivity of the modified analytical model for the exponential wind coefficient 83

Figure 3.24: Sensitivity of the original analytical solution for the shape factor in near-neutral stability 84
Figure 3.25: Sensitivity of the original analytical solution for the shape factor in unstable case 84
Figure 3.26: Sensitivity of the original analytical solution for the shape factor in stable case 85
Figure 3.27: Sensitivity of the original analytical solution for the empirical constant c in near-neutral condition 85
Figure 3.28: Sensitivity of the original analytical solution for the empirical constant c in unstable condition 86
Figure 3.29: Sensitivity of the original analytical solution for the empirical constant c in stable condition 86
Figure 3.30: Vertical profile of σ_w at the Howland forest from the mini-SODAR in slightly unstable condition 87
Figure 3.31: Comparison of footprint predictions from the modified analytical solution and a Lagrangian formulation using a realistic σ_w profile.....87
Figure 4.1: Satellite image of the Howland *Ameriflux* site 106
Figure 4.2: Frequency distribution of wind speed and direction at Howland forest in the year 2001.....107
Figure 4.3: Frequency distribution of wind direction and CO_2 concentration at Howland forest in the year 2001.....108
Figure 4.4: Frequency distribution of wind speed and direction at Howland forest for one day, one week, one month and one season in the year 2001.....109

Figure 4.5: Footprint climatology at Howland forest for one day, one week, one month and one season in the year 2001 110
Figure 4.6: Frequency distribution of wind speed and direction at Howland forest for stable, neutral and unstable conditions (above) and corresponding footprint climatology distributions (below) 111
Figure 4.7: Frequency distribution of wind speed and direction at Howland forest for the period 1996–2001 112
Figure 4.8: Footprint climatology at the Howland forest for the period 1996–2001.....113
Figure A1.1: Flux footprint distributions with upwind distance with and without RSL effects.....65
Figure A1.2: Variation of flux maximum with stability with and without RSL turbulent parameterization.....66
Figure A1.3: Variation of flux maximum with measurement height with and without RSL turbulent parameterization 66
Figure A1.4: Variation of the upwind distance corresponding to the flux maximum with measurement height with and without RSL turbulent parameterization 67
Figure A1.5: Percent change in flux maximum and corresponding upwind distance with respect to change in the empirical constant η 67

CHAPTER 1

INTRODUCTION

Continuous monitoring of atmospheric constituents has shown changes in the concentrations of gases such as CO_2, CH_4 and N_2O, the major greenhouse gases. Industrial and traffic emissions, fossil fuel combustion, increased use of nitrogen-based fertilizers, landfill releases and changing land use practices are possible causes for the rising amount of greenhouse gases in the atmosphere. Once these greenhouse gases are released, they remain in the atmosphere for decades or more causing increased terrestrial radiation absorption. Thus, in a way, heat energy is trapped in the atmosphere causing the air temperature to rise and creating changes in the Earth's energy budget. Some of the possible changes of high levels of atmospheric greenhouse gases are increased global temperature, rise in the sea level and perturbations of precipitation and soil moisture patterns. According to the Intergovernmental Panel on Climate Change (IPCC), since the industrial revolution, carbon dioxide levels in the atmosphere have increased 31% and methane levels have increased 151% (Weier, 2002). On going measurements at Mauna Loa in Hawaii, show that the annual average CO_2 concentration has increased from 315 *ppm* to approximately 370 *ppm* from 1960 to 2000 (Weier, 2002). Correspondingly the global annual temperature is increased by 0.4–0.6°C and worldwide measurements of sea level show a rise of 0.1 to 0.2m over the past century. Recent climate modeling studies report that the Earth's surface temperature is expected to rise between 0.5 and 1°C over the next 50 years (Weier, 2002).

This increasing threat on the environment has opened up investigations related to the global carbon cycle. It is known that chemical reactions in oceans and plant photosynthesis are the major processes by which carbon is removed from the atmosphere. About 40 to 60% of the anthropogenically emitted CO_2 remains in the atmosphere while the fate of the remainder is not known. It might be possible that the "missing" CO_2 is sequestered in oceans, vegetation and soil. In order to investigate the potential of vegetation as carbon sinks, continuous flux measurement systems are established over forest ecosystems. These systems measure the exchange of CO_2, water vapor, heat energy, momentum etc. between the vegetation and the atmosphere using eddy-covariance flux methodology. At present, about 200 tower sites are established in an international network (*Fluxnet*), most of them being in the Americas and Europe (known as *Ameriflux* and *Euroflux* respectively). A few sites are established in China, Korea, Australia, New Zealand and Thailand forming corresponding small regional networks.

The eddy-covariance technique relies on point measurements of momentum or scalar fluxes such as water vapor, temperature and trace gases. When turbulent flux sensors are deployed, the objective is to measure signals that reflect the influence of the underlying surface on the turbulent exchange (Schimd, 2002). This point measurement is assumed to be representative of the surrounding area only when the underlying terrain is uniform or of the same physical and thermal properties over several kilometers. Over such a terrain, turbulence is assumed to be homogenous; in other words, at any point, fluxes from all parts of the surface can be considered equal. In this simple case, the eddy flux tower can be placed at any point above the surface.

However in real situations the terrain is rarely homogeneous and so the assumption of uniform turbulence is not valid. Over inhomogeneous surfaces, in order to decide the exact

location of the flux tower, it is important to study the behavior of the turbulence and the influence of each point on the surface. The footprint of a turbulent flux measurement defines the spatial context of the measurement or estimates the area sensed by a flux tower at any point above the surface (Leclerc and Thurtell, 1990; Schuepp et al., 1990). Horst and Weil (1992) defines the footprint as the contribution per unit emission of each element of the upwind surface source area to the vertical scalar flux measured at a certain height. Although the flux footprint analysis is commonly discussed in the context of flux measurements over homogeneous vegetated surfaces, the method is also used to investigate to all boundary layer diffusion problems. For example, in odor pollution, footprint models can be used to determine the safe separation distance between the odor source and residential areas.

1.1. Objectives

The footprint methodologies are originally developed for flux measurements over smooth terrains such as flat grasslands. But most of the present day interests are centered around the exchange of fluxes between tall forest canopies and the atmosphere. For practical purposes it is common to use the original footprint models without much modifications for flow over canopies. It is known that flow properties above forest canopies (in the Roughness Sub Layer (RSL)) are different from those in the Inertial Sub Layer (ISL) and cannot be dealt with ISL turbulent parameterizations. The present study is an attempt to calculate the footprint fluxes for a tall forest canopy at the Howland *Ameriflux* site at Maine, USA. The footprint analysis is done based on the analytical approach proposed by Horst and Weil (1992, 1994). This study also estimates the time-averaged footprint fluxes or the footprint climatology for the same site. The objectives of the study are:

1) to incorporate the effects of roughness sub layer (RSL) into a widely used analytical approach to estimate the footprint
2) and to develop footprint climatology for the Howland Ameriflux site at Maine.

The second chapter is a detailed literature survey on analytical footprint approaches. The existence of RSL, its characteristics and recent studies in this area are also discussed briefly in the second chapter. The third chapter suggests a simple method to incorporate RSL effects in the analytical footprint solution and compares the results with and without the modifications. The fourth chapter is on footprint climatology analysis and uses the modified analytical solution discussed in the third chapter. A summary of the results is provided in the fifth chapter.

References

Horst, T.W., Weil, J.C., 1992. Footprint estimation for scalar flux measurements in the atmospheric surface layer. Bounday-Layer Meteorol. 59, 279–296.

Horst, T.W., Weil, J.C., 1994. How far is far enough?: The fetch requirements for micrometeorological measurements of surface fluxes. J. Atmos. Ocean. Tech. 11, 1018–1026.

Leclerc, M.Y., Thurtell, G.W., 1990. Footprint prediction of scalar fluxes using a Markovian analysis. Boundary-Layer Meteorol. 52, 247–258.

Schmid, H.P., 2002. Footprint modeling for vegetation atmosphere exchange studies: a review and perspective. Agric. For. Meteorol. 113, 159–183.

Schuepp, P.H., Leclerc, M.Y., Macpherson, J.I., Desjardins, R.L., 1990. Footprint predictions for scalar fluxes from analytical solutions of the diffusion equation. Boundary-Layer Meterol. 50, 355–373.

Weier, J., 2002. Global warming. http://earthobservatory.nasa. (accessed on 09-15-2003).

CHAPTER 2

LITERATURE REVIEW

2.1. Introduction

The problem of estimating fetch for micrometeorological measurements has been discussed since the late 1950s (Elliot, 1958; Peterson, 1969) though the issue was not formally addressed until 1972 (Pasquill 1972). Most of the present day thoughts on footprint analysis stems from Pasquill's method of estimating fetch for measurements over patchy surfaces. During the past decade, significant progress was seen in this subject mainly due to the increasing interest in global warming issues and flux estimations over the terrestrial ecosystems. A review on footprint models by Schmid (2002) points out the growing relevance of footprint studies by quoting the large number of articles published in this field. About 325 articles were published during the 1987–2000 period that either mentions footprint, source area, effective fetch or refers a published article on footprint. The footprint models were initially developed based on analytical diffusion approaches (Gash, 1986; Schuepp et al., 1990, Horst and Weil, 1992, Schmid, 1994). The Lagrangian (Leclerc and Thurtell, 1990; Horst and Weil, 1992; Flesch, 1996) as well as Large Eddy Simulation (LES) (Leclerc et al., 1997, Su and Leclerc, 1998) concepts are also applied in footprint models. The following is a brief overview on existing analytical footprint methodologies. The main advances in the analytical footprint models reported in the literature are listed in Table 2.1.

2.2. Evolution of the concept of footprint

The following sections briefly describe the evolution of the concept of footprint mentioning major works in the field.

2.2.1. Internal boundary layer approach

Prior to the development of the footprint concept into its present form, scientists tackled the question of representativeness by addressing the growth of the internal boundary layers (IBLs) over surface transitions. The IBLs are formed when the air mass flows over a surface of thermal or physical discontinuities. The growth of the IBL depends on the strength of horizontal advection, size of the discontinuity and differences in thermal and diffusive characteristics of both surfaces. When an air mass flows over a surface, the flow gradually comes into equilibrium with the thermal and physical properties of the surface beneath. In other words, there exists an energy balance between the air and the surface. Such an air mass, when it encounters with a surface of different thermal and physical characteristics, the adjustment of the flow to the new surface is not abrupt, but occurs gradually in space and time. Thus the layers close to the new surface get adjusted to the new properties and the height of this adjusted layer grows with downwind distance. This atmospheric layer, which is immediately above the new surface and in equilibrium with its characteristics, is called the IBL. One of the earlier researchers in this field, Elliot (1958) computed the height of the IBL for a step change in surface roughness in neutral conditions by using the logarithmic wind profile and Karman integral theorem (Lamb, 1932). Assuming conservation of momentum, the loss of momentum by advection from the IBL is equal to the net gain of momentum due to vertical flux into the region. This is also equal to the difference in shearing stress between the IBL and the layer above. The resulting theoretical expression was approximated by a power-law equation with an exponent 0.8, by which the height of the IBL increases with distance from the point of discontinuity. This distance to height ratio was further approximated to 1/100 and was used as a rule of thumb in micrometeorological measurements. However this assumption was proved to be inaccurate by Leclerc and Thurtell

(1990). Peterson (1969) obtained the energy balance in the IBL by using the equations of conservation of mass and horizontal momentum and turbulent kinetic energy. The vertical transfer of turbulent kinetic energy was expressed using the gradient transfer hypothesis. Garratt (1990) provides a comprehensive review on IBL studies.

2.2.2. Reverse plume approach

The internal boundary layer approach is confined to cases where a single crosswind inhomogenity exists. However, real terrain is characterized by crosswind as well as along wind transition zones and hence it is necessary to study the flow response to a wide spectrum of surface characteristics. Pasquill (1972) suggested an alternative procedure where he treated the surface as an array of elementary sources (or sinks in the case of momentum) from which a property is emitted (or absorbed). He suggested an analogy between the developing zone of influence downwind from a point of discontinuity and a diffusing plume of a scalar emitted at that surface element. He illustrated this analogy by plotting the height of the boundary layer from the derivations of Peterson (1969) and the mean height of the plume using Lagrangian similarity arguments (Batchelor, 1964), both against the downwind distance from the point of discontinuity. These two curves were found to be surprisingly similar and the curve for $3\bar{z}$ ($\bar{z}$ representing mean plume height) was seen to fit closely over Peterson's curve. By using the gradient transfer approach for vertical diffusion from a ground level source and adopting logarithmic wind profile, estimates of the mean plume height (which now is the height of the IBL) can be obtained. This criterion allowed Pasquill to calculate the IBL height to longer downwind distances where Peterson's calculations were limited to short distances. This new approach also permits to calculate the IBL height in a thermally stratified atmosphere. Using this analogy, Pasquill states that the momentum deficit produced at a height by a roughness element

situated on the surface will rise to a maximum at a certain distance and fall off continuously as the distance is further increased. This functional form is precisely that contained in the ground level distribution from an elevated source if the reciprocal relation between distributions from ground and elevated sources (Smith 1957) is adopted. The reciprocal theorem states that the concentration at x' due to a source at x'' with the flow in the positive x direction is equal to the concentration at x'' due to an identical source at x' when the direction of the flow is reversed. This suggests that in order to find the influence of a ground level source at a height say, z_m the ground level concentration distribution for a similar source at z_m, can be used. Pasquill (1972) tabulated the dimensions of this region relative to the receptor location for a set of heights, roughness lengths and stability conditions. The dimensions of the source area were found to be dependent on sensor height, surface roughness and atmospheric stability. This approach, which basically involves a geometric inversion of the plume, is called reverse plume method and is the basis for the majority of current footprint models. The concept of the footprint is illustrated on Fig. 2.1.

2.2.3. The fetch concept

Gash (1986) adopted Pasquill's concept of reverse plume model for micrometeorological evaporation measurements. He considered the upwind area, the area of transpiring vegetation as a continuum of line sources of water vapor each occupying an infinitesimal strip of δx. A sensor mounted at z_m, will sense concentration $\rho_v(x, z_m)$ of water vapor diffusing from a distance x upwind. This concentration can be calculated from basic diffusion equation.

$$u\frac{\partial \rho_v(x, z_m)}{\partial z_m} = K_{z_m}(\partial \rho_v(x, z_m)/\partial z_m) \qquad (2.1)$$

Here u is the time averaged horizontal wind velocity, K_{z_m} is the approximate eddy diffusivity at height z_m. Using the expression for diffusion from an infinite crosswind line source of passive particles proposed by Calder (1952), equation (2.1) can be modified to

$$\rho_v(x, z_m) = \frac{Q}{ku_* x}.\exp-(\frac{Uz_m}{ku_* x}). \tag{2.2}$$

Here k is the von Karman's constant, u_* is the friction velocity, U is the uniform wind speed and Q is the source strength of the line source per unit length. Here the assumptions of neutral stratification and uniform wind speed independent of height are used. After differentiating with respect to z_m and integrating over a certain upwind distance X_L, Gash obtained an equation describing the vertical gradient of water vapor concentration from a uniform strip of steamwise dimension X_L.

$$\frac{\partial \rho_v(z_m)}{\partial z_m} = -\frac{E}{ku_* z_m}\exp\left[-\frac{Uz_m}{ku_* x_L}\right] \tag{2.3}$$

In (eqn. 2.3), $E = Q/\delta x$. If the upwind distance is considered infinity, equation 2.3 simplifies without the exponential term. A percentage of that gradient, in the case of the infinite upwind distance, will be the result of molecules diffusing from within a distance X_F away from the point of measurement. This distance was termed as *F %* fetch by Gash. This distance X_F, which contributes *F%* of the measured concentration at z_m, is given by

$$x_F = -\frac{Uz_m}{ku_*}\frac{1}{\ln(F/100)} \tag{2.4}$$

The ratio U/u_* needed to solve the above equation is obtained from the following relation, where u can be substituted using the integrated logarithmic wind profile.

$$U = \int_{z_0}^{z_m} u dz \Big/ \int_{z_0}^{z_m} dz \qquad (2.5)$$

Hence X_F is expressed as a function of roughness length and measurement height.

$$x_F = -\frac{z_m(\ln(z_m / z_0) - 1 + z_0 / z_m}{k^2 \ln(F/100)} \qquad (2.6)$$

This same approach was used for a terrain with a step change in evaporation. The main disadvantage of this method is that it assumes both uniform wind speed and eddy diffusivity, whereas in reality, there is a height dependency for both parameters. However the method was shown to be adequate for practical purposes, with errors less than 20%.

Schuepp et al. (1990) found the simple solutions proposed by Gash (1986) are satisfactory approximations to numerical simulations over a wide range of heights, zero plane displacements and roughness lengths. They used an equivalent of equation 2.3. and their results compared favorably with aircraft measurements of CO_2 flux profiles and predictions by a Lagrangian simulation (Leclerc and Thurtell 1990).

2.2.4. Source area model

Pasquill's reverse plume approach is based on the reciprocal theorem proposed by Smith (1957). One of the main assumptions for the reciprocal theorem is that the distribution of velocity fluctuations in any direction is symmetrical and so dispersion is Gaussian in both the horizontal and vertical. Although Gaussian distribution is acceptable for horizontal dispersion, it is not realistic for vertical dispersion (Weil, 1985). Schmid and Oke (1990) presented a slightly different concept of reciprocity. The diffusion from a point source on the surface is measured at height z_m. The source location, which produces maximum concentration at the sensor, is termed the maximum source location. An arbitrary criterion say P is used to define the minimum

sensed concentration, χ_p for a source to belong to P source area. If a source is moved away from the maximum source location, the sensed concentration will eventually become χ_p. The geometric location of all point sources, whose effect level at the sensor equals χ_p, forms a closed curve, which is the boundary of the P source area. The source weight distribution function $\Omega(x, y)$ with $\omega = \Omega(x, y)$ is a geometric translation of the concentration or effect level distribution function at level z_m.

$$P = \iint_{\omega=\omega_p} \Omega(x, y)dxdy \Big/ \int_{-\infty}^{+\infty} \int_{0}^{+\infty} \Omega(x, y)dxdy. \qquad (2.7)$$

They showed that the source area $\Omega(x, y)$ could be obtained by reversing the wind direction and placing a virtual source at the ground below the sensor and projecting the virtual effect level distribution at z_m. This is a modified reverse plume approach and is not dependent on Smith's (1957) reciprocal theorem and is not limited by Gaussian distribution in the vertical. But this concept is not strictly valid in the case of non-passive scalars (where chemical reactions also play a role in deciding the concentrations) or of turbulence parameters, where the diffusivity field is affected by the horizontal variability of the property; or by the level of surface inhomogenity. To obtain $\Omega(x, y)$ Schmid and Oke (1990) used the plume diffusion model of Gryning et al. (1983), which considers non-Gaussian diffusion in the vertical. Schmid and Oke (1990) suggested that the flux footprint is proportional to the concentration distribution for a unit surface source. However Horst and Weil (1990) states that they found this assumption correct for the dependence of flux footprint on crosswind location it is not correct for the dependence of crosswind integrated flux footprint on measurement height.

2.3. Footprint models with stability effects and realistic wind profile

The analytical solution proposed by Horst and Weil (1992) is based on Pasquill's reverse plume approach where the vertical eddy flux measured at a height z_m can be considered as the integral of the contributions from all upwind surface emissions. A summary of the major steps in the model is given in the form of a flowchart in figure 2.2.

$$F(x, y, z_m) = \int_{-\infty}^{\infty} \int_{-\infty}^{x} F(x', y', 0) f(x - x', y - y', z_m) dx' dy' \tag{2.8}$$

For a special case when $F(x', y', 0) = Q\delta(x')\delta(y')$ where Q is the rate of emission form the source, we can write

$$f(x, y, z_m) = \frac{F(x, y, z_m)}{Q} \tag{2.9}$$

This suggests the flux footprint to be equal to the vertical flux downwind of a unit surface point source. Horst and Weil (1992) showed that the dependence of flux footprint on crosswind location is identical to the crosswind concentration distribution downwind of a unit surface point source. The crosswind-integrated footprint $\overline{f}^y$ is equal to the crosswind-integrated flux downwind of a unit surface point source and thus related to the crosswind integrated concentration distribution $\overline{C}^y$ through advection diffusion equation.

$$\overline{u} \frac{\partial}{\partial x} \overline{C}^y = -\frac{\partial}{\partial z} \overline{f}^y \tag{2.10}$$

This by integration gives

$$\overline{f}^y(x, z_m) = -\int_0^{z_m} \overline{u}(z) \frac{\partial}{\partial x} \overline{C}^y(x, z) dz \tag{2.11}$$

This equation is further evaluated using the analytic expression for the vertical concentration distribution downwind of a unit surface point source proposed by van Ulden (1978). This is given as

$$\overline{C}^{y}(x,z) = \frac{A}{U\overline{z}} e^{-(z/b\overline{z})^{r}} \tag{2.12}$$

Here $\overline{z}$ is the mean height of the particles at any downwind distance and U is the mean horizontal speed of these particles. van Ulden (1978) gives equations for $\overline{z}$ and U as follows,

$$\overline{z} = \int_0^\infty zCdz \Big/ \int_0^\infty Cdz \tag{2.13}$$

and

$$U = \int_0^\infty uCdz \Big/ \int_0^\infty Cdz\,. \tag{2.14}$$

The above analytical solution is derived from the power law profiles for wind and eddy diffusivity. They are given by

$$u(z) = u_1 z^m \qquad \text{and} \qquad K(z) = K_1 z^n \tag{2.15, 2.16}$$

The shape factor r in equation 2.12 is related to m and n by $r = 2 + m - n$. A and b are functions of r and are given by $A = r\Gamma(2/r)\big/\Gamma^2 1/r$ and $b = \Gamma(1/r)/\Gamma(2/r)$ where Γ is the gamma function.

From equation 2.13 it follows that

$$\frac{d\overline{z}}{dx} = \frac{K(p\overline{z})}{\overline{u}(p\overline{z})\,p\overline{z}} \tag{2.17}$$

where

$$p = \left\{\left[\Gamma(2/r)/\Gamma(1/r)\right]^r\right\}^{1/(1-r)} \tag{2.18}$$

The equation 2.17 can be further evaluated by substituting for $\bar{u}$ and K from similarity theory, i.e.,

$$K(z, z/L) = \frac{u_* kz}{\phi(z/L)} \tag{2.19}$$

where $\phi(z/L)$ expresses the dependence of K on stability.

$$\bar{u}(z/L) = \frac{u_*}{k}\left[\ln(z/z_0) - \psi(z/L)\right] \tag{2.20}$$

where $\psi(z/L)$ describes the departure of the wind profile from the logarithmic profile in neutral conditions, k the von Karman's constant and u_* the friction velocity. Surface layer expressions of $\phi(z/L)$ and $\psi(z/L)$ are adopted from Dyer (1974) and Paulson (1970) respectively. The above formulations give the horizontal gradient of mean plume height as follows:

$$\frac{d\bar{z}}{dx} = \frac{k^2}{\left[\ln(p\bar{z}/z_0) - \psi(p\bar{z}/L) + \psi(pz_0/L)\right]\phi(p\bar{z}/L)} \tag{2.21}$$

Apart from $\bar{z}$, we need to know U, the mean plume speed in equation (2.12). The mean plume speed is found according to the Lagrangian similarity theory.

$$U = \bar{u}(c\bar{z}) \tag{2.22}$$

This defines the mean particle speed as the flow speed at a fraction of the mean plume height. This fraction expressed by c is $e^{-\gamma}$, where γ is the Euler constant (Chatwin, 1968). Horst (1979) gives the values of c as $c = 0.66$ for $r = 2$, 0.63 for $r = 1.5$ and 0.56 for $r = 1$. Gryning et al., (1983) proposed theoretical expressions for the shape factor r as,

$$m(z_1) = \left[\frac{\partial \ln u(z)}{\partial \ln(z)}\right]_{z_1} \qquad n(z_1) = \left[\frac{\partial \ln K(z)}{\partial \ln(z)}\right]_{z_1} \tag{2.23, 2.24}$$

This fit should apply to an interval of the order of the height of the plume, which was taken as $c\bar{z}$ by Gryning et al., (1983). Using the Dyer (1974) surface layer similarity corrections for stability, Finn et al., (1996) showed that

$$r = \frac{1+5c\bar{z}/L}{\ln(c\bar{z}/z_0)-\psi(c\bar{z}/L)} + \frac{1+10c\bar{z}/L}{1+5c\bar{z}/L} \qquad \text{for } \bar{z}/L > 0 \qquad (2.25)$$

and

$$r = \frac{\left(1-16c\bar{z}/L\right)^{-1/4}}{\ln(c\bar{z}/z_0)-\psi(c\bar{z}/L)} + \frac{1-8c\bar{z}/L}{1-16c\bar{z}/L} \qquad \text{for } \bar{z}/L < 0\,. \qquad (2.26)$$

The above equations express r as a function of $\bar{z}$ and hence a function of x, the downwind distance. Haenel and Grunhage (1999) points out that the basic assumption in the analytical solution is the horizontal homogeneity of $u(z)$ and $K(z)$. This implies that m and n should be constants and hence r ($r = 2+m-n$) should be a constant also or $\partial r/\partial x = 0$. However Finn et al., (1996) has validated the Gryning et al., (1983) theoretical expressions. They support use of Gryning et al., (1983) formulations in analytical footprint models. They state that the sensitivity of the footprint to the value of r is small for $L > 0$ and relatively large for $L < 0$. Horst and Weil (1992) gave approximate constant values for r such as $r = 1$ for unstable conditions, $r = 1.5$ for near neutral conditions and $r = 2.0$ for stable conditions. Substituting for $\overline{C}^{y}(x,z)$ in equation 2.12 and changing the variable of integration to $\xi \equiv z/\bar{z}$, Horst and Weil (1994) showed that

$$\overline{f}^{y} = -\frac{d\bar{z}}{dx}\frac{\partial}{\partial\bar{z}}\int_0^{z_m/\bar{z}} \frac{\bar{u}(\xi\bar{z})}{U} A e^{-(\xi/b)^r}\, d\xi \qquad (2.27)$$

Further they define a normalized crosswind integrated footprint Φ which depends only on $\bar{z}/z_m$ and the shape factor r.

$$\Phi = \frac{z_m \overline{f}^{y}(x,z_m)}{d\bar{z}/dx} \approx \left(\frac{z_m}{\bar{z}}\right)^2 \frac{\bar{u}(z_m)}{U(\bar{z})} A e^{-(z_m/b\bar{z})^r} \qquad (2.28)$$

Equation 2.28 avoids the direct integration of the wind profile from zero to z_m and only the wind speed at the height z_m is required.

2.4. Flux footprint for profile techniques

Most of the footprint analysis (Schuepp et al.1990; Horst and Weil, 1992,1994; Leclerc and Thurtell, 1990; Weil and Horst, 1992; Schmid, 1994) was done for direct eddy-covariance flux measurements. Horst (1999) extended the footprint analysis for flux estimations from vertical concentration profiles. Earlier Schmid (1994) calculated the surface source area for the measurement of scalar concentration and reported that the source area is about an order of magnitude greater than that for an eddy-covariance flux measurement. Stannard (1997) calculated the uniform-fetch requirements for accurate Bowen ratio measurements in the simple case of a streamwise step change in surface fluxes, neutral stability and constant wind speed with height. Stannard found that the equilibration of the Bowen-ratio flux measurements to the surface downwind of the discontinuity is equivalent to the equilibration of an eddy-covariance measurement made at the geometric mean of the two Bowen ratio measurement heights, assuming that the available energy is constant across the flux discontinuity. Horst (1999) assumed for his comparison between the footprints for eddy-covariance and concentration gradient flux measurements that the vertical concentration gradient was measured at a single height even though in practice, measurements are made at several heights. It is found that the upwind extent of the footprint associated with concentration-profile flux estimates is similar to that of the footprint for eddy-covariance flux measurements, when the eddy-covariance measurements are made at a height equal to the arithmetic mean of the highest and lowest profile measurement height for stable stratification or geometrical mean for unstable stratification. The concentration profile flux footprint envelope extends closer to the measurement location than

does the eddy-covariance flux footprint, because the flux estimated from the profile is influenced by the concentration measurements made at heights lower than that of equivalent eddy-covariance flux measurement. The concentration profile flux footprint depends on the ratio of the highest to the lowest measurement height but is insensitive to the number of measurement levels. Measurements of surface fluxes by Bowen ratio technique were also examined by Horst (1999). The Bowen ratio footprint is identical to that of profile measurements when the reference flux is homogeneous, a scenario limited to few cases. In the more general case, Horst (1999) states that it is not permissible to define a Bowen ratio footprint, because the technique is a non-linear function of the surface fluxes.

2.5. Recent developments

Haenel and Grunhage (1999) present an improved analytical footprint model based on the existing theoretical background. They mainly address the fact that the analytical footprint solutions by Horst and Weil (1992, 1994) do not satisfy the constraint that the cumulative footprint must approach unity for an upwind distance tending towards infinity. They examine analytical models proposed by Horst and Weil (1992, 1994) and reach a concluding remark on the asymptotic behavior of the variation of the cumulative footprint with respect to upwind distance that the basis of this unsatisfactory results lies within the equation adopted for the shape factor 'r'. The shape factor, which describes the crosswind integrated concentration distribution ($\overline{D}^{y}(x,z)$) in Horst and Weil models is adopted from Gryning et al., (1983) and is based on the empirical power laws for wind speed and eddy diffusivity (eqns. 2.15, 2.16). The basic assumption to obtain an analytical solution for $\overline{D}^{y}(x,z)$ is that wind speed and eddy diffusivity must be horizontally homogeneous. This implies m and n to be constants in equations. 2.15 and 2.16 and there by r which is by definition $2+m-n$. However this is not true when r is

calculated from Gryning et al (1983) formula because it defines r as a function of $\bar{z}$ and thereby upwind distance x. Thus they recommend using a constant r value instead of a distance dependent function and show that the constraint that the cumulative footprint should approach unity at infinity cannot be satisfied if r is taken as a monotonic function of x or of $\bar{z}$. The use of Gryning et al (1983) formulations also requires the use of Monin-obukhov theory at this stage of model development and brings about a change from the power law world to the real world. Haenel and Grunhage (1999) uses Schmidt's conjugate powers which defines

$$r = 1 + 2m . \tag{2.29}$$

They further adopt m from Haenel and Siebers (1995) and by substituting into (2.29) gives

$$r = 1 + 2\left(\frac{\phi_m(z_m / L)}{\ln(z_m / z_0) - \psi_m(z_m / L) + \psi_m(z_0 / L)} \right). \tag{2.30}$$

Consequently their normalized crosswind integrated footprint is given as

$$\Phi = Ab\left(\frac{z_m}{\bar{z}} \right)^{(3+r)/2} e^{-\left(z_m / b\bar{z}\right)r} \tag{2.31}$$

All variables in the above equations are defined in section (2.3) except the new definition of the shape factor r, which is given in equation (2.29). Thus in this new model, the derivation of the crosswind integrated footprint is completely carried out within the power law world. They also suggest to employ Monin-Obukhov similarity theory at a later stage in the derivation namely on the dependence of plume height on upwind distance. As plume height enters as an independent variable this does not cause any inconsistency in the model.

Hsieh et al. (2000) proposed an approximate analytical footprint model for thermally stratified atmospheric flows. They use similarity theory and results from Lagrangian simulations

to construct the relationships between flux, fetch, stability, surface roughness and measurement height. They define a new length scale z_u by combining z_m and z_0 such that

$$z_u = z_m\left(\ln\left(z_m/z_0\right)-1+z_0/z_m\right). \tag{2.32}$$

Two dimensionless groups are then proposed and are interrelated.

$$\frac{x}{L} = f\left(\frac{z_u}{L}\right) \tag{2.33}$$

Using the Lagrangian model proposed by Thomson (1987), Hsieh et al. (2000) find the relationship between these two dimensionless groups, i.e.,

$$\left(\frac{x}{L}\right) = \frac{-1}{k^2\ln\left(F/S_0\right)} D\left(z_u/L\right)^P \tag{2.34}$$

Here, D and P are similarity constants and found for stable, neutral and unstable conditions from the regression analysis of the results from the Lagrangian model. The flux footprint $f(x,z_m)$ is derived from the above equation based on Gash (1986) expressions. The main advantage of Hsieh et al. (2000) model is that it explicitly describes the relationship between footprint, stability, measurement height and surface roughness and presents an analytically solvable model. The model performance was compared with Eulerian and Lagrangian models as well as with field observations of water vapor flux from an irrigated potato site followed by a transition to a desert.

Kormann and Meixner (2001) address the same problem of the inconsistent asymptotic behavior of Horst and Weil (1992, 1994) models. Similar to Haenel and Grunhage (1999), Kormann and Meixner (2001) choose to retain the power law profiles for both wind speed and eddy diffusivity. The basic difference between these two works is that Kormann and Meixner (2001) use power laws even in the calculation of the horizontal gradient of plume height (2.17)

while Haenel and Grunhage (1999) shift to the Monin-Obukhov similarity theory at this stage of derivation. Kormann and Meixner (2001) then derive a simple expression for the footprint based on power law profiles and finally relate the power law profiles to those described by Monin-Obukhov theory. They use an analytical approach by Huang (1979) and a numerical error minimization method for this purpose.

Leclerc et al. (2003a) observe that little attention has been given to the possible contributions of sources well outside the footprint region in the presence of non-local circulation. Their tracer release experiment over 9.8 m tall slash pine canopy found that in advective conditions, particularly when the air mass flows over large surface inhomogeneities, the observed footprint fluxes are significantly different from the predicted fluxes. Their site characterized a recently logged area forming an arc in North West direction extending up to 350 to 500 m from the flux site. The measured footprint fluxes compared well with the Lagrangian and analytical models in cases where the wind originated from NNE-NE directions. They observed significantly high values of the measured fluxes when the wind blows from NNW-NW directions and noticed poor comparison with modeled fluxes. This dramatic difference is attributed to the presence of the clearcut in NNW-NW direction, which modifies the flow due to the contrasting heat, mass and momentum budgets. Their results suggest that the effects of surface inhomogeneities should be properly quantified and accounted for when the flux measurements are carried out over tall forest canopies.

2.6. Model validation

In their 1992 paper Horst and Weil compared the analytical solutions with a stochastic model based on Thompson (1987). They found the agreement between the two models is quite good in stable and neutral atmospheric stratifications. However their solutions were for a smooth

terrain with (z_m/z_0) values ranging form 100 to 300. Finn et al. (1996) was the first to report experimental evaluations of analytical and Lagrangian footprint models. They selected analytical solutions by Horst and Weil (1992, 1994) and Lagrangian model by Leclerc and Thurtell (1990) for their study. The models were evaluated with the results of an SF_6 tracer release experiment conducted over a sagebrush canopy of 1 to 1.5m heights. The vertical flux of SF_6 was measured at 10m and 5m above the ground using eddy-covariance technique. The results were in good comparison with all the three model predictions in moderately unstable to moderately stable conditions ($-0.01 < z_0/L \leq 0.005$). The theoretical expressions for the shape factor (Gryning et al., 1983) in the analytical models were also evaluated with the experimental data. Their analysis supports the use of the Grynning formulation of the shape factor in analytical solution. The sensitivity of the footprint to the shape factor was found to be small in stable conditions and relatively large in unstable conditions. Leclerc at al. (2003a) reported experimental verification of the analytical footprint model (Horst and Weil, 1994) over a slash pine canopy of 9.8m height. They found excellent agreement between the experimental data and model predictions in the absence of large inhomogenities upwind in the landscape. Leclerc et al. (2003b) compared tracer flux measurements obtained over peach orchard with the results from two widely used footprint models (Horst and Weil, 1994; Leclerc and Thurtell, 1990). Their results show that both models work well over a canopy of intermediate roughness under unstable to near neutral conditions. At distances close to the source, the analytical model showed slight deviations from the experimental values while the Lagrangian model gave closer estimates.

2.7. Roughness sub layer over tall canopies

The surface layer is the bottom one-tenth of the planetary boundary layer (PBL) in which wind shear changes rapidly, where the friction is predominant and the Coriolis force has little

influence on the flow. The Surface Layer over vegetated areas can be divided into two layers; roughness sub layer (RSL) which extends from the ground to approximately three times the canopy height including the canopy air space, and inertial sub layer (ISL) beginning from the top of the RSL and extending throughout the surface layer (fig.2.3). RSL can be defined as the region where the turbulence characteristics are modified mechanically and thermally by the presence of the canopy elements (Kaimal and Finnigan, 1994). The Monin-Obukhov similarity theory, which is widely used in surface layer dispersion models, has been found not applicable in the RSL by a number of researchers since the early 1970s (Thom et al., 1975, Raupach, 1979, Denmead and Bradley, 1985). The diabatic influence functions used in Moin-Obukhov similarity theory are derived from experiments over smooth savannah type surfaces (Dyer and Hicks, 1970; Businger et al., 1971; Hicks, 1976). The use of these empirical functions for flow over rough surface such as forests is questionable. The flow over surfaces of different roughnesses can be assumed to be similar only at heights much greater than the largest length scales characterizing the surface (Raupach, 1979). Below such levels, the flow is influenced by dynamical and thermal effects created by the characteristics of the surface. Researchers have conducted flux profile measurement campaigns above vegetated surfaces using eddy-covariance or aerodynamic methods and compared the non-dimensional stability functions predicted by similarity theory for momentum, heat and water vapor with the corresponding functions calculated from experimental data. It has been found that similarity theory considerably underestimates the turbulence above plant canopies; in other words the eddy diffusivities for momentum, heat and scalar are enhanced in the RSL from their surface layer values.

In agricultural and forest meteorology studies, we often make flux measurements over tall-vegetated areas where it is impossible to build very tall flux towers extending above the RSL

due to practical difficulties. It is desirable to make flux measurements close to the canopy top (1.5-1.7h) as flux gradients become weaker and fetch requirements become important as the height increases. Due to these reasons, flux measurements above canopies are usually made well within the RSL. Researchers have investigated the increased turbulence in the RSL and reported empirical values by which momentum and scalar diffusivities are enhanced within this region (Thom et al., 1975; Garratt, 1978; Raupach, 1979; Denmead and Bradley, 1985; Cellier and Brunet, 1992, Simpson et al., 1998). The enhancement factor ($\gamma_{m,h,v}$), the magnitude by which similarity theory underestimates the diffusivities is given by Garratt, 1978 and by Raupach, 1979.

$$\gamma_{m,h,v} = \frac{\phi_{m,h,v}}{\phi^*_{m,h,v}} \tag{2.35}$$

where $\phi_{m,h,v}$ is the stability function for momentum, heat and water vapor based on Monin-Obukhov similarity theory and $\phi^*_{m,h,v}$ represents stability function in the RSL. Thom et al. (1975) were amongst the first to compare the vertical flux of sensible heat and latent heat estimated from profile gradient relationship against those obtained from energy balance estimates of observed data. Their experiment was over a pine forest of approximate height 15m. They found that independent energy balance estimates are 2 to 3 times greater than those obtained from profile gradient relationship in unstable and near neutral conditions ($-0.04 \leq Ri \leq -0.01$) while no similar discrepancy was observed in stable conditions ($Ri > 0.02$). Thom et al. (1975) pointed out two mechanisms, which could possibly cause this discrepancy, namely thermal seeding and wake diffusion. They observed that the values of Ri are several times larger than their canopy top values at measurement levels close to $z = d$ and that similar inflection points exist in the profiles of wind speed and potential temperature as well. This suggests that free convective

thermals of characteristic dimension z_0 can be originated within the canopy and moved into the turbulent boundary layer just above the canopy producing additional mixing and thereby enhanced eddy diffusivity. This process which is associated with substantially negative Ri is described as thermal seeding by Thom et al., (1975). Another mechanism by which diffusion could be enhanced is wake diffusion, originally proposed by Schlichting (1955). Schlichting (1955) observed that in the wake behind a row of heated bars the eddy diffusivity of heat (K_H) is twice that of momentum (K_M). Similarly, it is possible that mixing generated by individual rough elements in a forest canopy produces additional diffusion mechanism contributing more effectively to K_H and K_V than to K_M. Therefore the profiles of temperature and humidity are less steep than the velocity profiles.

Garratt (1978) obtained similar results form the experimental data obtained over a surface of mixed roughness. The site comprised of scattered live trees and shrubs of average height 8m occupying about 25% of the total area, dry grass of 1m height with 60-70% area cover and patches of burnt grass on the rest of the area. The results suggest enhanced eddy diffusivities for the region $\xi = z/z_0 = 20-85$ ($z_0 = 0.4m$) and the enhancement decreasing as the non-dimensional height (ξ) increases. He observed no significant difference between K_H and K_M at any of the measurement levels. The experimental data suggests that the depth of this transition layer above the canopy (RSL) is approximately $4.5h$ for momentum transfer and $3h$ for heat transfer where h is the height of the main roughness elements.

Raupach (1979) is one of the earliest publications on the issue of validity of similarity theory over tall forest canopies. His results from the data obtained over a pine forest of height 16.6m substantially contradict Garratt's (1978) findings. Raupach (1979) found no enhancement for momentum for all stabilities while for the scalar entity an enhancement factor of 2 is found

for slightly stable conditions and 3.5 for slightly unstable cases, all at a height of 1.2h. This means that $K_H = 2K_M$ and $\phi_m = \phi^*_m$ while Garratt (1978) finds $K_H = K_M$ and $\phi_m = 0.6\phi^*_m$. The difference in turbulent diffusivities (K_H, K_M) is discussed in the context of mixing lengths. The presence of pressure forces enables a vertically migrating air parcel to exchange momentum with its surroundings more quickly than other properties causing momentum mixing lengths to be shorter than property mixing lengths. No such equivalent of pressure force exists for heat or scalar entity. It is possible to observe higher scalar eddy diffusivity in the wake region behind a heated object and in the unstable boundary layer over a heated surface. While the former is attributed as a possible cause for the enhanced diffusivity by Thom et al. (1975), Raupach (1979) discusses the buoyant convective effects that might originate as a results of horizontally distributed sources and sinks in the canopy.

Most of the earlier works in this field reported the enhancement factor only at one or two heights close to the canopy. Over a maize canopy of 2.3 m height and 3.4 LAI, Cellier and Brunet (1992) reported enhancement factors ($\gamma_{m,h,v}$) at 5 heights up to 2.3h. They obtained a smooth profile where $\gamma_{h,v} \cong 1.7\gamma_m$ at $1.2h$. They also used a power law profile for the height dependent γ as $\gamma_{h,v} = z_*/z$ and $\gamma_m = (z_*/z)^\eta$ where η should be an empirical constant depending on the canopy density and z_* is the height of the RSL.

More recently the validity of similarity theory over tall forests was examined by Simpson et al. (1998). Diabatic influence functions are calculated based on observations at 4 levels over a mixed deciduous forest canopy of 20m height. The scalar diffusivity enhancement they observed is relatively small ($\gamma_h = 1.8$ at $1.3h$) compared to previously rported results. However it is

believed that, in their studies, scalar concentration differences are observed more precisely than that of previous measurements with the high resolution Trace Gas Analysis System (TGAS).

The problems in modeling of dispersion in the RSL is still being investigated and no concrete theories are developed which can be applied to different canopies. Researchers rely either on direct measurements of diabatic influence functions or use enhancement factors observed elsewhere for practical purposes. However a better defined RSL depth, its variation with stability, dependency of enhancement factor on stability all remain still to be investigated. Most of the data available are contradicting and no general conclusions are made in these topics. As an example Cellier Brunet (1992) finds no significant evolution in either of the enhancement factors from near neutral to unstable conditions. This is consistent with Garratt (1980) while Raupach (1979) and Chen and Schwerdtfeger (1989) found γ_h to be stability dependent. This shows the necessity of more data over a wide range of canopies from accurate experiments.

2.8. Footprint estimation in the RSL

As mentioned previously, footprint analysis is widely used for the flux measurements in the RSL over forest canopies. It is known that the present footprint models are developed for the ISL and it is necessary to modify them to take into account the flow properties in the RSL. Lee (2003) studies the characteristics of flux footprint in the RSL in a Lagrangian framework. His model combines the localized near-field (LNF) theory of Raupach (1989) and in canopy turbulence formulation. In the LNF theory, the scalar concentration resulting from the canopy source is separated into a non-diffusive near field and a diffusive far-field component. In the RSL, the footprint prediction from LNF is more contracted than the models based on ISL turbulence parameterizations.

2.9. Footprint climatology

From the previous discussions it can be seen that the footprint models are not developed in a way to use them for practical field applications. Despite the growing interest in flux measurement studies, it has not yet become a customary step to use footprint analysis in deciding the sensor location. Amiro (1998) applied the Horst and Weil (1992) model to micrometeorological monitoring of evapotranspiration in a boreal forest catchment. He used this model in a practical way to illustrate patterns of footprint envelopes over long time periods. This allows to easily map out regions on the site where evapotranspiration might have originated. The study shows that two 12-m high towers would be needed to fully sample the 90% footprint contour of evapotranspiration in the 0.5 km^2 catchment study area on a seasonal basis.

It is important to note that the time averaged footprint flux gives only a weighting factor for the sources and it is necessary to know the actual source distribution for an actual estimation of fluxes. There is increasing interest in carbon sequestration studies to upscale the field measurements to a landscape or regional level. Soegaard et al. (2003) summarizes the major methods used in upscaling the local flux measurements. 1) Different types of surfaces or vegetation can be assigned characteristic fluxes by parallel flux measurements and by linear averaging of the fluxes, the landscape level flux can be derived by area weighting. 2) Footprint modeling can be used to obtain an integrative flux measurement by raising the measurement height and thereby increasing the source area. 3) Plant photosynthesis and soil respiration models can be combined to simulate the net ecosystem exchange. 4) Remotely sensed and satellite data can be used as an input in spatial modeling of carbon fluxes. Soegaard et al. (2003) uses an analytical footprint model (Schuepp et al., 1990) in a geographic information system (GIS) framework for the eddy- covariance data obtained over an agricultural landscape. Their

experiment consisted of five eddy-covariance systems operating in parallel over the important crop classes and a sixth system mounted on a 48m tower to enable landscape wide flux measurement. The landscape level CO_2 measurement is further weighted by footprint fluxes and compared with direct measurements over five crop types and these estimates are found to be in good agreement.

2.10. Conclusions

This chapter discusses the concept of footprint, its evolution and some commonly used models developed in this area. Over the past two decades the concept of footprint has become an important research area. At present, simple analytical models are available for practical purposes of source area estimation, which require the friction velocity and a measure of atmospheric stability, typically taken to be the Obukhov length. The theoretical treatment of diffusion in these models contains empirical constants and can be a concern for users. Another problem associated with analytical solutions is the inconsistency in the use of wind and diffusivity profiles as both power laws and Monin-Obukhov similarity profiles are used within the same theoretical framework. The analytical solutions are developed for flux measurements in inertial sub layer (ISL) and their applications for flux measurements immediately above forest canopies is not recommended. An important underlying assumption in these solutions is that the terrain is horizontally homogeneous which might not be the case usually. Despite these facts these models are validated against more sophisticated stochastic solutions and also against observations above smooth and rough surfaces.

References

Amiro, B.D., 1998. Footprint climatologies for evapotraspiration in a boreal catchment. Agric. For. Meteorol. 90, 195–201.

Batchelor, G.K., 1964. Diffusion from sources in a turbulent boundary layer. Arch. Met. Stosowanej. 3, 661–670.

Businger, J.A., Wyngaard, J.C., Izumi, Y., Bradley, E.F., 1971. Flux-profile relations in the atmospheric surface layer. J. Atmos. Sci. 28, 189–191.

Calder, K.L., 1952. Some recent work on the problem of diffusion in the lower atmosphere. *Proc. U.S. Tech. Conf. Air Poll*., McGraw-Hill, New York. 787–792.

Cellier, P., Brunet, Y., 1992. Flux gradient relationships above tall plant canopies. Agric. For. Meteorol. 58, 93–117.

Chatwin, P.C., 1968. The dispersion of a puff of passive contaminant in the constant stress region. Quart. J. Roy. Meteorol. Soc. 94, 401–411.

Chen, F., Schwerdtfeger, P., 1989. Flux-gradient relationships for momentum and hear over a rough natural surface. Quart. J. Roy. Meteorol. Soc. 115, 335–352.

Denmead, O.T., Bradley, E.F., 1985. Flux-gradient relationships in a forest canopy. in: B.A. Hutchison and B.B. Hicks (eds), The forest-atmosphere interaction. Reidel, Dordrecht, pp. 421–442.

Dyer, A.J., 1974. A review of flux-profile relationships. Boundary-Layer Meteorol. 7, 363–372.

Dyer, A.J., Hicks, B.B., 1970. Flux gradient relationships in the constant flux layer. Quart. J. Roy. Meteorol. Soc. 96, 715–721.

Elliot, W.P., 1958. The growth of the atmospheric internal boundary layer. Trans. Amer. Geophys. Union. 39, 1048–1054.

Elliot, W.P., 1961. The vertical diffusion of a gas from a continuous source. Int. J. Air and Water poll. 4, 33–46.

Finn, D., Lamb, B., Leclerc, M.Y., Horst, T.W., 1996. Experimental evaluation of analytical and Lagrangian surface-layer flux footprint models. Boundary-Layer Meteorol., 80, 283–308.

Flesch, T.K., 1996. The footprint for flux measurements, from backward lagrangian stochastic models. Boundary-Layer Meteorol. 78, 399–404.

Garratt, J.R., 1978. Flux profile relations above tall vegetation. Quart. J. Roy. Meteorol. Soc. 104, 199–211.

Garratt, J.R., 1980. Surface influence upon vertical profiles in the atmospheric near-surface layer. Quart. J. Roy. Meteorol. Soc. 106, 803–819.

Garratt, J.R., 1990. The internal boundary layer – A review. Boundary-Layer Meteorol. 50, 171–203.

Gash, J.H.C., 1986. A note on estimating the effect of a limited fetch on micrometeorological evaporation measurements. Boundary-Layer Meteorol. 35, 409–413.

Gryning, S.E., van Ulden, A.P., Larsen, S.E., 1983. Dispersion from a continuous ground-level source investigated by a K model. Quart. J. Roy. Meteorol. Soc. 109, 355–364.

Haenel, H.-D., Grunhage, L., 1999. Footprint analysis: A closed analytical solution based on height-dependent profiles of wind speed and eddy viscosity. Boundary-Layer Meteorol. 93, 395–409.

Haenel, H.D., Siebers, J., 1995. Lindane volatilization under field conditions: Estimation from residue disappearance and concentration measurements in air. Agric. For. Meteorol. 76, 237–257.

Hicks, B.B., 1976. Wind profile relationships from the ‘Wangara Experiment’. Quart. J. Roy. Meteorol. Soc. 102, 535–552.

Horst, T.W., 1979. Lagrangian similarity modeling of vertical diffusion from a ground-level source. J. Appl. Meteorol. 18, 732–740.

Horst, T.W., Weil, J.C., 1992. Footprint estimation for scalar flux measurements in the atmospheric surface layer. Bounday-Layer Meteorol. 59, 279–296.

Horst, T.W., Weil, J.C., 1994. How far is far enough?: The fetch requirements for micrometeorological measurements of surface fluxes. J. Atmos. Ocean. Tech. 11, 1018–1026.

Horst, T.W., 1999. The footprint estimation of atmosphere-surface exchange fluxes by profile techniques. Boundary-Layer Meteorol. 90, 171–188.

Hsieh, C., Katul, G., Chi, T., 2000. An approximate analytical model for footprint estimation of scalar fluxes in thermally stratified atmospheric flows. Advances in Water Resources. 23, 765–772.

Huang, C.H., 1979. A theory of dispersion in turbulent shear flow. Atmos. Environ. 13, 453–463.

Kaimal, J.C., Finnigan, J.J., 1994. Atmospheric boundary layer flows: their structure and measurement. Oxford University Press, Oxford, 289 pp.

Kormann, R., Meixner, F.X., 2001. An analytical footprint model for non-neutral stratification. Boundary-Layer Meteorol. 99, 207–224.

Lamb, H., 1932. Hydrodynamics. Dover Publications, New York, 730 pp.

Leclerc, M.Y., Thurtell, G.W., 1990. Footprint prediction of scalar fluxes using a Markovian analysis. Boundary-Layer Meteorol. 52, 247–258.

Leclerc, M.Y., Shen, S., Lamb, B., 1997. Observations and large-eddy simulation modeling of footprints in the lower convective boundary layer. J. Geophys. Res.102, 9323–9334.

Leclerc, M.Y., Karipot, A., Prabha,T., Allwine, G., Lamb, B., Gholz, H.L., 2003a. Impact of non-local advection on flux footprints over a tall forest canopy: a tracer flux experiment. Agric. For. Meteorol. 115, 17–34.

Leclerc, M.Y., Meskhidze, N., Finn, D., 2003b. Comparison between measured tracer fluxes and footprint model predictions over a homogeneous canopy of intermediate roughness. Agric. For. Meteorol. 117, 145–158.

Lee, X., 2003. Fetch and footprint of turbulent fluxes over vegetative strands with elevated sources. Boundary-Layer Meteorol. 107, 561–579.

Pasquill, F., 1972. Some aspects of boundary layer description. Quart. J. Roy. Meterol. Soc. 98, 469–494.

Paulson, C.A., 1970. The mathematical representation of wind speed and temperature profiles in the unstable atmospheric surface layer. J. Appl. Meteorol. 9, 857–861.

Peterson, E.W., 1969. Modification of mean flow and turbulent energy by a change in surface roughness under conditions of neutral stability. Quart. J. Roy. Meteorol. Soc. 95, 561–575.

Raupach, M.R., 1979. Anomalies in flux-gradient relationships over forest. Boundary-Layer Meteorol. 16, 467–486.

Raupach, M.R., 1989. A practical Lagrangian method for relating scalar concentrations to source distributions in vegetation canopies. Quart. J. Roy. Meteorol. Soc. 115, 609–632.

Schlichting, H., 1955. Boundary layer theory. Pergamon, London, 535 pp.

Schmid, H.P., Oke, T.R., 1990. A model to estimate the source area contributing to the turbulent exchange in the surface layer over patchy terrain. Q. J. R. Meteorol. Soc. 116, 965–988.

Schmid, H.P., 1994. Source areas for scalars and scalar fluxes. Boundary-Layer Meteorol. 67, 293–318.

Schmid, H.P., 2002. Footprint modeling for vegetation atmosphere exchange studies: a review and perspective. Agric. For. Meteorol. 113, 159–183.

Schuepp, P.H., Leclerc, M.Y., Macpherson, J.I., Desjardins, R.L., 1990. Footprint predictions for scalar fluxes from analytical solutions of the diffusion equation. Boundary-Layer Meterol. 50, 355–373.

Simpson, I.J., Thurtell, G.W., Neumann, H.H., Hartog, G.D., Edwards, G.C., 1998. The validity of similarity theory in the roughness sublayer above forests. Boundary-Layer Meteorol. 87, 69–99.

Smith, F.B., 1957. The diffusion of smoke from a continuous elevated point source into a turbulent atmosphere. J. Fluid. Mech. 2, 49–76.

Soegaard, H., Jensen, N.O., Boegh, E., Hasager, C.B., Schelde, K., Thomsen, A., 2003. Carbon dioxide exchange over agricultural landscape using eddy correlation and footprint modeling. Agric. For. Meteorol. 114, 153–173.

Stannard, D.I., 1997. A theoretically based determination of Bowen-Ratio fetch requirements. Boundary-Layer Meteorol. 83, 375–406.

Su, H.B., Leclerc, M.Y., 1998. Large eddy simulation of trace gas footprints from infinite crosswind line sources inside a forest canopy. Preprints, 23rd *Conference on Agricultural and Forest Meteorology*. Amer. Meteorol. Soc., Boston, MA. 388–391.

Sutton, 1953. Micrometeorology: A study of physical processes in the lowest layers of the Earth's atmosphere. McGraw-Hill Book Company, Inc., New York. 323 pp.

Thom, A.S., Stewart, J.B., Oliver, H.R., Gash, J.H.C., 1975. Comparison of aerodynamic and ennrgy budget estimates of fluxes over a pine forest. Quart. J. Roy. Meteorol. Soc. 101, 93–105.

Thomson, D.J., 1987. Criteria for the selection of stochastic models of particle trajacteries in turbulent flows. J. Fluid. Mech. 180, 529–556.

Van Ulden, A.P., 1978. Simple estimates for vertical diffusion from sources near the ground. Atmospheric Environment. 12, 2125–2129.

Weil, J.C., 1985. Updating applied diffusion models. J. Climatol. Appl. Meteorol. 24, 1111–1130.

Weil, J.C., Horst, T.W., 1992. Footprint estimates for atmospheric flux measurements in the convective boundary layer. *Precipitation Scavenging and Atmosphere-Surface Exchange*, Vol. 2, S.E. Schwartz and W.G.N. Slinn (eds), Hemisphere Publishing. 717–728.

Table. 2.1. Summary of major works in footprint analysis

Model	Characteristics
Roberts (unpublished, see Sutton, 1953)	Solved the advection diffusion equation assuming a power law for wind speed and eddy diffusivity.
Elliot (1958)	Computed the height of the internal boundary layer assuming a logarithmic wind speed distribution and found the IBL to grow as the 4/5 power of the downwind distance in neutral conditions.
Pasquill (1972)	Introduced the concept of the reverse plume approach and estimated fetch distances for point measurements.
Gash (1986)	Calculated fetch distances for evaporation measurements for uniform wind profile and neutral stability.
Schuepp et al. (1990)	Calculated footprint for uniform wind field and neutral stability and evaluated against Lagrangian simulations of Leclerc and Thurtell (1990).
Schmid and Oke (1990)	Developed a source area model with Monin-Obukhov similarity profiles of wind and diffusivity.
Horst and Weil (1992)	Included the effects of atmospheric stability in footprint.
Horst and Weil (1994)	Proposed an approximate analytical solution using Monin-Obukhov similarity profiles of wind speed and eddy diffusivity.
Finn et al. (1996)	Validation of Horst and Weil (1994) analytical solution with observations above a short canopy.
Horst (1999)	Developed footprint formulation for measurements of Bowen ratio.
Haenel and Grunage (1999)	Suggested the use of a constant value for shape factor instead of a distance dependent function.

Kormann and Meixner (2000)	Suggested the use of power laws in order to avoid the inconsistency in the derivation and presented a simple numerical error minimization and a purely analytical approach to relate the power laws to similarity profiles.
Hsieh et al. (2000)	Developed a hybrid solution based on analytical dispersion formula as well as results from Lagrangian simulations. Analytically related the stability, measurement height and surface roughness to flux footprint.
Leclerc et al. (2003a)	Observed the influence of surface inhomogenities (non-local advection) in the measured flux and the incapability of present models to incorporate them.
Leclerc et al. (2003b)	Compared the observed fluxes over a canopy of intermediate roughness with analytical and Lagrangian model outputs and found good agreement.

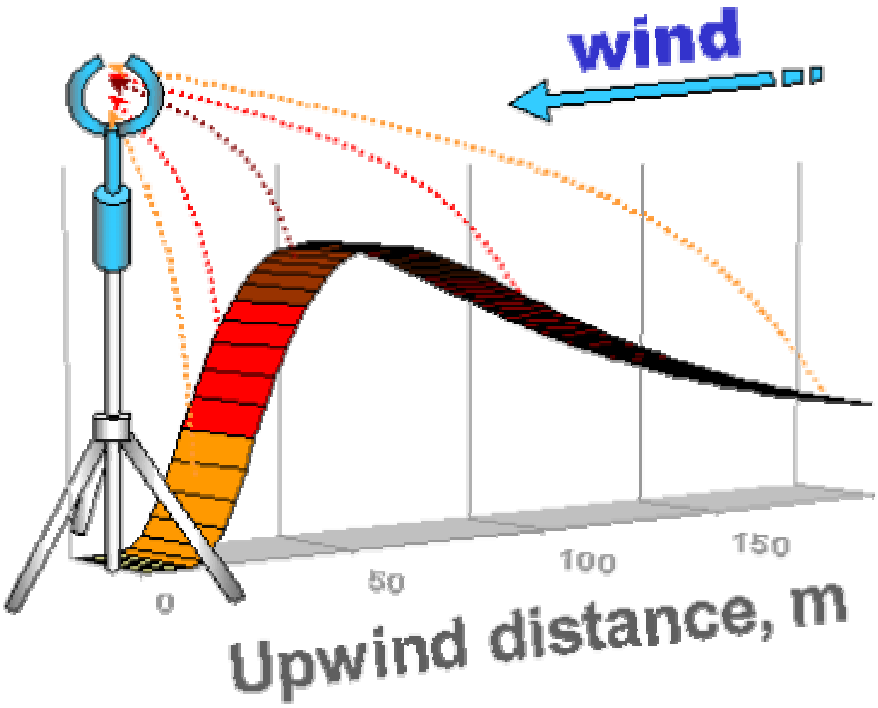

Figure 2.1. Illustration of flux footprint

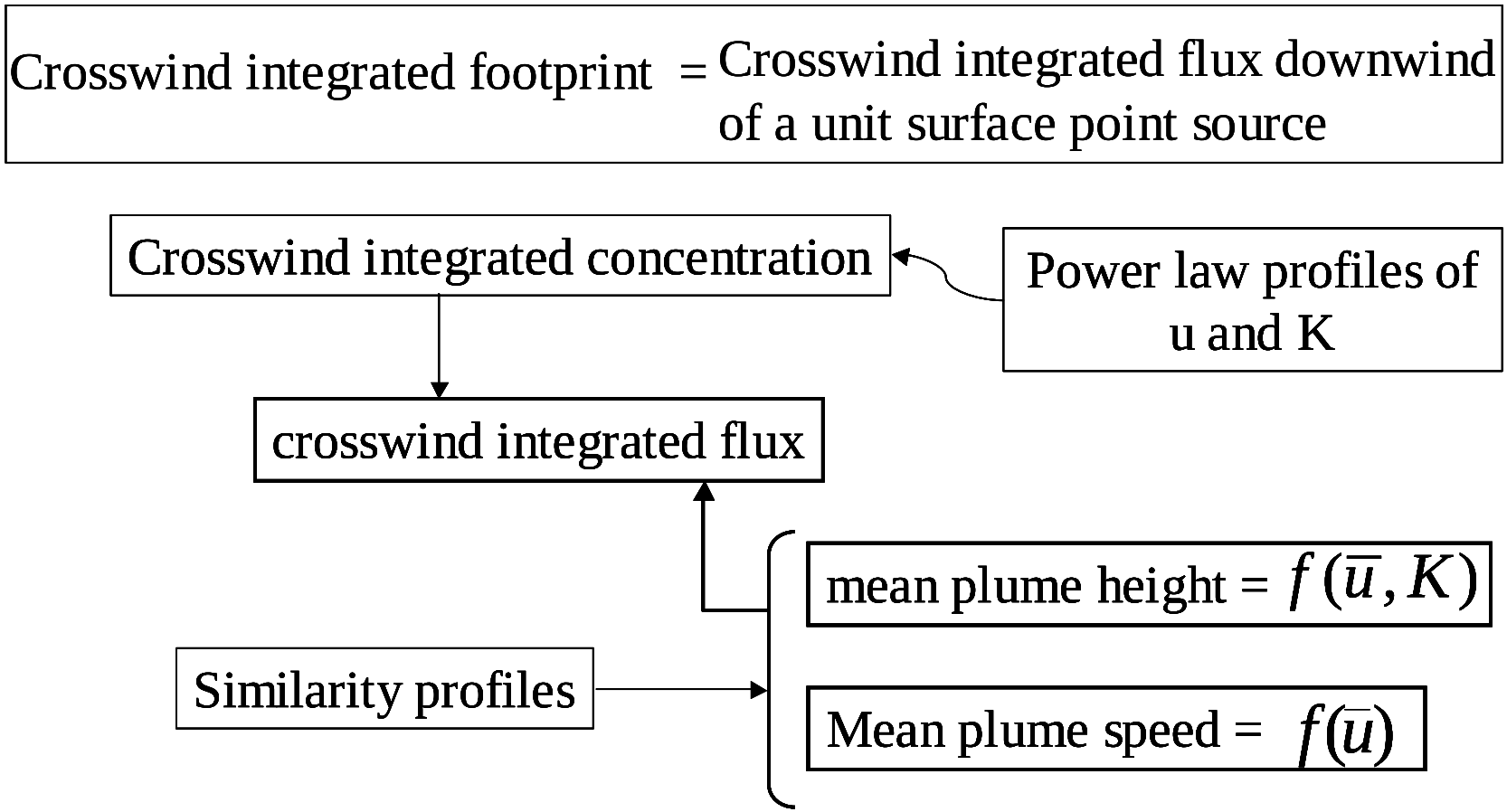

Figure 2.2. Major steps in the analytical footprint model

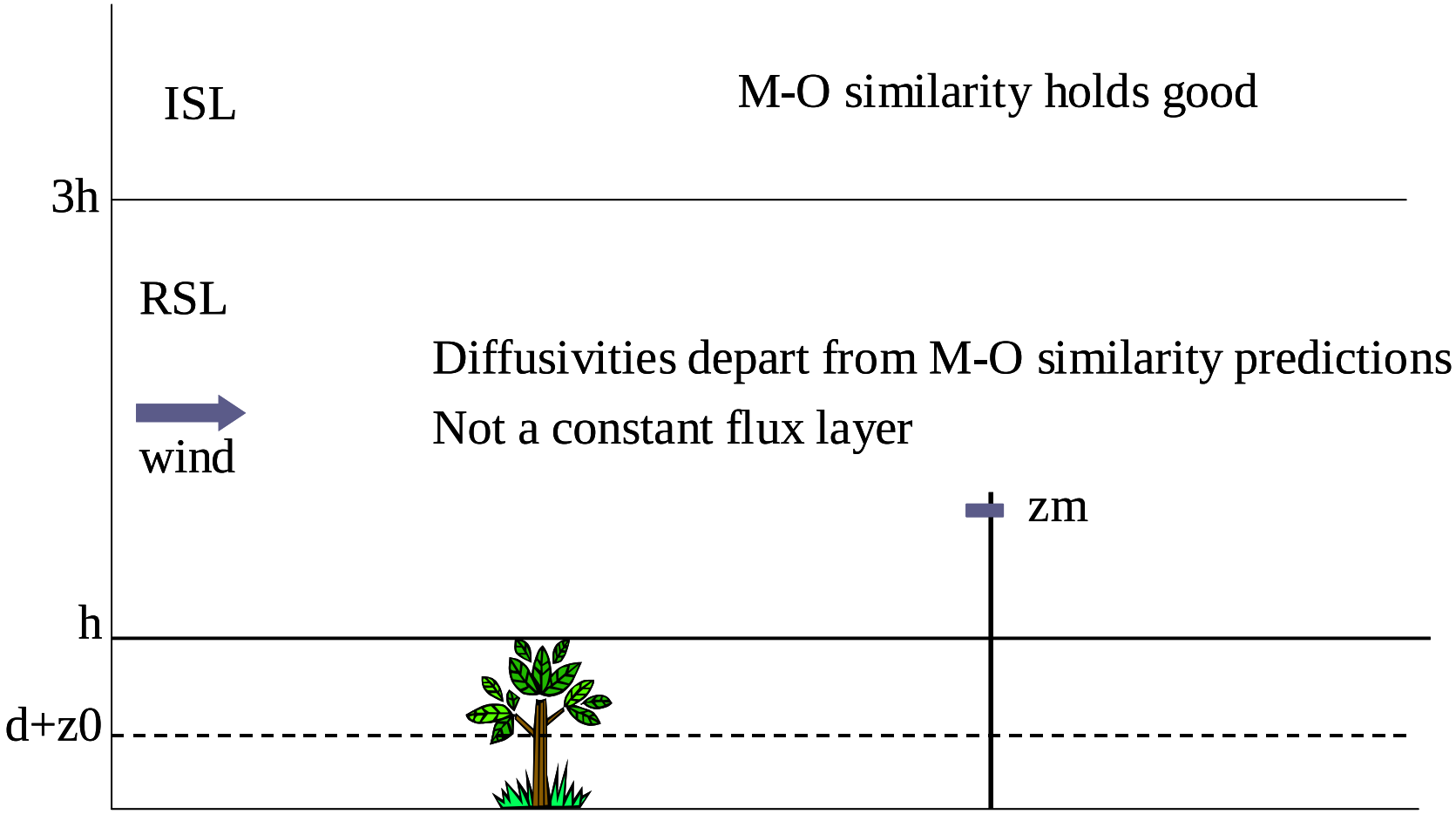

Figure 2.3. Diagram showing roughness sub layer and flux measurements above forest canopies

CHAPTER 3

IMPACT OF ROUGHNESS SUB LAYER ON FLUX FOOTPRINT PREDICTIONS OVER TALL FOREST CANOPIES[1]

[1]Achuthavarier, D. and M.Y. Leclerc. To be submitted to *Agricultural and Forest Meteorology*

3.1. Introduction

Observations of the interaction between the Earth's surface and the overlying atmosphere are important in understanding various exchange processes. This exchange is usually measured in terms of fluxes. In micrometeorology, we usually come across fluxes of momentum and scalars such as heat energy, water vapor, CO_2 and other atmospheric constituents. Attempts are being made worldwide to understand the fate of the greenhouse gases (CO_2, CH_4, N_2O etc.) and their sources and sinks (Baldocchi et. al., 1988, 1996, 2000; Hollinger et al., 1994; Denning et al., 1996; Falge et al., 2002). This has also generated an unparalleled interest in spurring efforts to better understand carbon sequestration capacity of forests. As a result, continuous monitoring systems are established over forest canopies where they measure fluxes of CO_2, water vapor, heat energy and momentum. The most common method to observe surface-atmosphere exchanges is using flux sensors installed at a given level above the site of interest (Baldocchi, 1988). In this method the sensors are employed to record fluxes continuously at a given point. To provide estimates of net exchange, one has to know the spatial context of the measurements. In other words, it is required to understand the source area for a point measurement at a given height. The footprint of a flux measurement, a term originally coined by Schuepp et al. (1990) and by Leclerc and Thurtell (1990) in companion papers, defines the upwind extent of the source area or simply the "field of view" of the flux sensor. The footprint provides a relationship between the vertical flux measured at a given level and the upwind source/sink distribution. The flux footprint is the contribution per unit emission of each element of a surface area source to the vertical scalar flux measured at a height (Horst and Weil, 1992).

Several studies can be found in the literature since the pioneering efforts of Schuepp et al. (1990) and Leclerc and Thurtell (1990). While the analytical solution by Schuepp et al. (1990)

was limited to neutral atmospheric stability, a Lagrangian approach proposed by Leclerc and Thurtell (1990) showed the dependence of flux footprint on atmospheric stability, surface roughness and measurement height. The analytical solution was later modified to take into account the stability effects by Horst and Weil (1992). The less realistic uniform wind profile in the analytical model was further replaced by the logarithmic wind equation (Horst and Weil, 1994). Some of the other works in the analytical footprint approach are the source area model (SAM) by Schmid (1994), model with a constant shape factor by Haenel and Grunage (1999), model using power law profiles for wind and eddy diffusivity by Kormann and Meixner (2000) and a hybrid solution based on analytical dispersion formula as well as results from Lagrangian simulations by Hsieh et al. (2000).

Typically, analytical footprint models are based on equations intended primarily to describe the diffusion over smooth surfaces like grassland. However these models have been widely used outside their original scope for flux measurements over rough surfaces such as forests. It has been known for the last two decades that turbulence properties above forests vary significantly from those described by the atmospheric surface layer similarity theory. (Thom et al., 1975; Raupach, 1979; Denmead and Bradley, 1985). The atmospheric layer immediately above a rough surface, (e.g. a vegetation stand) is called roughness sub layer (RSL), and the rest of the surface layer extending above RSL is called inertial sub layer (ISL). The RSL extends to 2 to 3 canopy heights from the ground.

The growing interest in flux measurements over forest canopies emphasizes the necessity for footprint models that are adapted for RSL. Recent works by Rannik et al., (2000) and Lee (2003) show modified models for flux footprint estimation over rough surfaces using the Lagrangian approach. This study attempts to include the RSL turbulence equations in a simple

analytical footprint model. I choose the footprint solutions proposed by Horst and Weil (1994) for this purpose. This solution is easy to use for practical purposes and requires a minimum of input variables. Despite its simplicity, it uses height-dependent wind and eddy diffusivity profiles and provides good agreement with results obtained using the stochastic simulations and/or field measurements (Finn et al., 1996; Leclerc at al., 2003a, 2003b; Cooper et al., 2003).

The objectives of this study are 1) to characterize the influence of the RSL parametrizations on footprint predictions over tall forest canopies and 2) to develop a simple analytical footprint solution that can be used for measurements within the RSL.

3.2. Theory

3.2.1. Analytical footprint model

In this section, I briefly discuss the basic analytical footprint model by Horst and Weil (1994). The vertical eddy flux measured at a point x, y, z_m, $F(x, y, z_m)$ can be considered as the integral of the contributions from all upwind surface emissions, $F(x', y', 0)$, x', y' being the coordinates of the source, multiplied by an appropriate source weight function or footprint, $f(x - x', y - y', z_m)$.

$$F(x, y, z_m) = \int_{-\infty}^{\infty} \int_{-\infty}^{x} F(x', y', 0) f(x - x', y - y', z_m) dx' dy' \qquad (3.1)$$

For a special case when $F(x', y', 0) = Q\delta(x')\delta(y')$ where Q is the rate of emission from the source, it can be written that

$$f(x, y, z_m) = \frac{F(x, y, z_m)}{Q}. \qquad (3.2)$$

This suggests that the flux footprint equals the vertical flux downwind of a unit surface point source. Horst and Weil (1992) showed the dependence of the flux footprint on crosswind

location to be identical to the crosswind concentration distribution downwind of a unit surface point source. The cross wind integrated footprint ($\overline{f}^{y}$) is equal to the crosswind integrated concentration distribution ($\overline{C}^{y}$) from a unit surface point source and is given by

$$\overline{f}^{y}(x, z_m) = -\int_0^{z_m} \overline{u}(z) \frac{\partial}{\partial x} \overline{C}^{y}(x, z) dz \,. \tag{3.3}$$

By substituting for $\overline{C}^{y}$ from Van Ulden (1978) and assuming a logarithmic wind profile, we obtain (Horst and Weil, 1994)

$$\Phi = \frac{z_m \overline{f}^{y}(x, z_m)}{d\overline{z} / dx} \approx (\frac{z_m}{\overline{z}})^2 \frac{\overline{u}(z_m)}{U(\overline{z})} A e^{-(z_m / b\overline{z})^r} \tag{3.4}$$

Here $\overline{z}$ is the mean plume height, $\overline{u}$ is the mean wind speed, $U(\overline{z})$ is the mean particle velocity at height $\overline{z}$ and r is the shape factor. A and b are functions of r and are given by $A = r\Gamma(2/r)/\Gamma^2(1/r)$ and $b = \Gamma(1/r)/\Gamma(2/r)$ where Γ is the gamma function. Φ is defined as a universal footprint function. The dependence of footprint on measurement height, stability, downwind distance and surface roughness are assumed to be contained in the dependence of $\overline{z}/z_m$ on measurement height, stability, downwind distance and surface roughness. The use of height-dependent logarithmic wind profile is the major difference between the two solutions proposed by Horst and Weil in 1992 and 1994. However equation 3.4 is a simplified form where the integration of $\overline{u}$ from 0 to z_m is approximated to $\overline{u}(z_m)$.

Further evaluation of (3.4) requires values of $\overline{z}$ and $U(\overline{z})$. van Ulden (1978) estimated $d\overline{z}/dx$ in terms eddy diffusivity (K_c) and mean wind speed.

$$\frac{d\overline{z}}{dx} = \frac{K_c(p\overline{z})}{\overline{u}(p\overline{z})p\overline{z}} \tag{3.5}$$

Here p is a function of r and is given by

$$p = \left\{ \left[\Gamma(2/r)/\Gamma(1/r) \right]^r \right\}^{1/(1-r)} \tag{3.6}$$

The mean particle speed or mean plume speed is taken as the mean flow speed at a fraction (c) of the mean plume height i.e.,

$$U(\bar{z}) = \bar{u}(c\bar{z}) \tag{3.7}$$

Chatwin (1968) solved for c and found to be equal to 0.562. According to this relation, the plume speed at the top of the canopy is equal to the wind speed at $0.562h$, h being the height of the canopy, which shows the particle speed at the top of the canopy to be equal to the flow speed inside the canopy. For this reason, the model will require wind speed values in the region $d < z \le h$ despite the fact that the analytical solution is not compatible for in-canopy footprint estimations. Here d is the displacement length. It is known that the logarithmic profile often underestimates the wind speed inside the canopy (Shaw et al., 1974; Wilson et al., 1982; Raupach et al., 1986). The use of more realistic exponential profile (eqn. 3.8) is recommended in the region $d < z \le h$ (Cionco, 1965)

$$u(z) = u(h)\exp\left(-\alpha_u \left(1 - z/h\right)\right) \tag{3.8}$$

α_u is the exponential wind coefficient. The stability dependent logarithmic profile is used in the region $z > h$ and is given as

$$\bar{u}(z, z/L) = \frac{u_*}{k}\left[\ln(z/z_0) - \psi(z/L) + \psi(z_0/L)\right] \tag{3.9}$$

Here u_* is the friction velocity and $k = 0.4$ and is the von Karman constant. The stability correction ($\psi(z/L)$ is adopted from Paulson (1970). The term $\psi(z_0/L)$ is used in this study and is justified by the recent results published by Nakamura and Mahrt (2001). They observe that

the term $\psi(z_0 / L)$ becomes significant with relatively large roughness lengths and small measurement heights, as is usually the case over forest canopies. The eddy diffusivity is given by

$$K_c(z, z/L) = \frac{u_* kz}{\phi_c(z/L)} \tag{3.10}$$

where $\phi_c(z, z/L)$ expresses the stability dependence and is adopted from Dyer (1974). Equation 3.5 is evaluated by substituting from (eqn. 3.7) and (eqn. 3.10).

3.2.2. Roughness sub layer

Several studies have been published on the validity of similarity theory in the RSL going back to the 1970s (Thom et al., 1975; Garratt, 1978; Raupach, 1979; Denmead and Bradley, 1985; Cellier and Brunet, 1992; Simpson et al., 1998). Findings from these studies suggest that diffusivities for momentum and scalar quantities are enhanced within the RSL compared against predictions from Monin-Obukhov similarity theory. Thom et al. (1975) postulated two phenomena in an attempt to explain the enhancement of diffusivities in the RSL. Firstly, it is possible that free convective thermals originating within the canopy emerge into the turbulent air above the canopy and generate additional mixing, thereby enhancing turbulent diffusivities. Secondly, forests could be acting as a row of heated rods creating turbulent wakes behind each tree. The former mechanism is termed as thermal seeding while the latter is known as wake diffusion. Some of the other explanations put forwarded for the RSL effect are horizontal inhomogenity in forests (Raupach, 1979) and the vertical location of sources and sinks (Denmead and Bradley, 1985). The factor by which diffusivity is enhanced ($\gamma_{m,h,v}$ where m, h and v represent momentum, heat and water vapor respectively) is given by Garratt, 1978 and by Raupach, 1979 as

$$\gamma_{m,h,v} = \frac{\phi_{m,h,v}}{\phi^*_{m,h,v}} \tag{3.11}$$

where $\phi_{m,h,v}$ is the stability function derived from Monin-Obukhov similarity and $\phi^*_{m,h,v}$ is the observed stability function in the RSL. The value of the enhancement factor is highest close to the canopy and found to decrease with height. These profiles, however, vary from canopy to canopy and the enhancement of momentum diffusivity differs from that of scalar diffusivity. Cellier and Brunet (1992) proposed a simple diffusive model for the height-dependent γ based on their experimental data over a maize canopy. They suggest $\gamma_{h,v} = z_*/z$ and $\gamma_m = \left(z_*/z\right)^{\eta}$, where z_* is the height of the RSL, z the reference height and η a constant value depending on the canopy density. The value of η tends towards 1 for low-density canopies and 0 for high-density canopies. According to their study, the enhancement of scalar diffusivity is the same for all canopies while that of momentum is maximum for sparse canopies and minimum for dense canopies. A review of previous results shows that γ_m lies between 1.5 – 2.5 for bushland and savannah type canopies (Garratt, 1978, 1980; Chen and Schwerdtfeger, 1989) of roughness concentration (λ) ranging from 0.01-0.32. λ is a measure of canopy density and is defined as the total roughness frontal area per unit horizontal area (Raupach et al., 1991). It is approximately equal to $PAI/2$, where PAI is the plant area index or the cumulative element area including the stems and leaves per unit ground area. Even though this method is attractive and simple to incorporate in footprint analyses, the results are not available for mature tall forest canopies. This is why enhancement factors obtained over forest canopies from two other studies (Simpson et al., 1998; Denmead and Bradley, 1985) available in the literature are adopted. However the simple diffusive model of Cellier and Brunet (1992) is also used in the footprint solutions for comparison purposes and results are shown in Appendix-1. In the present study, I use the results

of Simpson et al. (1998), obtained over a mixed deciduous forest of 20 m tall and 3.6-leaf area index (LAI), to describe the vertical profiles of scalar diffusivity enhancement. This is reasonably similar to the Howland forest when the trees are with full leaves. In the Simpson et al. (1998) study, simultaneous eddy-covariance and flux gradient measurements of CO_2 were made at 4 heights within the RSL for unstable, near neutral and stable conditions. Linear fits of the experimental values of γ_h are incorporated in the footprint model (Figs 3.1–3.3). The eddy diffusivity for a scalar is then determined according to equation 3.12.

$$K_c^* = \frac{k u_* z}{\phi_h^*(z/L)} \tag{3.12}$$

where $\phi_h^*(z/L)$ is defined in (3.11). Equation 3.12 is used within the RSL and 3.10 is used for $z > z_*$. A comparison between the modeled enhancement factors (Cellier and Brunet, 1992) and experimental values obtained by Simpson et al. (1998) is shown in figure 3.4. Even though the model agrees well with the observed values above $1.7h$, significant differences can be found close to the canopy for all stability conditions. The difference can be attributed to the change in canopy height and density between the two studies.

Momentum diffusivity enhancement is assumed to be unity according to Denmead and Bradley (1985). They found no significant enhancement for momentum at 1.2h for a pine forest with LAI 4.4 m^2m^{-2}. This suggests no variation in wind speed from the logarithmic profile above the canopy.

3.3. Site characteristics

The analytical solution modified for the RSL is used for the CO_2 flux data obtained over the Howland *Ameriflux* site at Maine (Figs 3.5 and 3.6). The Howland Forest research site is located about 56 km north of Bangor at 45° 12' N, 68° 44' W in Maine, USA. The topography of

the region varies from flat to gently rolling, with a maximum elevation change of less than 68 m within 10 km. The canopy consists chiefly of spruce-hemlock-fir, aspen-birch and hemlock-hardwood mixtures (Hollinger at al., 1999). The dominant species in a 3 ha plot within 100 m from the flux tower are red spruce (41%), eastern hemlock (25%), other conifers (23%) such as balsam fir, white pine, northern white cedar, and hardwoods (11%) such as red maple and paper birch (Table. 3.1.). The average canopy height is 20 m and the flux measurements are made at a height of 30m. The leaf area index (LAI) of the canopy is approximately 5.3 m^2m^{-2}.

3.4. Model inputs and constants

The inputs for the model are friction velocity (u_*), Obukhov length (L), roughness length ($z_0 = 0.1 \times h$) and displacement height ($d = 0.7 \times h$). The depth of the roughness sub layer is taken as twice the canopy height from the ground (Simpson et al., 1998). The shape factor r is treated as constant and is equal to 1.0 for unstable, 1.5 for neutral and 2.0 for stable atmospheric conditions. The corresponding c values are 0.56 for unstable, 0.63 for neutral and 0.66 for stable atmospheric conditions. The values of r and c are based on direct observations of vertical profiles of scalar concentrations (Horst and Weil, 1992). The analytical solution for the shape factor r proposed by Gryning et al., (1983) and later experimentally verified by Finn et al., (1996) is not used in the present study. This is explained by the dependency of r on upwind distance, which is in contradiction with the basic assumption of horizontal homogeneity of turbulence in analytical solutions (Haenel and Grunhage, 1999). However, the analytical expression for r is used in the sensitivity analysis in section 3.5. The value of the wind coefficient α_u is taken as 1.7 from the results of Denmead and Bradley (1987) from the 20m tall and 4.9 LAI Uriarra forest in Australia. The selection of α_u value is justified by the similarity between the Uriarra forest and Howland site in both canopy height and LAI.

3.5. Results and discussions

3.5.1. Surface roughness

The analytical solution by Horst and Weil (1994) is originally developed for smooth surfaces where the ratio between the measurement height and surface roughness, z_m/z_0 , ranges from 100 to 300. For a case of $z_m/z_0 = 300$, Horst and Weil (1994) found that the measured flux is unaffected by the region directly beneath the flux sensor. They show the contribution from the near source region ($\bar{z}/z_m < 0.2$) to the measured flux to be negligibly small when measurements are made over smooth terrain. They also determined the upwind extent of this region as 3-6 z_m, less than 2 z_m and more than 10 z_m in neutral, unstable and stable conditions respectively. Their results suggest that the flux footprint from the region directly beneath the sensor can be assumed to be zero. However for measurements above rough forest canopies, it is impractical to obtain a z_m/z_0 value of 100 or more. Values between15 and 20 ($1.5h/0.1h$) are more common for rough surfaces. The relationship between the universal footprint function (Φ) and $\bar{z}/z_m$ for different values of z_m/z_0 for neutral stability are presented in figure 3.7. When $z_m/z_0 = 20$, the footprint flux from the near field is significantly higher compared to the case when $z_m/z_0 = 30$. This shows that for small values of z_m/z_0 (which refers to small measurement levels over rough surfaces) it is not desirable to assume the near field source contributions to be zero.

The integrated stability function calculated at z_0 ($\psi(z_0/L)$) is very small for small surface roughness values and is usually omitted from the logarithmic wind profile equation. Recently, Nakamura and Mahrt (2001) showed that $\psi(z_0/L)$ becomes significant for large surface roughness and small measurement heights. The term is positive in unstable conditions

and negative in stable conditions. The inclusion of the expression $\psi(z_0/L)$ increases the wind speed in unstable conditions and decreases it in stable conditions. In unstable cases, the buoyancy production of turbulence is high causing enhanced mixing and low wind speeds. The influence of this term in the footprint model for different surface roughness values is examined. For measurements above grasslands or short crop canopies ($z_0 \leq 0.1m$), the footprint flux distribution with upwind distance does not show much difference with the inclusion of $\psi(z_0/L)$ for unstable as well as stable conditions (Fig 3.8). Over tall canopies, the footprint maximum is overestimated in unstable conditions (Fig 3.9) and underestimated in stable conditions (Fig 3.10) by omitting the term, $\psi(z_0/L)$.

3.5.2. Observed wind profile over the Howland forest

The vertical profile of wind speed in the RSL is expected to vary from the logarithmic profile due to the increase in shear production. Due to the shortage of measurements in the RSL over tall canopies, footprint models generally use logarithmic wind profile in the RSL. In this section, we examine the sensitivity of the analytical solution to the vertical wind profile and compare the flux footprint distributions obtained for actual and logarithmic wind profiles. The vertical profile of wind speed over the Howland forest site is obtained from short-term micrometeorological measurements using a mini-SODAR and a tethered balloon system. The measurements were made in August 2000 and 2001. The mini-SODAR was placed on a 12 m high platform near the top of the canopy and approximately 20 – 30 m away from the eddy flux tower (Fig 3.11). The mini SODAR range was set to 100 m above the antenna with a vertical resolution of 5 m. The tethered balloon was launched from a small opening near the eddy flux sensor (Fig 3.12). It provided wind seed profile information up to approximately 150 m. Our aim is to find the flux footprint distributions for a realistic wind profile and compare the results

against those obtained using the logarithmic profile. The measurements for unstable cases ($0 > (z_m - d/L) > -1.0$) were averaged to obtain a mean wind profile, Obukhov length and friction velocity (Fig. 3.13). The values of the Obukhov length and friction velocity are obtained from the sonic anemometer. The figure.3.13 shows the average of 12 hourly mean cases. One observation from the tethered balloon for a similar stability and friction velocity is compared with the SODAR profile. The vertical profile obtained from the balloon is smoothed using adjacent averaging with 5 points. The logarithmic profile shown on fig. 3.13 is plotted using the average Obukhov length and friction velocity values obtained from the sonic anemometer measurements on the flux tower.

The footprint model was run for all three cases. The model is found to be very sensitive to wind profile. We know from (3.4) that the footprint flux is a function of wind speed through the term $\bar{u}(z_m)/U(\bar{z})$. A comparison of the slopes of the three profiles on fig 3.13 shows that the term $\bar{u}(z_m)/U(\bar{z})$ at the canopy top is highest for the logarithmic profile and lowest for the SODAR while the data obtained with the tethered balloon lies between the two. This difference can be seen on the footprint flux as the logarithmic wind profile gives the largest flux maximum and the tethersonde profile the smallest. Due to the shortage of good quality data, the above analysis was performed only for unstable cases. However these results show that the variation of the wind speed from the logarithmic values causes significant changes in the flux footprint. The results suggest to use observed wind profiles in the footprint model whenever available.

3.5.3. Exponential wind profile

It is well known that the logarithmic wind equation often underestimates the wind profile within the crown region of the canopy (Raupach et al., 1986; Shaw et al., 1988; Amiro, 1990). In this region, approximately from 0.7h to 1.0h, the exponential wind profile (3.8) is often used.

The figure 3.15 shows a comparison between the logarithmic and exponential profiles for three stability conditions. It can be seen that the exponential wind equation gives non-zero wind speeds inside the canopy where the logarithmic profile decreases to near-zero values. In this section, the influence of this increased wind speed inside the canopy, on flux footprint estimations above the canopy is examined. The footprint distributions show a significant difference up to a downwind distance of 10 m in unstable, 40 m in neutral and 500 m in stable conditions (Fig 3.16). The flux footprint decreases with an increase in wind speed. Correspondingly, the footprint envelope expands in higher wind speeds. It can be assumed that an increased wind speed advects the plume in the along wind direction resulting in minimum vertical dispersion. This advection effect on the plume also increases the extent of the fetch. This relation between the vertical flux or concentration and the horizontal wind speed is inherent in the analytical dispersion equations and has been carried over to the footprint model as Horst and Weil (1992) adopts Pasquill's (1974) original solution to the vertical dispersion.

These results illustrate the importance of wind speed inside the canopy on flux footprint estimations for sources above or at the tree height and suggest the use of a more realistic wind profile than the logarithmic equation in the crown space. In analytical footprint solutions, though the plume height is always above the canopy, the plume speed is calculated as the wind speed at a fraction (0.56) of the plume height. Hence the model requires inside-canopy wind speed values. In section 3.5.1 we have seen that for measurements above a rough surface, the contribution from the upwind distance directly beneath the sensor is significant and often maximum. This follows that plume speed calculations near the sensor influence the model results considerably and hence an error in this can cause significant changes in the flux maximum. I therefore recommend using a realistic wind speed for these highly sensitive region near the sensor.

3.5.4. Influence of RSL on footprint

In this section, I discuss the footprint flux distributions obtained by examining the behavior of the analytical model when modified to include the RSL. Prior to the results and discussion, I summarize the modifications employed in the original Horst and Weil (1994) model from all previous sections in this chapter.

1) The flux footprint is not assumed to be zero in the first few meters upwind of the sensor. The flux footprint is calculated at each upwind distance at an interval of 1m, the first upwind distance being 1 m away from the flux sensor.
2) The integrated stability function evaluated at z_0, $\psi\left(z_0/L\right)$, is used in the logarithmic wind equation for all stabilities.
3) For the region $d < z \le h$, the exponential wind profile is used instead of the logarithmic one.
4) The momentum diffusivity within the RSL is assumed to be unity leading to a profile which remains logarithmic throughout the RSL.
5) The eddy diffusivity for scalars is enhanced based on observations of Simpson et al. (1998). Three different profiles for the enhancement factor are used for unstable, stable and near neutral conditions.

The measure of vertical dispersion in the analytical model is the mean plume height expressed as $\bar{z}$. The crosswind-integrated footprint is a function of this single variable ($\bar{z}/z_m$) and the dependence of footprint on stability, downwind distance and surface roughness are contained in this. Figure 3.17 shows the variation of mean plume height with upwind distance for unstable, near neutral and stable conditions. It can be seen that a plume released into the turbulent RSL rises faster than it's counterpart in the ISL. For unstable cases, in the presence of

thermally generated turbulence, the plume escapes from the RSL at a distance of approximately $2h$ from the sensor while in neutral and in stable cases it travels horizontally in the RSL for a longer distance. It can be seen that the horizontal gradient of the plume height ($d\bar{z}/dx$) is slightly greater when the RSL parameterization is employed. This effect is a clear manifestation of the increased eddy diffusivity used in the model.

The flux footprint maximum increases with the inclusion of the RSL parameterization in all three stability conditions (Fig 3.18). The difference in flux footprint is clearly seen up to 0.5h in unstable cases, 2.5h in neutral and more than 5h in stable conditions for both the measurement heights presented. In unstable and neutral cases, the flux footprint distribution is slightly contracted when the RSL turbulent enhancement is employed. The flux footprint is increased by approximately 25% in unstable and neutral cases and by 60% in stable cases by the modifications adopted (Fig 3.18). It can be assumed that the plume emanating from the sources close to the tower base is transported vertically and immediately reaches the vicinity of the sensor due to the high turbulence observed in the RSL. The cumulative footprint (Fig 3.19) shows the percentage contributed to the flux with upwind distance. The footprint envelope corresponding to 35-40% flux contribution shows a slight contraction in the presence of RSL turbulence. This is approximately 10m in unstable, 100m in near neutral and more than 100m in stable conditions.

In section 3.5.3, I pointed out the importance of exponential wind profile in the analytical footprint model. The use of such a non-zero wind speed at the displacement height is expected to enhance the horizontal advection of the plume, and thereby decreasing vertical dispersion effects in the model. The above results show that the inclusion of RSL turbulence parameterization leads to an increase in mixing dominating over the effect of wind speed.

Figure 3.20 shows the variation of flux maximum with stability. The modified model shows a profile similar to that of the original Horst and Weil (1994) model except that the flux maximum is higher in the RSL. The flux maximum decreases with an increase in measurement height in both cases (Fig 3.21), with slightly higher fluxes in the RSL case. However it has to be noted that the difference between both models remains significant even for measurement heights above the RSL ($z_m/h > 2.0$). The extent of the upwind distance corresponding to 50, 80 and 90% of the total flux contribution is shown with respect to stability in figure 3.22. The behavior of the fetch with stability is similar in both models as the footprint envelope expands as the atmosphere goes from unstable to stable cases. The effect of enhanced turbulence is most pronounced within the 50% footprint envelope as we observe a slight contraction in fetch when the modified model is used.

3.5.5. Sensitivity analysis

In this section, the sensitivity of the modified model for three important empirical parameters is investigated. They are the exponential wind coefficient α_u, shape factor r and the constant c used in the calculation of the mean plume speed. For each parameter, a value is selected based on the available data in the literature and is fixed as default in the present sensitivity analysis. An increase in α_u causes a decrease in wind speed and an increase in flux footprint (Fig 3.23). The sensitivity of the model to α_u is negligible as a 20% change from its default value (α_u = 1.7) produces only less than 5% change in flux footprint. The change in the shape factor by approximately 13% in near-neutral conditions produces very small changes in flux maximum and fetch (Fig 3.24) whereas it found more sensitive to r in unstable and stable cases (Figs 3.25 and 3.26). The use of Finn et al. (1996) analytical formulations of r causes an increase in flux maximum in unstable cases and a decrease in stable cases. The sensitivity of the

model to c is small in neutral and unstable cases while in stable conditions, a change by 3% causes approximately 6% difference in the flux footprint maximum (Figs 3.27, 3.28 and 3.29). The use of empirical values of c from Finn et al. (1996) increases the flux maximum in unstable case and decreases in stable conditions.

3.5.6. Comparison with Lagrangian model

The suggested modifications are evaluated against predictions from a Lagrangian model (Leclerc and Thurtell, 1990). The wind profile obtained from the SODAR (Fig 3.13) is used in both the analytical and Lagrangian models. The analytical model carries the RSL parameterizations of the eddy diffusivity discussed in section 3.2.2 while the Lagrangian model uses a realistic σ_w profile obtained from the SODAR (Fig 3.30). The σ_w and wind speed profiles are averages of 12 one hour cases with the stability range of $-0.5 < (z_m - d/L) < -0.1$. The values of $(z_m - d)/L$ and u_* used in both models are –0.3 and 0.64 respectively. Results compare well against one another in terms of footprint. For the parameters used, there is however a clear difference in the flux footprint up to an upwind distance of approximately1h.

3.6. Conclusions

The present study attempts to modify a widely used analytical model for flux footprint estimations over tall rough surfaces such as forests. Simple empirical equations are used to simulate the enhanced turbulence in the RSL above forest canopies based on prior observations. The main findings are the following. A summary on the modifications employed in the original model and corresponding results is given in Table 3.2.

1) The flux maximum always occurs directly beneath the flux tower for small measurement heights above rough surfaces. This is significant given the usual practice of assuming the contribution from sources close to the tower as zero.

2) It is important that the integrated stability function evaluated at z_0 ($\psi(z_0/L)$) be included in the wind profile for measurements made above rough canopies. The omission of this term results in underestimation of flux in stable and overestimation in unstable conditions.

3) The inclusion of RSL turbulence in the footprint model produces an increase in flux maximum for all stabilities. As a result of increased dispersion in the RSL, the footprint envelope of 50% contribution contracts.

4) The flux footprint is found to be less sensitive to the empirical constant (α_u) describing the wind speed in the canopy crown space.

5) The modified model is evaluated against results obtained from a Lagrangian simulation using a realistic σ_w and wind profiles and found to agree reasonably well.

The model parameterizations are based on observations from two similar forest canopies. I have selected data from forests with characteristics that of Howland forest in Maine. The comparison between forests is logical, given that two key parameters such as mean tree height (h) and leaf area index (LAI) are directly comparable. It is particularly difficult to obtain information about plant area index or the mean tree spacing. Such information would provide more accurate comparisons between canopy types as pointed out by Cellier and Brunet (1992). Another difficulty is the evident contradictions observed in the available data in the literature. For instance, the scalar eddy diffusivity enhancements I adopted in the present study (Simpson et al.,1998) are substantially small when compared to previous results by Thom et al., 1975, Garrat (1978), Raupach (1979) and Cellier and Brunet (1992). Nevertheless the high resolution of the gas analyzer used for the measurement of CO_2 concentration in Simpson et al., 1998 provides a more precise comparison between measured and calculated fluxes. In this study, I have used

different vertical profiles of enhancement factor for three stability conditions. Discrepancies exist in the dependence of enhancement factor on stability. Garratt (1980) and Cellier Brunet (1992) find no apparent evolution of γ_h with instability while Raupach (1979) and Chen and Schwerdtfeger (1989) found an increase of γ_h with instability. No clear picture has evolved on the variation of enhancement factors with stability. A direct comparison between the available data on the RSL is not possible as the canopy height and type are different in each study. Similar challenges are present in the selection of the RSL depth and on its possible evolution with instability. Some studies point out that the anomalies in the RSL vanishes by adjusting the zero plane displacement height or by introducing separate displacement heights for momentum and scalar properties (Hicks et al., 1979). All these factors further compound the difficulties in modeling RSL adequately.

Future work in this field should focus on the application of two-dimensional footprint models considering the spatial variability in species composition and canopy density encountered in natural forest ecosystems (Baldocchi, 1997; Rannik et al., 2000, 2003; Kljun et al., 2002).The assumption of horizontally homogeneous turbulence above a forest canopy is an oversimplification of the problem and often leads to erroneous conclusions (Schmid and Lloyd, 1999). Further studies should also be directed toward the development of integrated footprint algorithms as part of signal processing package in the field during long-term measurement campaigns. Accurate field measurements in the RSL over a wide range of canopies are also required to improve parameterization efforts.

References

Amiro, B.D., 1990. Drag coefficients and turbulence spectra within three boreal forest canopies. Boundary-Layer Meteorol. 52, 227–246.

Baldocchi, D.D., Hicks, B.B., Meyers, T.P., 1988. Measuring biosphere-atmosphere exchanges of biologically related gases with micrometeorological methods. Ecology. 69,1331-1340.

Baldocchi, D.D., Valentini, R., Running, S., Oechel, W., and Dahlman, R. 1996. Strategies for measuring and modelling carbon dioxide and water vapor fluxes over terrestrial ecosystems. Global Change Biology. 2,159-168.

Baldocchi, D.D., 1997. Flux footprints within and over forest canopies. Boundary-Layer Meteorol. 85, 273–292.

Baldocchi, D.D., Finnigan, J., Wilson, K., Paw, U.K.T., Falge, E., 2000. On measuring net ecosystem carbon exchange over tall vegetation on complex terrain. Boundary Layer Meteorol. 96, 257–291.

Cellier, P., Brunet, Y., 1992. Flux gradient relationships above tall plant canopies. Agric. For. Meteorol. 58, 93–117.

Chatwin, P.C., 1968. The dispersion of a puff of passive contaminant in the constant stress region. Quart. J. Roy. Meteorol. Soc. 94, 401–411.

Chen, F., Schwerdtfeger, P., 1989. Flux-gradient relationships for momentum and hear over a rough natural surface. Quart. J. Roy. Meteorol. Soc. 115, 335–352.

Cionco, R.M., 1965. A mathematical model for air flow in a vegetated canopy. J. Appl. Meteorol. 4, 517

Cooper, D.I., Eichinger, W.E., Archuleta, J., Hipps, L., Kao, J., Leclerc, M.Y., Neale, C.M., Prueger, J., 2003. Spatial source-area analysis of three dimensional moisture fields from lidar, eddy covariance and a footprint model. Agric. For. Meteorol. 114, 213–234.

Denmead, O.T., Bradley, E.F., 1985. Flux-gradient relationships in a forest canopy. in: B.A. Hutchison and B.B. Hicks (eds), The forest-atmosphere interaction. Reidel, Dordrecht, pp. 421–442.

Denmead, O.T., Bradley, E.F., 1987. On scalar transport in plant canopies. Irrig. Sci. 8, 131–149.

Denning, A.S., Random, D. A., Collatz, G. J., Sellers, P.J., 1996. Simulations of terrestrial carbon metabolism and atmospheric CO_2 in a general circulation model. Part 2: Simulated CO_2 concentrations. Tellus 48B, 543–567.

Falge, E., Baldocchi, D., Tenhunen, J., Aubinet, M., Bakwin, P., Berbigier, P., Bernhofer, C., Burba, G., Clement, R., Davis, K.J., Elbers, J.A., Goldstein, A.H., Grelle, A., Granier, A., Guðmundsson, J., Hollinger, D., Kowalski, A.S., Katul, G., Law, B.E., Malhi, Y., Meyers, T., Monson, R.K., Munger, J.W., Oechel, W., Paw U, K.T. Pilegaard, K., Rannik, Ü., Rebmann, C., Suyker, A., Valentini, R., Wilson, K., Wofsy, S., 2002. Seasonality of ecosystem respiration and gross primary production as derived from FLUXNET measurements. Agric. For. Meteorol. 113, 53–74.

Finn, D., Lamb, B., Leclerc, M.Y., Horst, T.W., 1996. Experimental evaluation of analytical and Lagrangian surface-layer flux footprint models. Boundary-Layer Meteorol., 80, 283–308.

Garratt, J.R., 1978. Flux profile relations above tall vegetation. Quart. J. Roy. Meteorol. Soc. 104, 199–211.

Garratt, J.R., 1980. Surface influence upon vertical profiles in the atmospheric near-surface layer. Quart. J. Roy. Meteorol. Soc. 106, 803–819.

Gryning, S.E., van Ulden, A.P., Larsen, S.E., 1983. Dispersion from a continuous ground-level source investigated by a K model. Ouart. J. Roy. Meteorol. Soc. 109, 355–364.

Haenel, H.-D., Grunhage, L., 1999. Footprint analysis: A closed analytical solution based on height-dependent profiles of wind speed and eddy viscosity. Boundary-Layer Meteorol. 93, 395–409.

Hick, B.B., Hess, G.D., Wesely, M.L., 1979. Analysis of flux-profile relationships above tall vegetation- an alternate view. Quart. J. Roy. Meteorol. Soc. 105, 1074–1077.

Hollinger, D.Y., Kelliher, F.M., Byers, J.N., Hunt, J.E., McSeveny, T.M., Weir, P.L., 1994. Carbon dioxide exchange between an undisturbed old-growth temperate forest and the atmosphere. Ecology 75, 134–150

Hollinger, D.Y., Goltz, S.M., Davidson, E.A., Lee, J.T., Tu, K., Valentine, H.T., 1999. Seasonal patterns and environmental control of carbon dioxide and water vapour exchange in an ecotonal boreal forest. Global Change Biology. 5, 891–902.

Horst, T.W., Weil, J.C., 1992. Footprint estimation for scalar flux measurements in the atmospheric surface layer. Bounday-Layer Meteorol. 59, 279–296.

Horst, T.W., Weil, J.C., 1994. How far is far enough?: The fetch requirements for micrometeorological measurements of surface fluxes. J. Atmos. Ocean. Tech. 11, 1018–1026.

Hsieh, C., Katul, G., Chi, T., 2000. An approximate analytical model for footprint estimation of scalar fluxes in thermally stratified atmospheric flows. Advances in Water Resources. 23, 765–772.

Kljun, N., Rotach, M.W., Schmid, H.P., 2002. A three-dimensional backward Lagrangian footprint model for a wide range of boundary-layer stratifications. Boundary-Layer Meteorol. 103**,** 205–226.

Kormann, R., Meixner, F.X., 2001. An analytical footprint model for non-neutral stratification. Boundary-Layer Meteorol. 99, 207–224.

Leclerc, M.Y., Thurtell, G.W., 1990. Footprint prediction of scalar fluxes using a Markovian analysis. Boundary-Layer Meteorol. 52, 247–258.

Leclerc, M.Y., Shen, S., Lamb, B., 1997. Observations and large-eddy simulation modeling of footprints in the lower convective boundary layer. J. Geophys. Res.102, 9323–9334.

Leclerc, M.Y., Karipot, A., Prabha,T., Allwine, G., Lamb, B., Gholz, H.L., 2003a. Impact of non-local advection on flux footprints over a tall forest canopy: a tracer flux experiment. Agric. For. Meteorol. 115, 17–34.

Leclerc, M.Y., Meskhidze, N., Finn, D., 2003b. Comparison between measured tracer fluxes and footprint model predictions over a homogeneous canopy of intermediate roughness. Agric. For. Meteorol. 117, 145–158.

Lee, X., 2003. Fetch and footprint of turbulent fluxes over vegetation stands with elevated sources. Boundary-Layer Meteorol. 107, 561–579.
Nakamura, R., Mahrt, L., 2001. Similarity theory for local and spatially averaged momentum fluxes. Agric. For. Meteorol. 108, 265–279.

Pasquill, F., 1974. Atmospheric diffusion. John Wiley, Sussex, England.

Rannik, U., Aubinet, M., Kurbanmuradov, O., Sabelfeld, K.K., Markkanen, T., Velsa, T., 2000. Footprint analysis for measurements over a heterogeneous forest. Boundary-Layer Meteorol. 97, 137–166.

Rannik, U., Markkanen, T., Raittila, J., Hari, P., Vesala, T., 2003. Turbulence statistics inside and over forest: Influence on footprint prediction. Boundary-Layer Meteorol. 109, 163–189.

Raupach, M.R., 1979. Anomalies in flux-gradient relationships over forest. Boundary-Layer Meteorol. 16, 467–486.

Raupach, M.R., Coppin, P.A., Legg, B.J., 1986. Experiments of scalar dispersion within a model plant canopy. Part I. The turbulence structure. Boundary-Layer Meteorol. 35, 21–52.

Raupach, M.R., Antonia, R.A., Rajagopalan, S., 1991. Rough-wall turbulent boundary layers. Appl. Mech. Rev. 44, 1–25.

Schmid, H.P., 1994. Source areas for scalars and scalar fluxes. Boundary-Layer Meteorol. 67, 293–318.

Schmid, H.P., Lloyd, C.R., 1999. Spatial representativeness and location bias of flux footprints over inhomogeneous areas. Agric. For. Meteorol. 93, 195–209.

Schuepp, P.H., Leclerc, M.Y., Macpherson, J.I., Desjardins, R.L., 1990. Footprint predictions for scalar fluxes from analytical solutions of the diffusion equation. Boundary-Layer Meterol. 50, 355–373.

Shaw , R.H., Silversides, R.H., Thurtell, G.W., 1974. Some observations of turbulence and turbulent transport within and above plant canopies. Boundary-Layer Meteorol. 5, 429–449.

Shaw, R.H., Hartog, G.D., Neumann, H.H., 1988. Influence of foliar density and thermal stability on profiles of Reynolds stress and turbulence intensity in a deciduous forest. Boundary-Layer Meteorol. 45, 391–401.

Simpson, I.J., Thurtell, G.W., Neumann, H.H., Hartog, G.D., Edwards, G.C., 1998. The validity of similarity theory in the roughness sublayer above forests. Boundary-Layer Meteorol. 87, 69–99.

Thom, A.S., Stewart, J.B., Oliver, H.R., Gash, J.H.C., 1975. Comparison of aerodynamic and ennrgy budget estimates of fluxes over a pine forest. Quart. J. Roy. Meteorol. Soc. 101, 93–105.

Van Ulden, A.P., 1978. Simple estimates for vertical diffusion from sources near the ground. Atmospheric Environment. 12, 2125–2129.

Wilson, J.D., Ward, D.P., Thurtell, G.W., Kidd, G.E., 1982. Statistics of atmospheric turbulence within and above a corn canopy. Boundary-Layer Meteorol. 24, 495–519.

Appendix 1

A simple diffusive model for enhancement factors ($\gamma_{m,h}$) proposed by Cellier and Brunet (1992) is used in the analytical footprint solution for the RSL for comparison. The eddy diffusivities for momentum and scalar ($K_{m,h}$) are modeled based on values obtained from measurements in the RSL ($K^*_{m,h}$). The enhanced eddy diffusivities are given by

$$K^*_{m,h} = \frac{ku_* z}{\phi^*_{m,h}(z/L)} \qquad \text{(A1.1)}$$

Details of the analysis can be found in section 3.2. The flux footprint is found only for unstable and near-neutral cases as the modified empirical stability functions are available for these cases. Figure A1.1 shows the flux footprint distributions with respect to upwind distance. The inclusion of RSL turbulent effects increases the flux maximum in all cases. The influence of RSL is more pronounced when the Cellier and Brunet (1992) model is used for the RSL turbulent parameterization (Figs. 3.18 and A 1.1). This is caused by higher values of γ_h in Cellier and Brunet (1992). Figure A1.2 shows the behavior of the flux maximum with stability. The flux maximum is more than double with the inclusion of RSL. The difference in flux maximum between the two models reduces as the measurement height increases within the RSL (Figure A1.3). Figure A1.4 shows the variation of the upwind distance corresponding to the maximum flux ($x_{\max}$) with respect to measurement height. The influence of the RSL is not reflected on the $x_{\max}$ when measurement height is very close to the canopy ($z_m < 1.5h$). The inclusion of RSL shifts $x_{\max}$ to distances closer to the tower and this is evident when $z_m > 1.5h$. This implies a contraction in the flux footprint envelope in the presence of a turbulent RSL. The model is examined for its sensitivity for the empirical constant η, which determines the

dependency of the enhancement factor on canopy density (Figure A1.5). The flux maximum values remain the same for changes in η and the corresponding upwind distance shows slight variations (<1.0%). In general the parameter η can be considered not sensitive to the footprint solution proposed here.

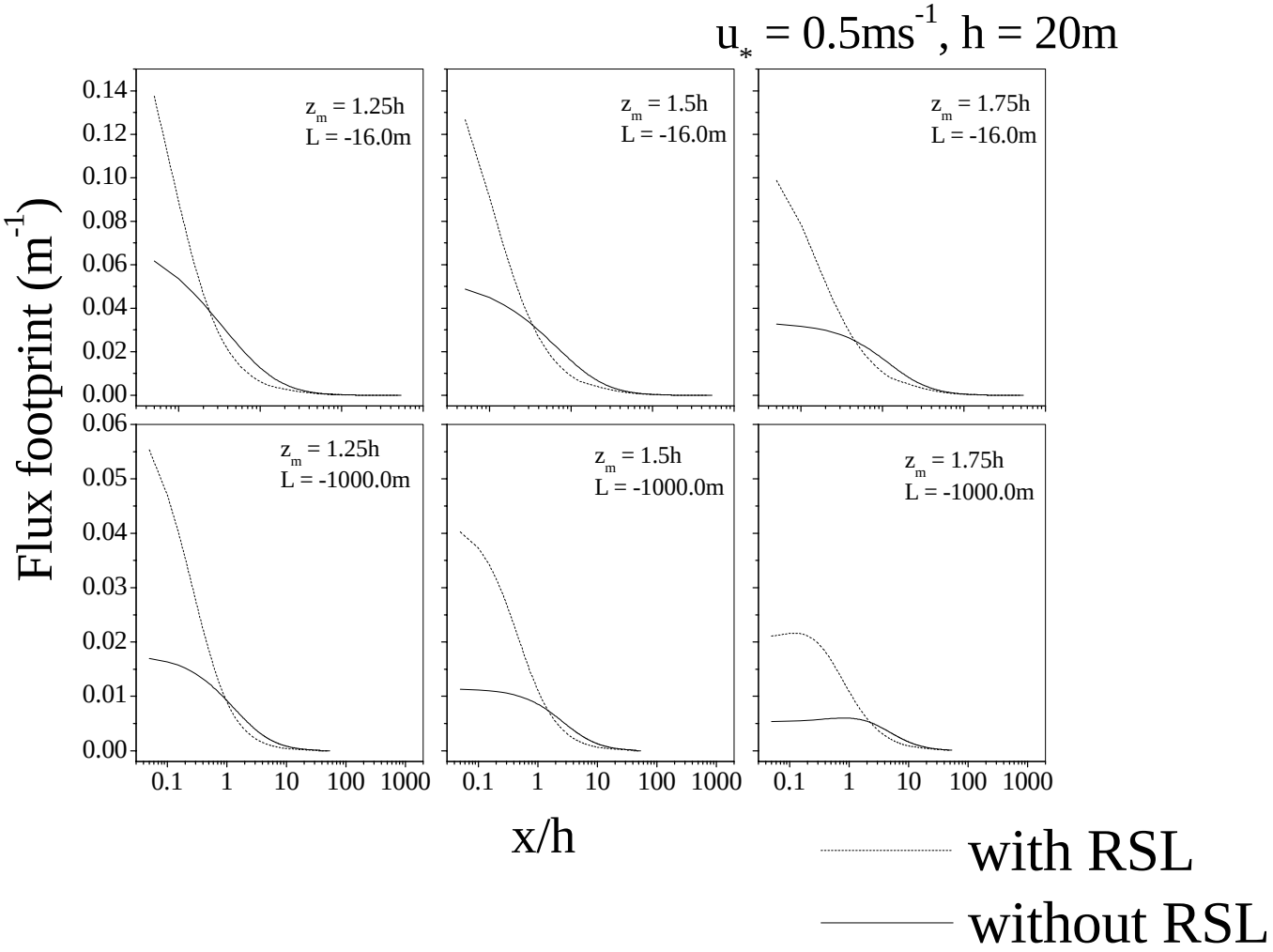

Figure A1.1. Flux footprint distributions with upwind distance with and without RSL effects

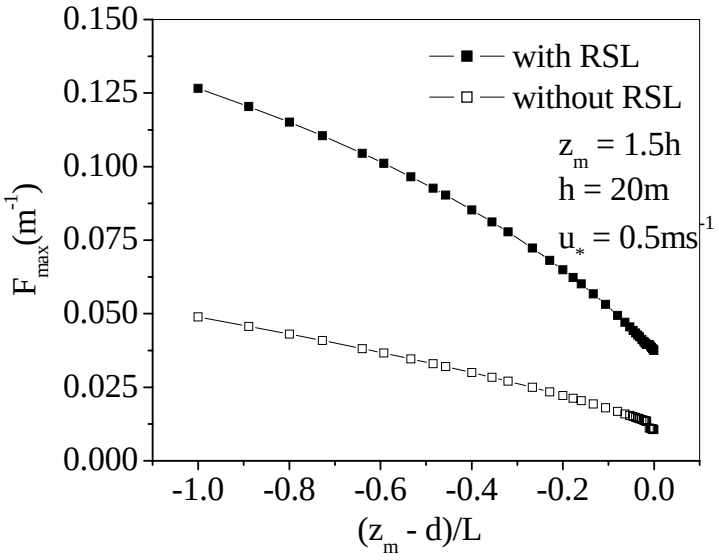

Figure A1.2. Variation of flux maximum with stability with and without RSL turbulent parameterization.

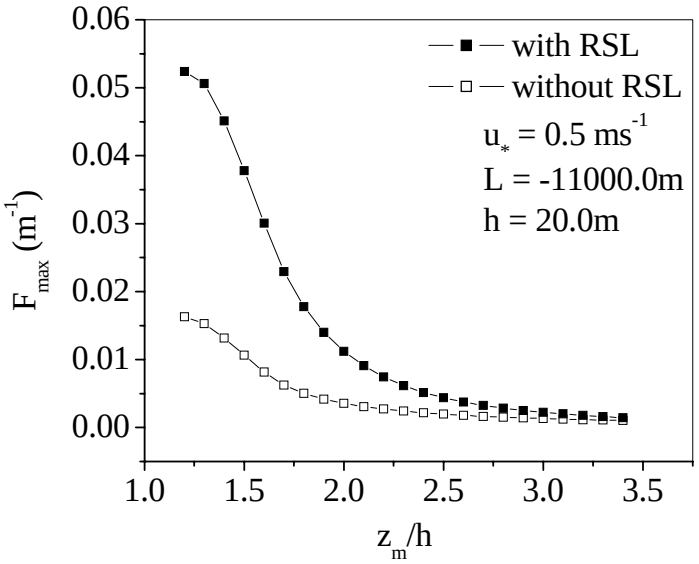

Figure A1.3. Variation of flux maximum with measurement height with and without RSL turbulent parameterization.

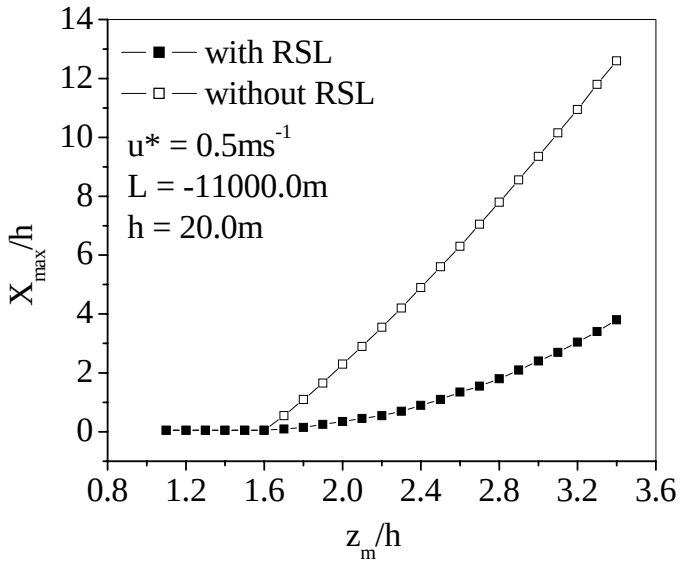

Figure A1.4. Variation of the upwind distance corresponding to the flux maximum with measurement height with and without RSL turbulent parameterization.

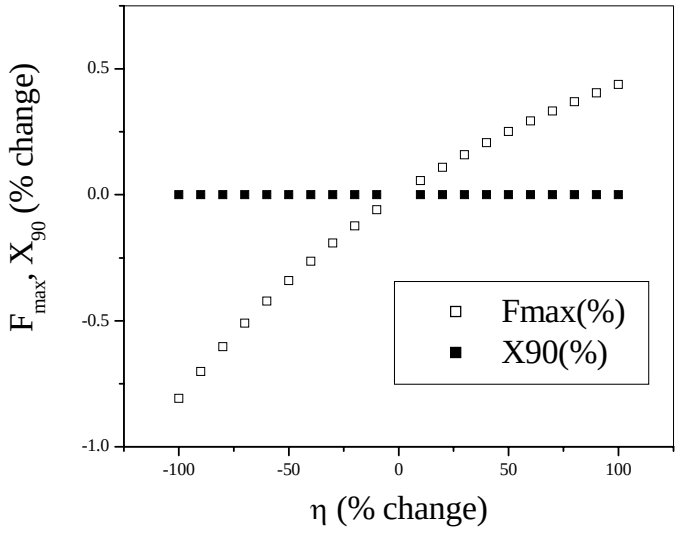

$(z_m - d)/L = -1.0$, $u_* = 0.5ms^{-1}$
default $\eta = 0.45$

Figure A1.5. Percent change in flux maximum and corresponding upwind distance with respect to change in the empirical constant η

Table 3.1. Tree density and basal area at the Howland site (Source: Hollinger et al., 1999)

Species	**Density (stems ha^{-1})**	**% of total living**	**Basal area (m^2 ha^{-1})**	**% of total living**
Picea rubens	816	40.5	14.20	44.1
Tsuga canadensis	509	25.3	8.45	26.2
Hardwoods	224	11.1	2.67	8.3
Thuja occodentalis	201	9.9	3.29	10.2
Abies balsamea	194	9.6	0.74	2.3
Pinus strobus	64	3.2	2.76	8.6
Total living	2017	100	32.2	100
Standing dead	585	-	4.7	-
Total	2602	-	36.9	-

Table 3.2. Summary of major results

No.	**Modification**	**Result**
1	Applied over a rough surface	Contribution from sources located close to the sensor can not be neglected
2	Included the integrated stability function evaluated at surface roughness in the logarithmic wind profile	Peak flux decreases in unstable conditions and increases in stable conditions compared to the original model results.
3	Used the exponential wind profile in the crown space of the canopy	Peak flux decreases and the footprint envelope expands.
4	Used enhanced eddy diffusivity in the RSL	Peak flux increases and the footprint envelope contracts.

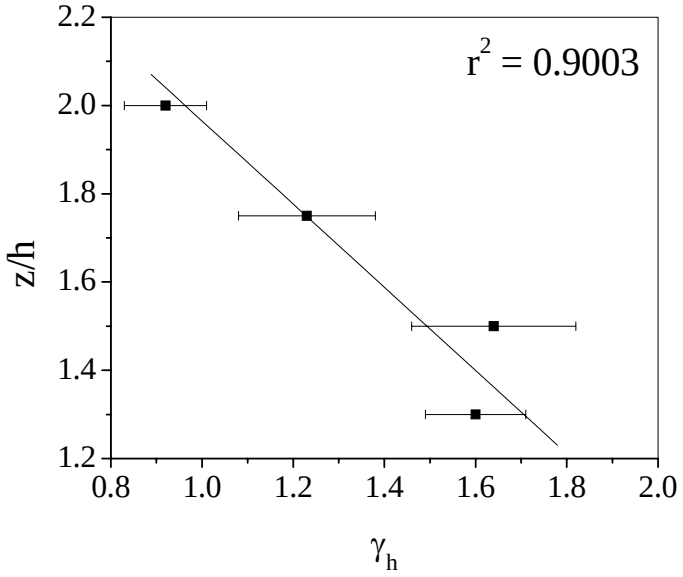

Figure 3.1. Vertical profile of scalar diffusivity enhancement in unstable conditions $(-2 < (z_m - d)/L \leq -0.05)$ from Simpson et al., 1999

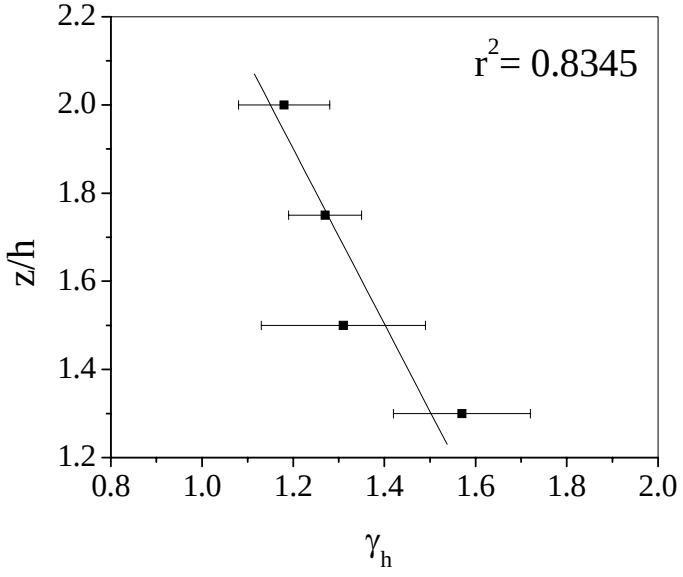

Figure 3.2. Vertical profile of scalar diffusivity enhancement in neutral conditions $(-0.05 < (z_m - d)/L \leq 0.05)$ from Simpson et al., 1999.

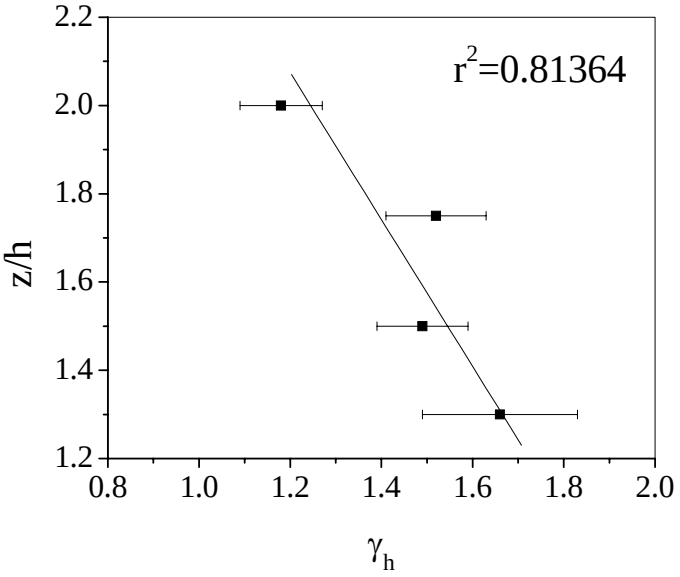

Figure 3.3. Vertical profile of scalar diffusivity enhancement in stable conditions ($0.05 < (z_m - d)/L < 0.4$) from Simpson et al., 1999.

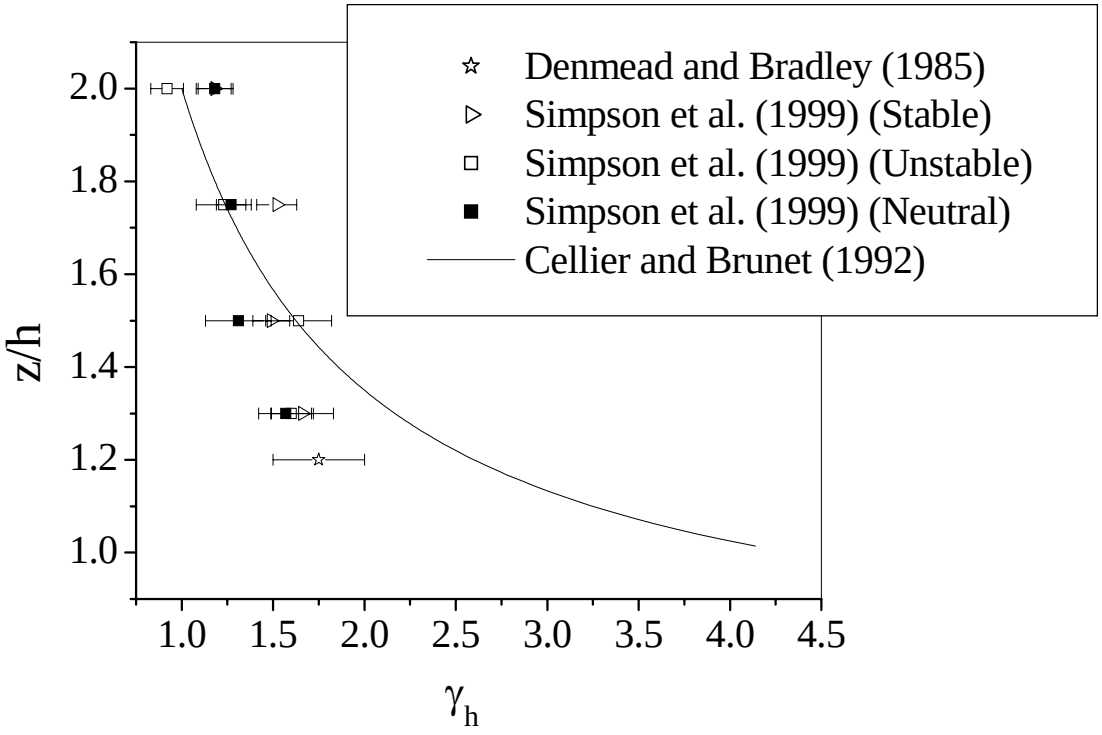

Figure 3.4. Comparison of scalar eddy diffusivity enhancement factors reported in the literature

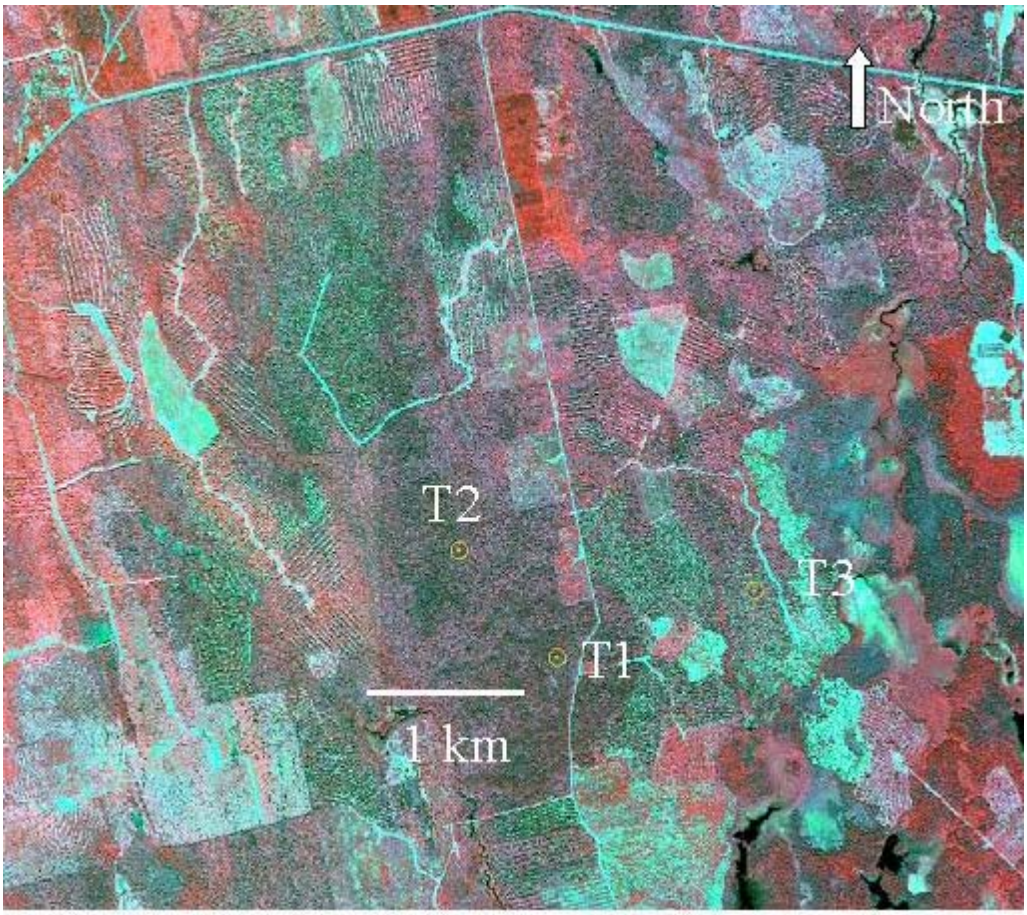

Figure 3.5. Satellite image of the Howland *Ameriflux* site. T1, T2 and T3 are eddy-flux sensor towers. This study uses the data obtained from tower T1. The bright red areas are generally hardwoods and the darker green areas are softwoods. Ground is seen in lightly green color. The long strips visible on the NW are due to the strip cutting.

Figure 3.6. Eddy-covariance flux measurement system at Howland, Maine
Source: http://www.daac.ornl.gov/FLUXNET/fluxnet.html

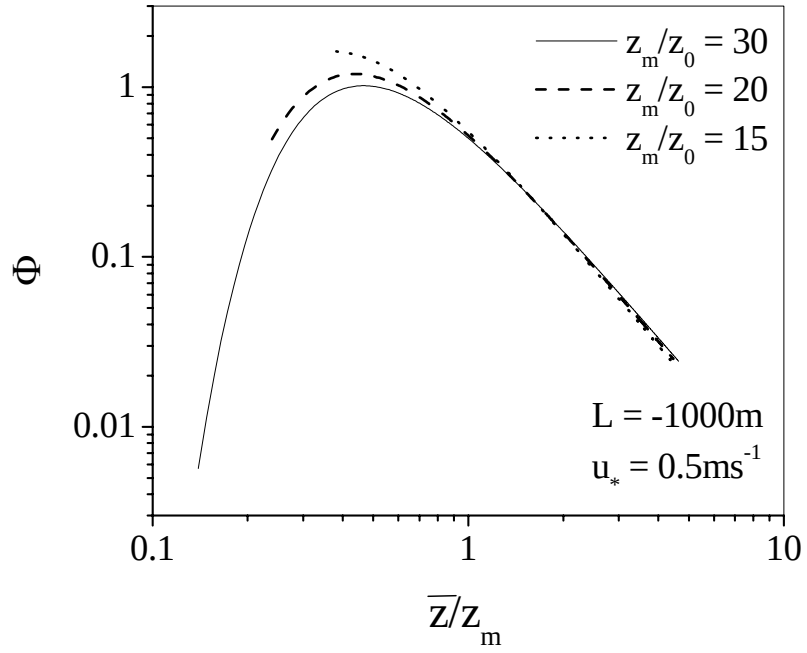

Figure 3.7. Variation of the universal footprint function (Φ) with normalized plume height

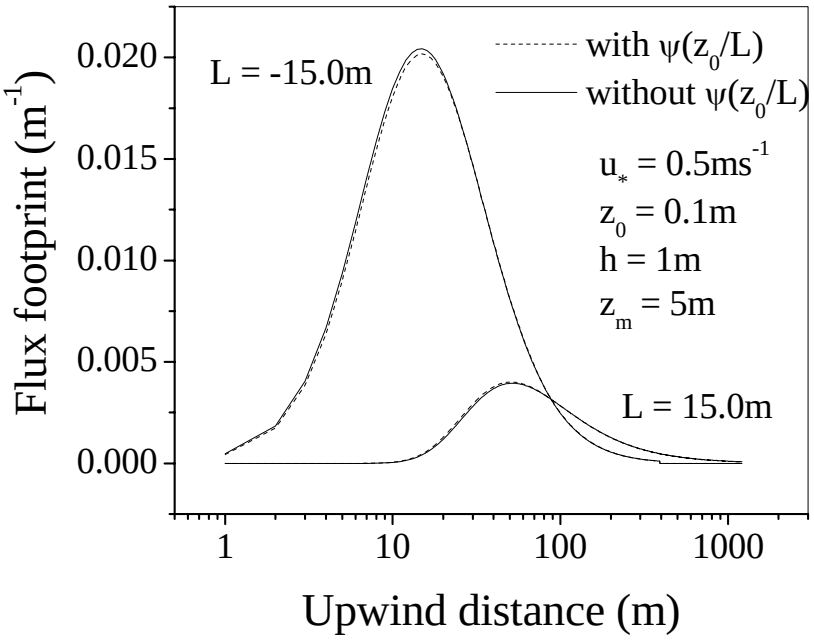

Figure 3.8. Influence of $\psi(z_0/L)$ on flux footprint over smooth terrain in stable and unstable conditions

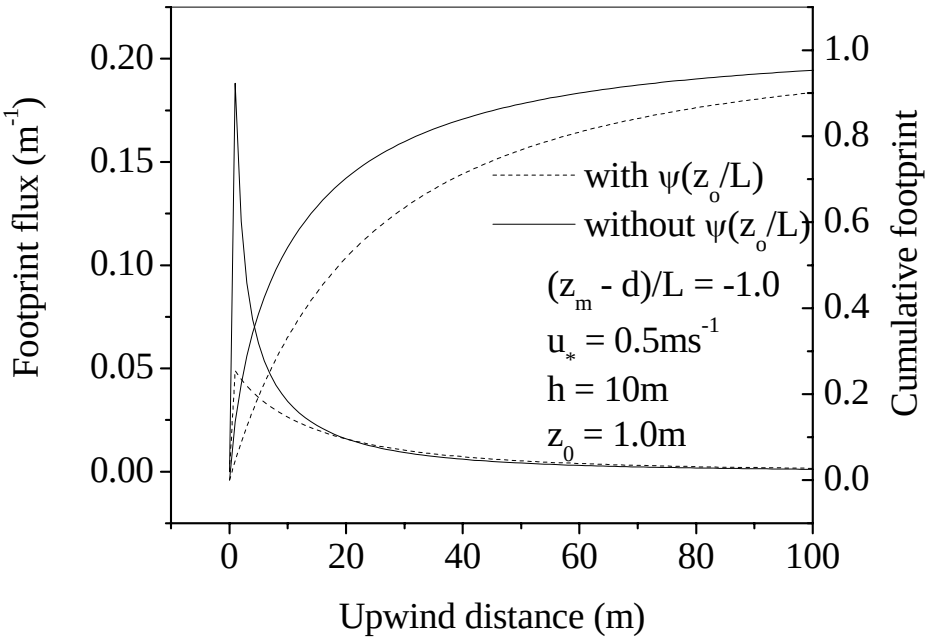

Figure 3.9. Influence of $\psi(z_0/L)$ on flux footprint over rough terrain (unstable case)

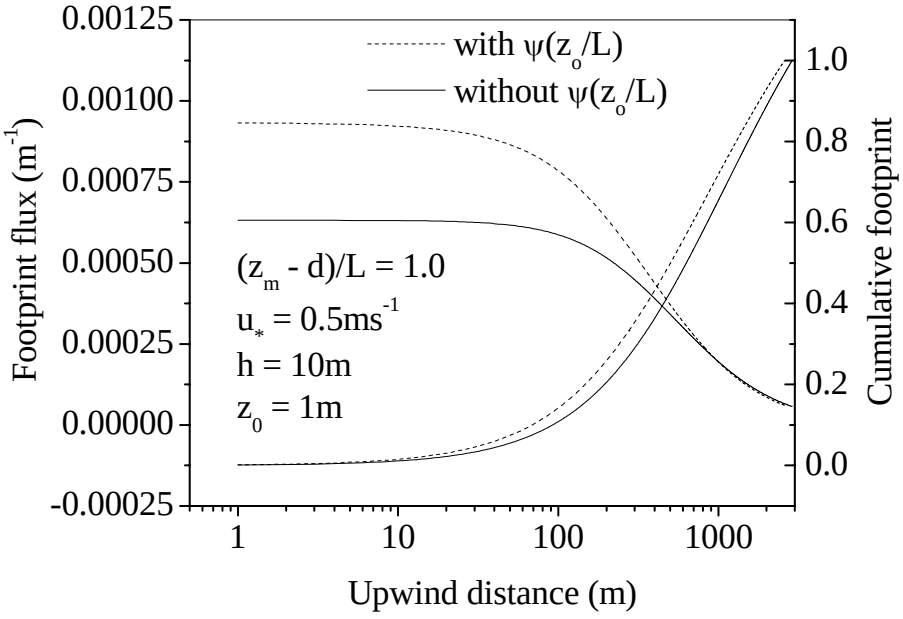

Figure 3.10. Influence of $\psi(z_0/L)$ on flux footprint over rough terrain (stable case)

Figure 3.11. Mini-SODAR installed at treetop

Figure 3.12. Tethered balloon being filled with Helium.

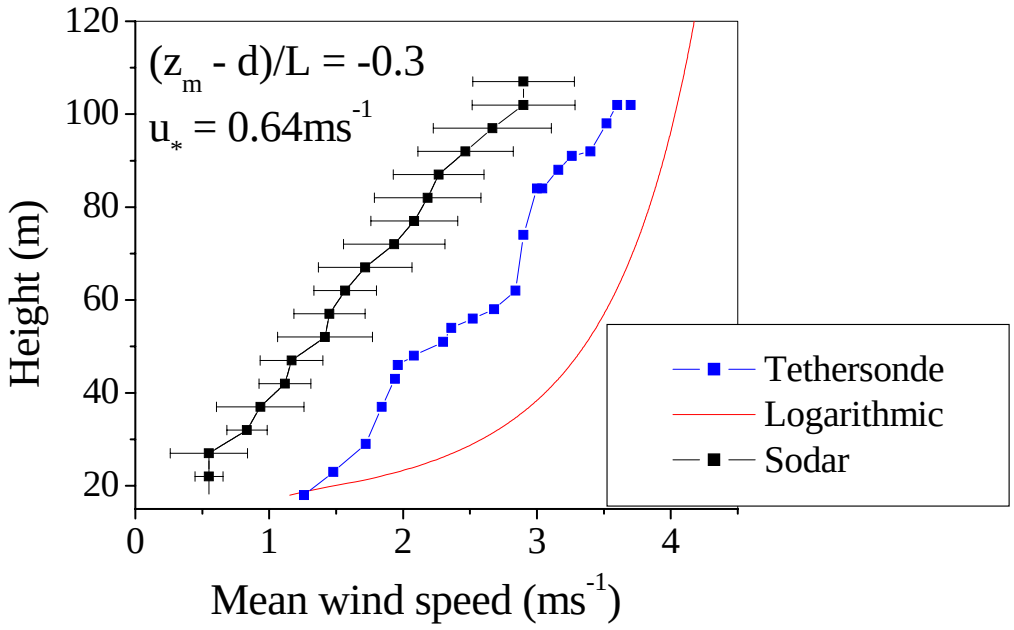

Figure 3.13. Comparison between the wind profiles obtained from the SODAR, tethersonde and the logarithmic profile.

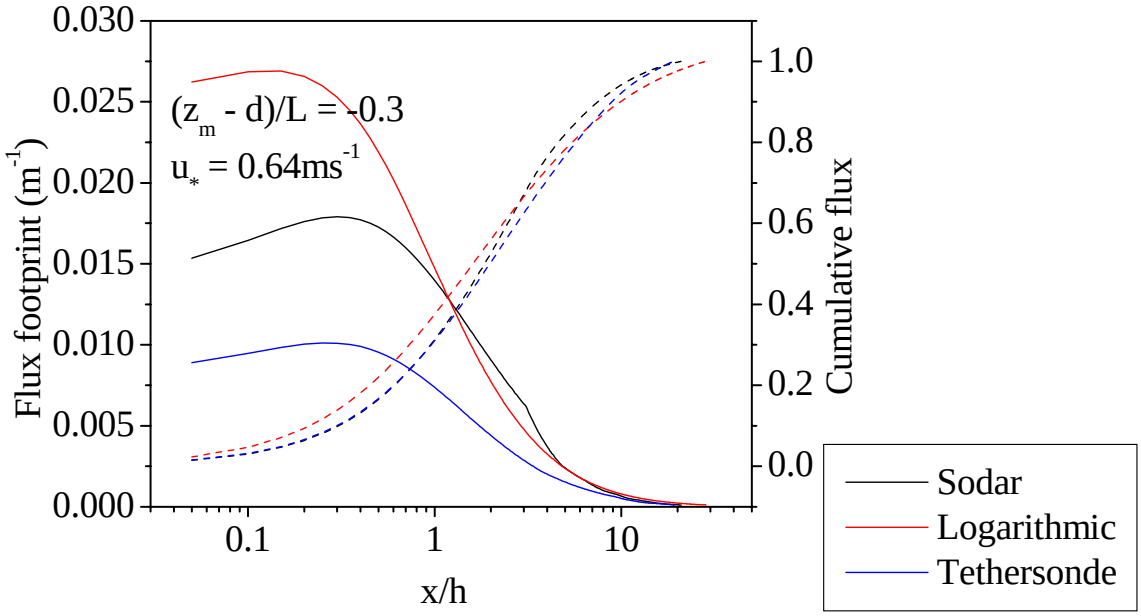

Figure 3.14. Comparison between the predicted footprints using wind profiles from the SODAR, tethersonde and logarithmic profile. The dashed lines represent cumulative footprints and the solid lines are the flux footprints.

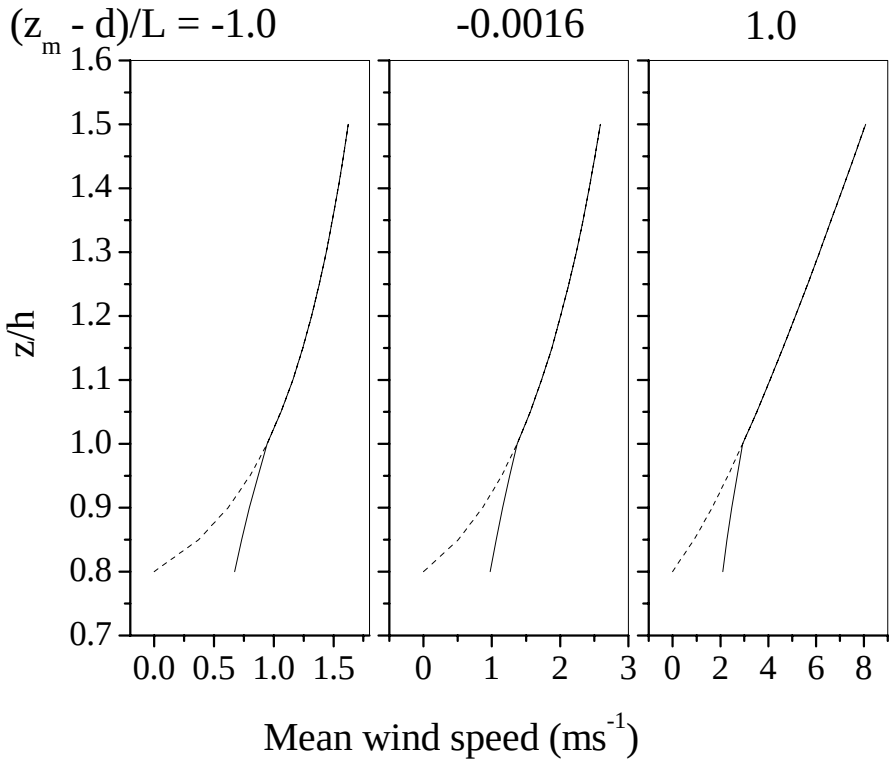

Figure 3.15. Vertical profiles of mean horizontal wind speed for different stability cases with logarithmic (dotted lines) and exponential relations (solid lines).

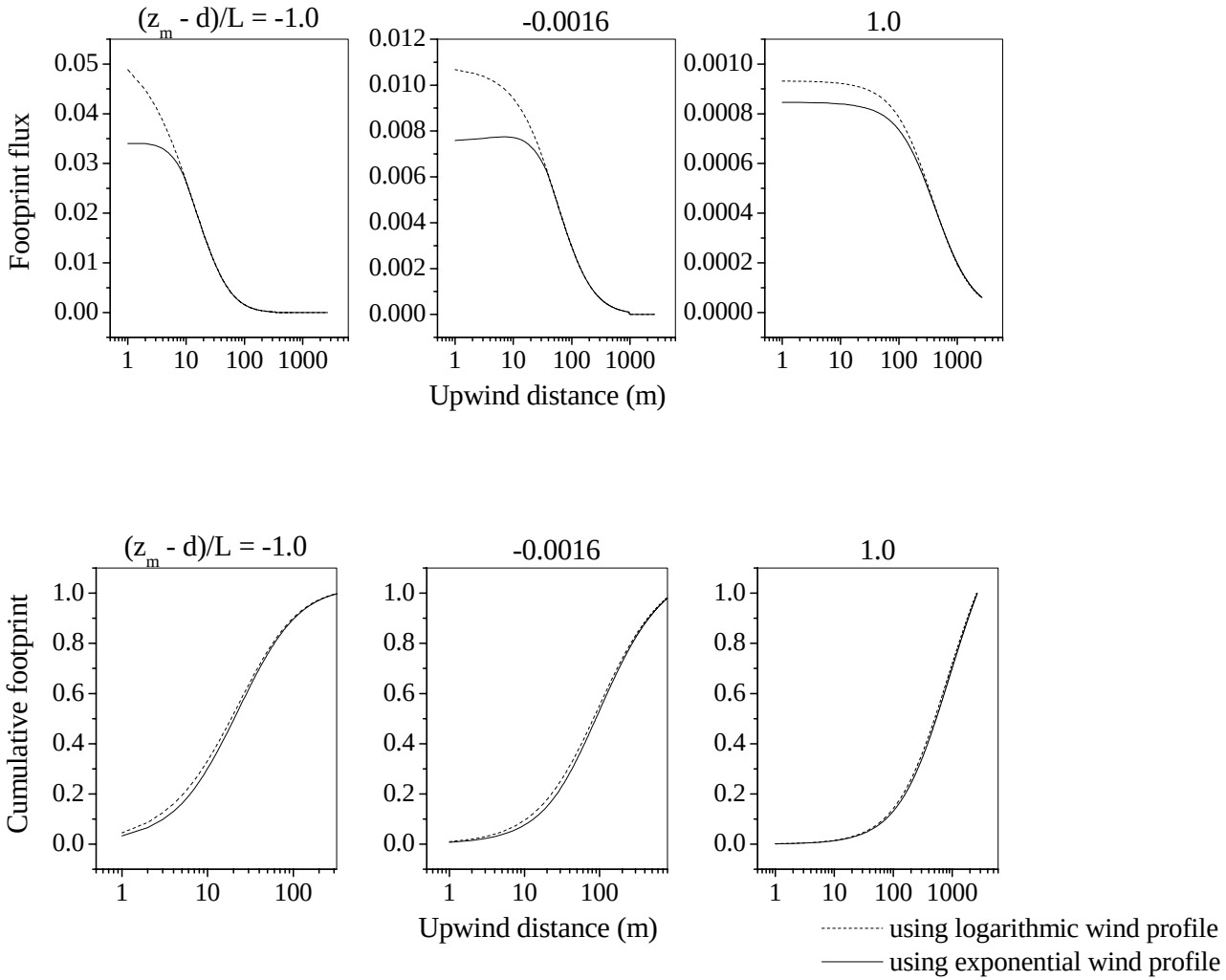

Figure 3.16. Comparison of flux footprint and cumulative flux with respect to upwind distance between original Horst and Weil (1994) model and modified analytical solution using an exponential wind profile in the crown space.

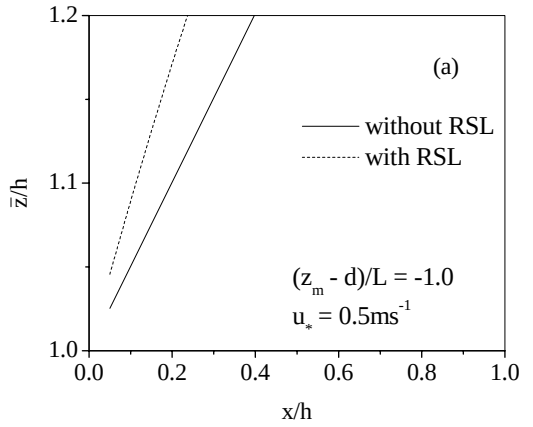

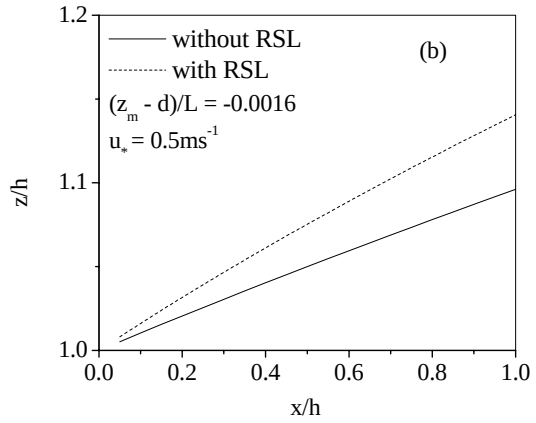

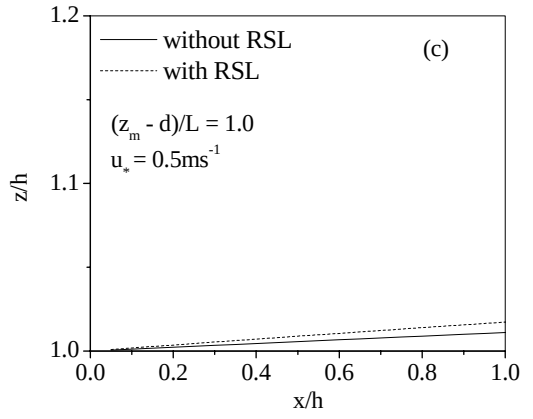

Figures 3.17. Variation of mean plume height with downwind distance for unstable (a), near neutral (b) and stable (c) conditions

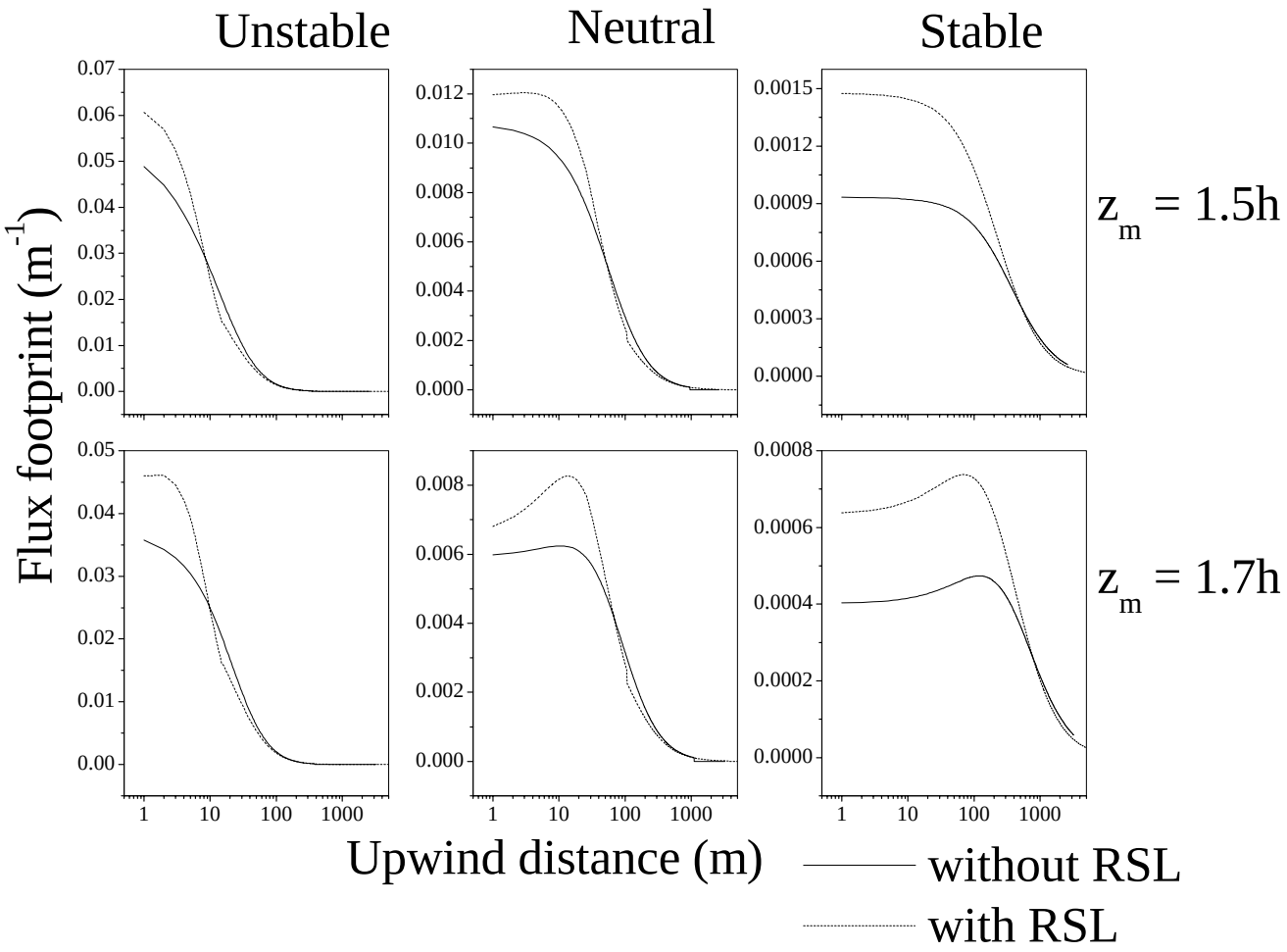

Figure 3.18. Variation of flux footprint with upwind distance with and without RSL parameterizations. u_* is 0.5ms^{-1} and L -30, -10000 and 30m in unstable, neutral and stable cases respectively.

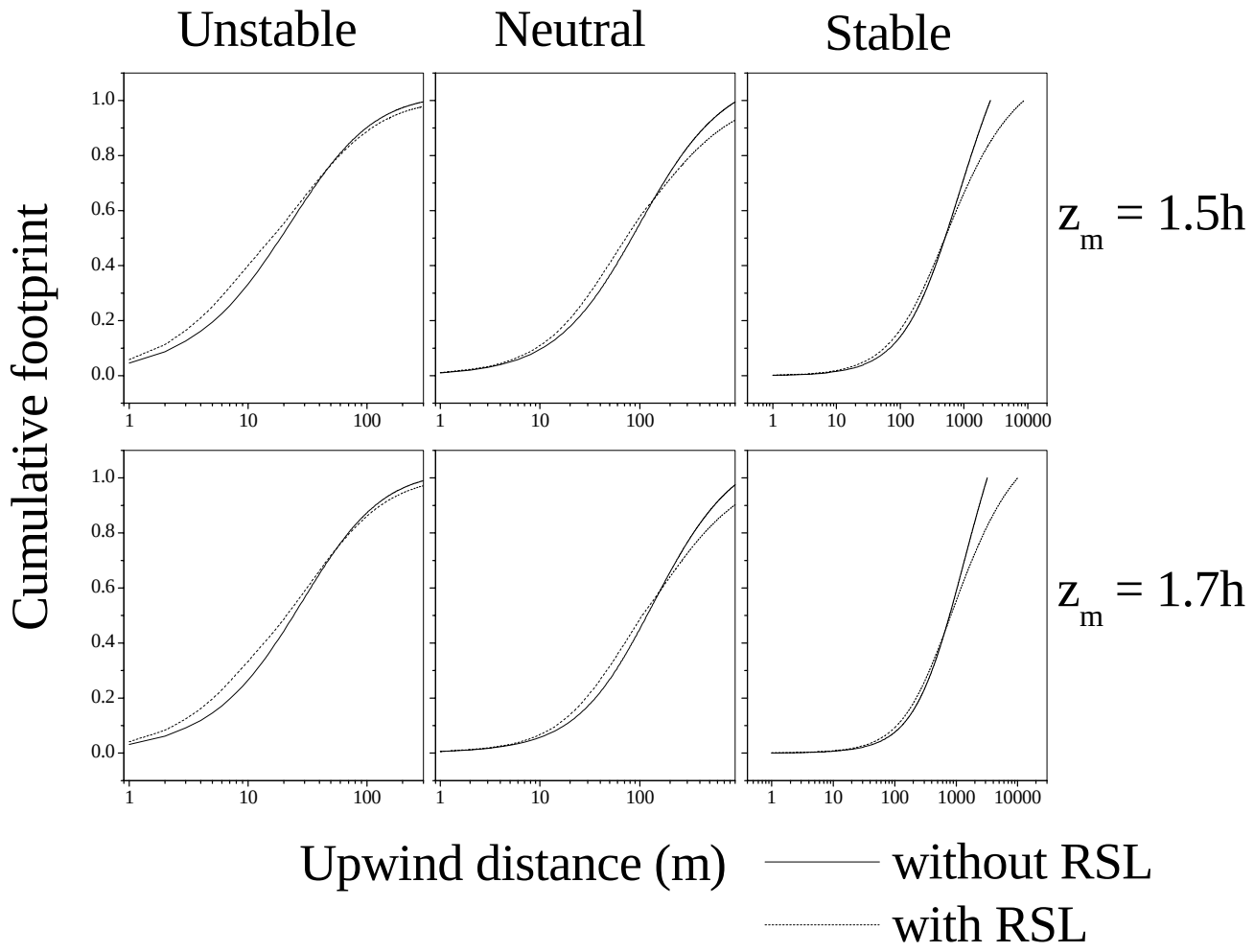

Figure 3.19. Variation of cumulative footprint with upwind distance with and without RSL parameterizations. u_* is 0.5ms^{-1} and L -30, -10000 and 30m in unstable, neutral and stable cases respectively.

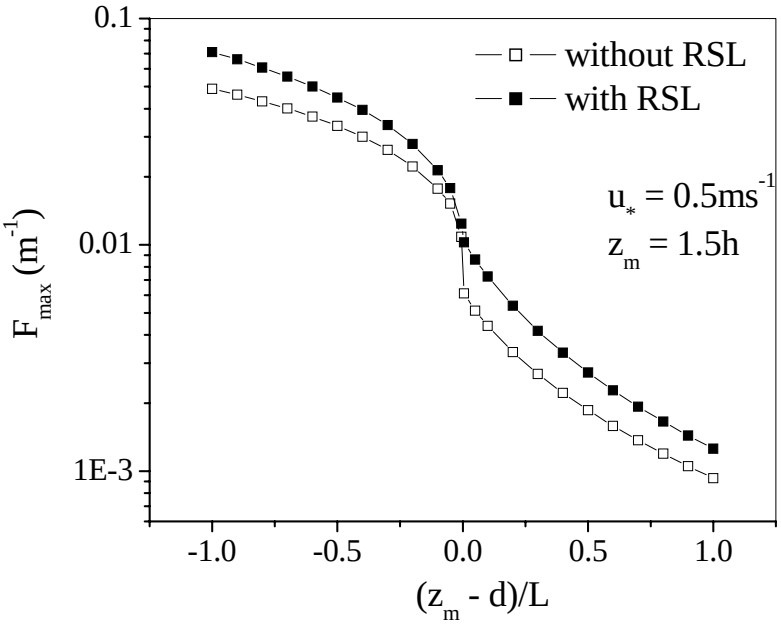

Figure 3.20. Variation of flux maximum with stability with and without RSL parameterization

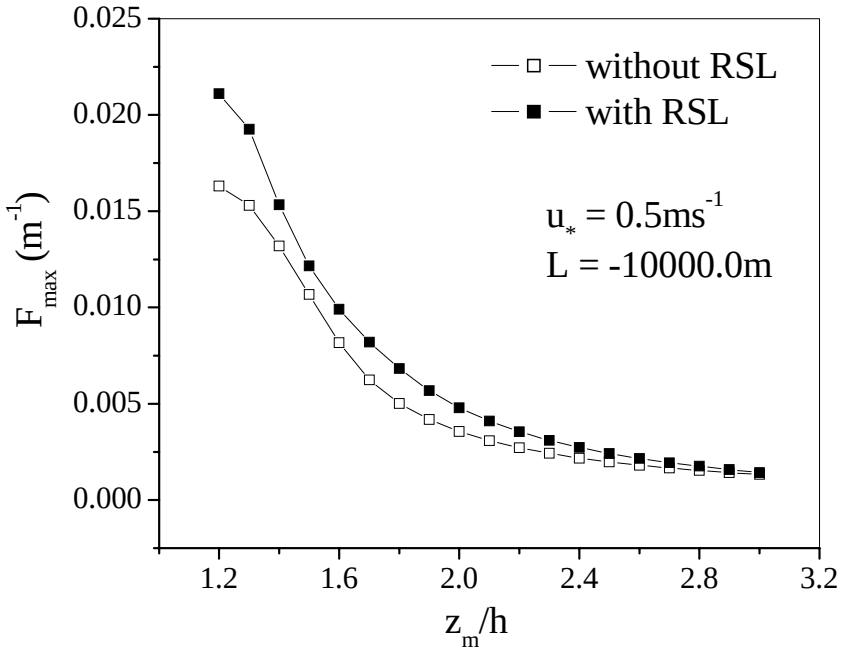

Figure 3.21. Variation of flux maximum with measurement height with and without RSL parameterization

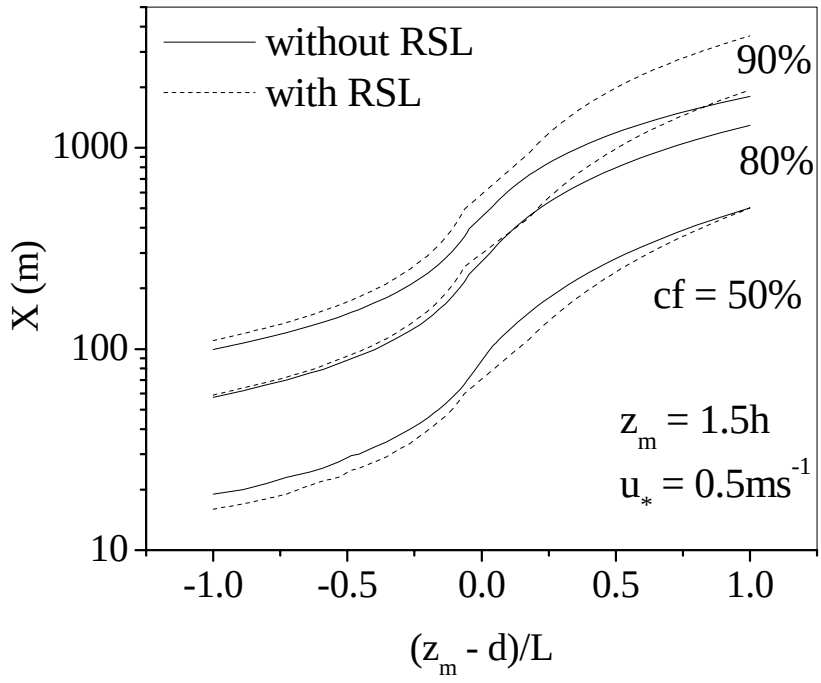

Figure 3.22. Comparison of fetch calculated with and without RSL parameterizations. cf represents cumulative footprint.

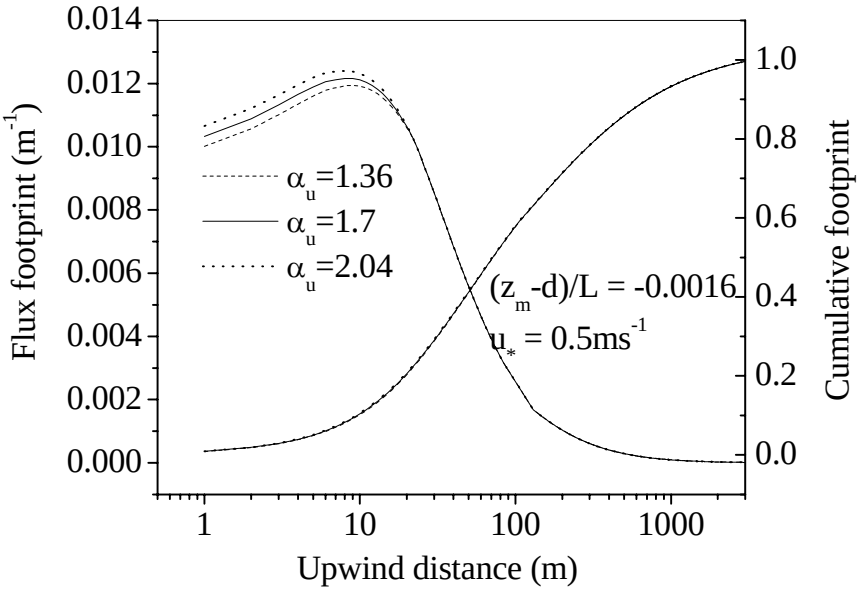

Figure 3.23. Sensitivity of the modified analytical model for the exponential wind coefficient

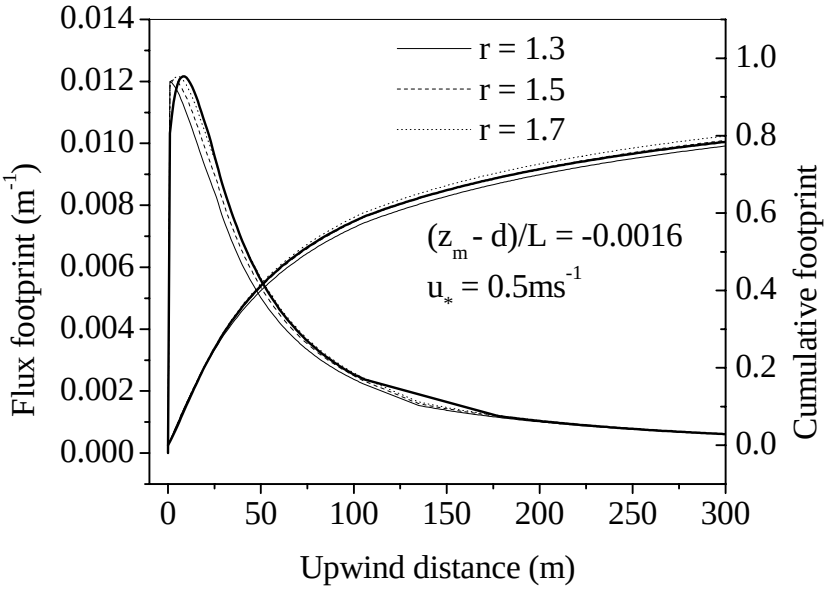

Figure 3.24. Sensitivity of the original analytical solution for the shape factor in near neutral stability. The bold lines represent the flux footprint and cumulative footprint using the analytical formula for the shape factor from Finn et al. (1996).

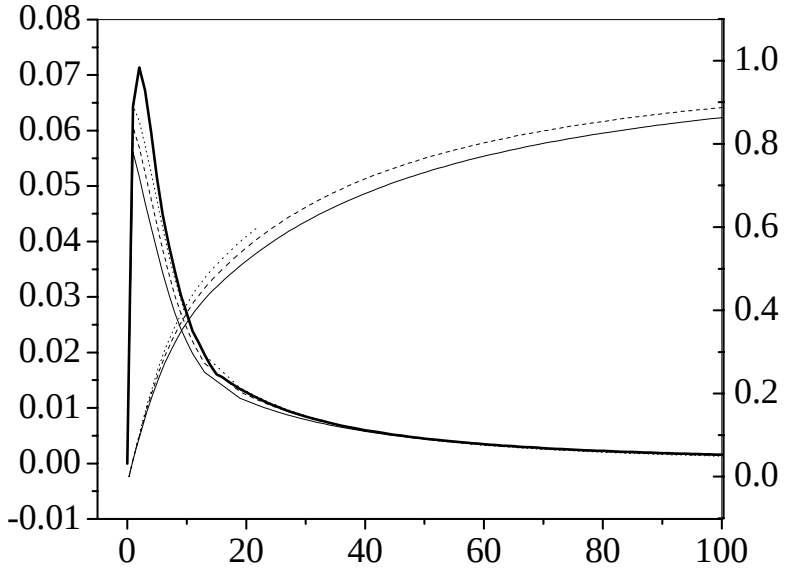

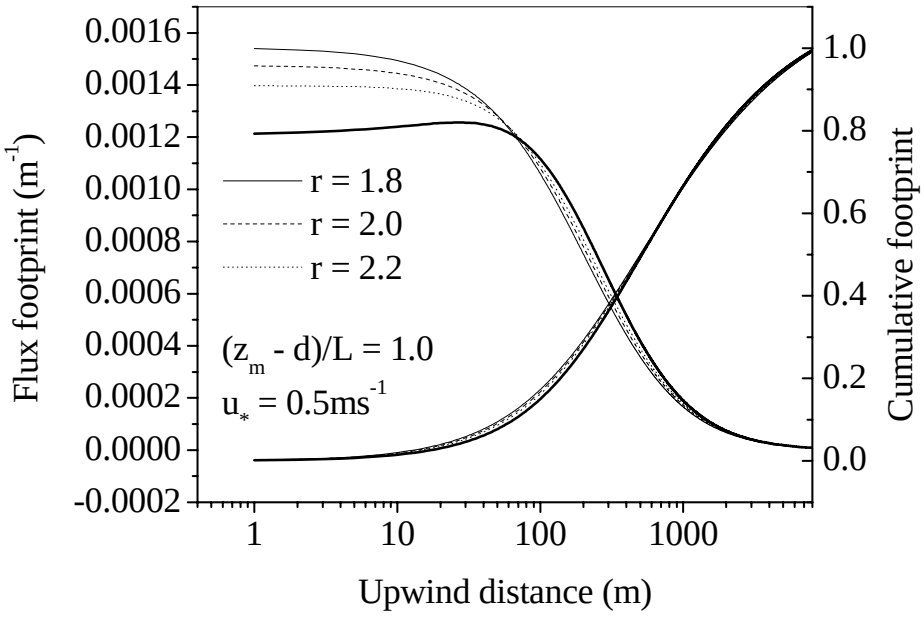

Figure 3.26. Sensitivity of the original analytical solution for the shape factor in stable case. The bold lines represent the flux footprint and cumulative footprint using the analytical formula for the shape factor from Finn et al. (1996).

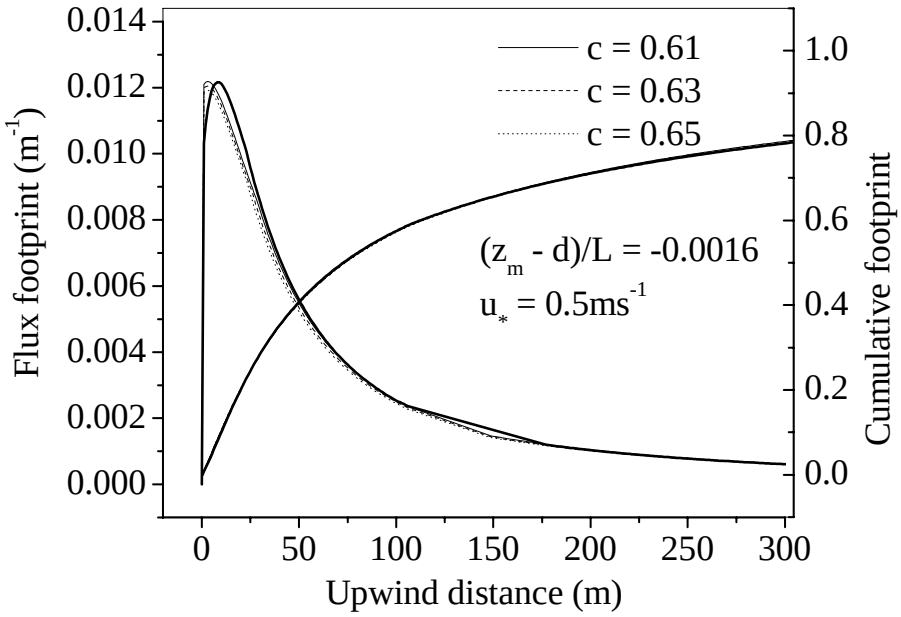

Figure 3.27. Sensitivity of the original analytical solution for the empirical constant c in near neutral condition. The bold lines represent the flux footprint and cumulative footprint using experimental values of c from Finn et al. (1996).

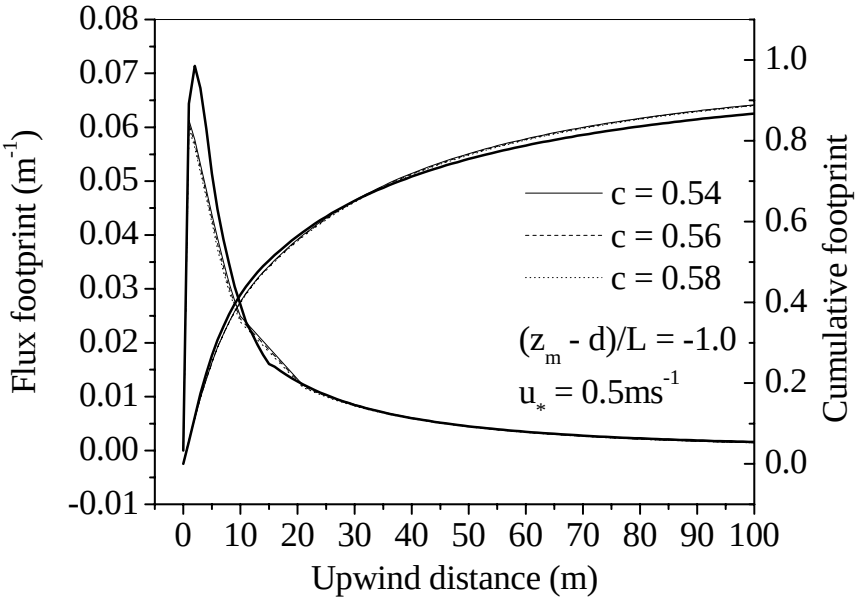

Figure 3.28. Sensitivity of the original analytical solution for the empirical constant c in unstable condition. The bold lines represent the flux footprint and cumulative footprint using experimental values of c from Finn et al. (1996).

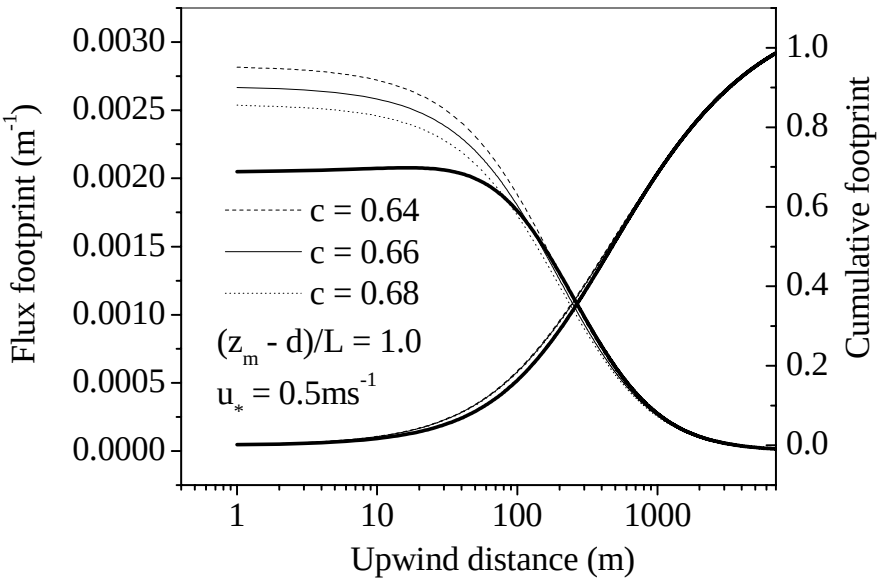

Figure 3.29. Sensitivity of the original analytical solution for the empirical constant c in stable condition. The bold lines represent the flux footprint and cumulative footprint using experimental values of c from Finn et al. (1996).

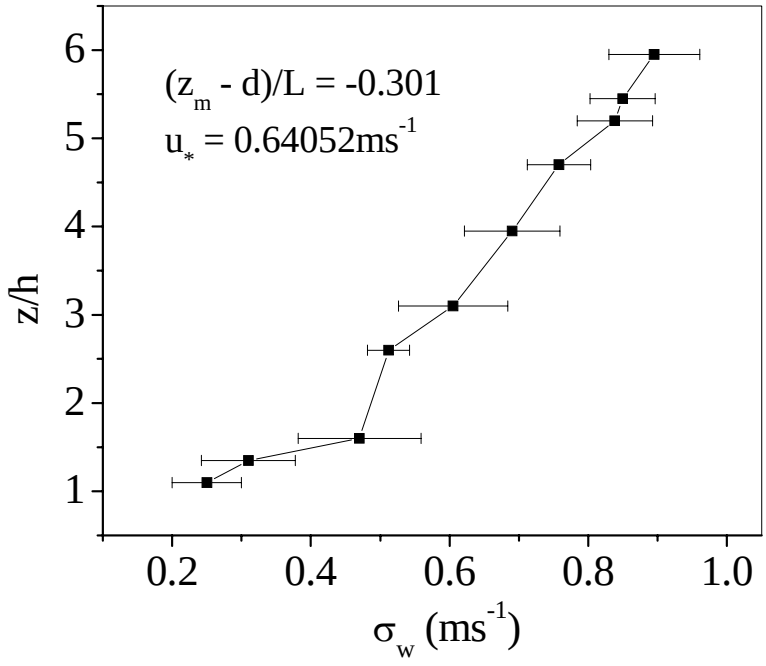

Figure 3.30. Vertical profile of σ_w at the Howland forest from the mini-SODAR in slightly unstable condition. The Obukhov length and friction velocity are obtained from the Sonic anemometer.

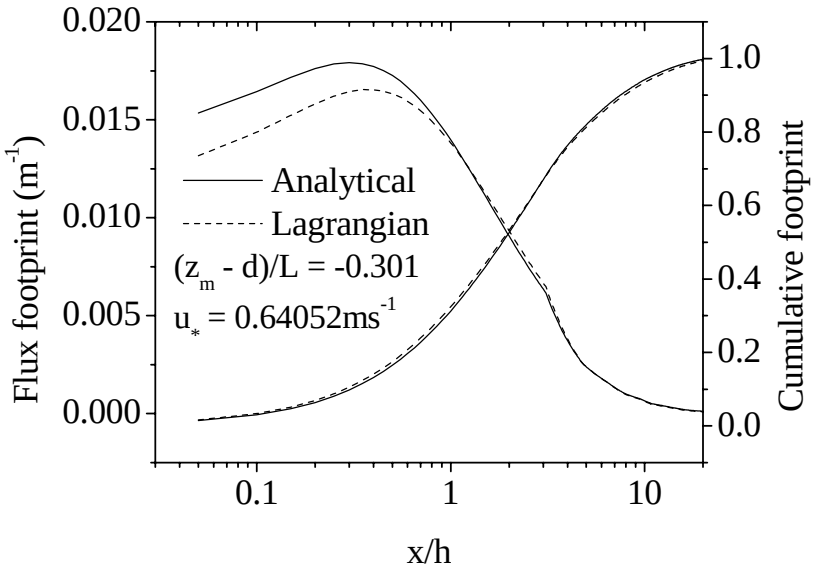

Figure 3.31. Comparison of footprint predictions from the modified analytical solution and a Lagrangian formulation using a realistic σ_w profile.

CHAPTER 4

FOOTPRINT CLIMATOLOGY FOR CO_2 FLUXES OVER HOWLAND AMERIFLUX SITE [1]

[1]Achuthavarier, D. and M.Y. Leclerc. To be submitted to *Agricultural and Forest Meteorology*

4.1. Introduction

In order to understand the exchange mechanisms between the Earth's surface and atmosphere we mainly rely on tower-based point measurements of fluxes of energy and mass. The main exception to this is aircraft based flux-measuring systems (Schuepp et al., 1987; Oechel et al., 1998), which are limited to short-term measurement campaigns and not suitable for long-term observations. Flux sensors monitor the uptake and release of CO_2 from and to the air above vast forest areas (Baldocchi et. al., 1988, 1996, 2000; Hollinger et al., 1994; Denning et al., 1996; Aubinet, 2000; Falge et al., 2002). These observations provide information on the ability of green plants to act as sinks for atmospheric carbon and thus in global warming studies (Chen et al., 2000; Griffis et al., 2003). The tower-based flux measurements, commonly referred to as eddy-covariance systems, consist of sonic anemometers which measure eddy velocities and co-located sensors to sample the concentration of the property of interest say CO_2, water vapor etc. The interpretation of data from the eddy-covariance systems pose a difficulty in most cases particularly when set up over inhomogeneous surfaces such as natural forests. The spatial context of the measurement is not provided by the sensors and to compound the problem, the dimensions of the sensing area varies with measurement height, atmospheric stability and surface roughness. The area or the distance (in one dimensional case) that covers all the contributory sources at the surface to the measured flux at a height is referred as effective fetch (Pasquill, 1972) or footprint (Schuepp et al., 1990; Leclerc and Thurtell, 1990) or source area (Schmid and Oke, 1990). The flux footprint can be defined as the contribution per unit emission from each element at the surface of the upwind source area to the vertical flux measured at a point above the surface (Horst and Weil, 1992). Since Pasquill's original work on effective fetch, several models are proposed to estimate the footprint based on analytical (Gash, 1986; Schmid and Oke, 1990;

Schuepp et al, 1990; Horst and Weil, 1992, 1994) as well as stochastic solutions (Leclerc and Thurtell, 1990; Flesch and Wilson, 1992; Flesch, 1996; Baldocchi, 1997; Rannik et al., 2000; 2003; Kljun et al., 2001). Recently large-eddy simulations (LES) are also used in footprint models (Leclerc et al., 1997).

Despite the availability of simple footprint models, traditional height to fetch ratios are often used in the placement of measurement towers. These ratios are based on the internal boundary layer growth and are proved to be inadequate for accurate upwind fetch estimations (Leclerc and Thurtell, 1990). Application of the footprint models to actual field measurements is generally limited to individual cases of half hourly averaged data mainly focusing on its dependency on stability, friction velocity and surface roughness. In order to use as an operational tool during and following actual field measurements, footprint models need to be modified to accommodate the large volume of observations. As the orientation of the footprint envelope depends on wind direction, it is important to study wind direction patterns observed at the site, which can be considered typical for a period of time such as a month or a season. Only a few attempts are reported in the literature where the footprint analysis is used for long-term field measurements (Amiro, 1998; Stoughton et al., 2000; Soegaard et al., 2003). Amiro (1998) was the first to apply the footprint model to field measurements over a climatological time scale. He introduced the footprint climatology, to map out the source area around the flux tower where potential sources/sinks are situated. He used the analytical solution proposed by Horst and Weil (1992) for the footprint climatology for evapotranspiration measurements in a boreal forest catchment. Following Amiro (1998), this study aims to estimate the footprint climatology for CO_2 flux measurements over a tall forest canopy.

4.2. Theory

The analytical footprint model suggested by Horst and Weil (1994) is used in the present footprint climatology analysis. This analytical solution is simple and easy to use with minimum input requirements. It uses height-dependent wind and eddy diffusivity profiles whereas the earlier model by Horst and Weil (1992) uses a uniform wind field. The analytical model by Horst and Weil (1994) has also been evaluated against tracer flux measurements over a short canopy (Finn et al., 1996) and outside the roughness sub layer of a canopy of intermediate roughness (Leclerc et al., 2003b) and over a tall forest canopy (Leclerc et al., 2003a) within the roughness sub layer.

In the present study, the basic footprint model for flux estimations over smooth terrain is modified to take into account roughness sub layer (RSL) effects as discussed in the previous chapter. In this section, we review the original analytical footprint solution by Horst and Weil (1994). The modifications employed for the RSL turbulent effects are briefly mentioned. The flux footprint is the contribution per unit emission from each element of a surface area source to the vertical scalar flux measured at a certain height above the surface. Horst and Weil (1992) showed the dependence of the flux footprint on crosswind location to be identical to the crosswind concentration distribution for a unit surface point source. The measured flux at a point (x, y, z_m) is an integral of the contributions from all upwind sources.

$$F(x, y, z_m) = \int_{-\infty}^{\infty} \int_{-\infty}^{x} F(x', y', 0)\, f(x - x', y - y', z_m)\, dx'\, dy' \qquad (4.1)$$

$F(x', y'0)$ is the source located at $(x', y', 0)$ and f is the footprint or the relative weight given to each source. Horst and Weil (1994) proposed a stability dependent universal footprint function (Φ) using the logarithmic wind profile

$$\Phi = \frac{z_m \overline{f}^{y}(x, z_m)}{d\bar{z}/dx} \approx (\frac{z_m}{\bar{z}})^2 \frac{\bar{u}(z_m)}{U(\bar{z})} A e^{-(z_m/b\bar{z})^r} \quad (4.2)$$

Here $\bar{z}$ is the mean plume height, $\bar{u}$ is the mean wind speed, $U(\bar{z})$ is the mean particle velocity at height $\bar{z}$ and r is the shape factor. A and b are functions of r and are given by $A = r\Gamma(2/r)/\Gamma^2(1/r)$ and $b = \Gamma(1/r)/\Gamma(2/r)$ where Γ is the gamma function. The horizontal gradient of the mean plume height is a function of scalar eddy diffusivity and mean wind speed. The mean plume speed is the mean wind speed at a fraction of height (c) and is given by

$$U(\bar{z}) = \bar{u}(c\bar{z}) \quad (4.3)$$

For $z > h$ the logarithmic profile is used (eqn. 4.4) and for $d \geq z \leq h$ the exponential profile proposed by Cionco, 1965 is used (4.5).

$$\bar{u}(z) = \frac{u_*}{k}\left[\ln(z/z_0) - \psi(z/L) + \psi(z_0/L)\right] \quad (4.4)$$

$$\bar{u}(z) = \bar{u}(h)\exp\left(-\alpha_u\left(1 - z/h\right)\right) \quad (4.5)$$

Here h is the height of the canopy and α_u is the exponential wind coefficient taken as 1.7 from Denmead and Bradley (1987), u_* is the friction velocity and k is the von Karman's constant. In order to take in to account the impact of RSL we used eddy diffusivity as,

$$K = \frac{u_* k z}{\phi^*(z/L)} \quad (4.6)$$

where $\phi^*(z/L)$ is the modified stability function adopted from Simpson et al., (1998). Details of this analysis are given in Chapter 3. The shape factor r is taken as constant and is equal to 1.0 for unstable, 1.5 for neutral and 2.0 for stable conditions. The corresponding c values are 0.56 for unstable, 0.63 for neutral and 0.66 for stable conditions (Horst and Weil 1992). The roughness length (z_0) is taken as 0.1h and the displacement height (d) as 0.7h.

4.3. Site and measurements

The footprint model is used to analyze the data obtained from the measurements over a forest canopy situated in northern Maine, USA. The site is one of the *Ameriflux* research locations where continuous monitoring of wind speed and fluxes of CO_2, heat, momentum and water vapor are performed by eddy-covariance method. The site is located at the Howland forest at latitude of 45.2° N and longitude of 68.7° W. The terrain varies from flat to gently rolling and the elevation of the site is approximately 60 m. The vegetation is of mixed type consisting of deciduous evergreen needle forest, boreal/northern hardwood ecoton, old coniferous, hemlock, douglas fir and evergreen coniferous with dominant species such as red spruce, eastern hemlock, balsam fir, white pine, northern white cedar, and hardwoods. The canopy is relatively dense with a leaf area index (LAI) of approximately 5.3 m^2m^{-2}.

The mean height of the canopy is 20 m.The flux sensors are placed at a height of 1.5 times the height of the canopy, hereafter referred as h. Figure 4.1 is a satellite (Ikonos) image of the location where the yellow circles show the three flux towers. On the picture, the bright red areas are mostly hardwoods and the darker green areas are softwoods. The bare ground is seen in light green color. The long strips visible to the NW of Tower1 represent strip-cutting areas. All analyses done in this study relate to the data obtained from Tower 1. Apart from the empirical constants (r, c and α_u, values of which are given in section 4.2), the inputs for the model are wind direction ($\bar{\theta}$), friction velocity (u_*) and Obukhov length (L). The friction velocity is obtained from sonic anemometer. The Obukhov length (L) is calculated according to Panofsky and Dutton (1984).

$$L = \frac{-\left(u_*^{\,3}\rho c_p T\right)}{kgH\left(1+0.07/B\right)} \tag{4.7}$$

Here ρ is the density of air, T air temperature in Kelvin, g acceleration due to gravity, H sensible heat flux, k is von Karman constant and B is the Bowen ratio defined as the ratio between the sensible and latent heat fluxes. Half-hourly averaged data obtained for 6 years (1996 to 2001) is utilized for the present study.

It is known that Monin-Obukhov similarity theory is not valid in very unstable or very stable conditions. The empirical stability functions (Dyer and Hicks, 1970; Dyer, 1974) are often found to be inaccurate to use under these limiting conditions (Thom et al., 1975; Garratt, 1978; Raupach, 1979; Denmead and Bradley, 1985; Cellier and Brunet, 1992; Simpson et al., 1998). Researchers often use local similarity and free convective similarity for very stable and unstable cases respectively (Stull, 1997). Again most of these formulations are developed for homogeneous terrain and studies are yet to suggest on alternatives when similarity theory becomes invalid over forest canopies. Recently, Nakamura and Mahrt (2001) found the empirical equations for the integrated stability function (ψ) (Paulson, 1970; Dyer, 1974) to be invalid for cases $z/L > 0.5$ and $z/L < -1.0$. The available data at the Howland site shows on average 4% of the observations in any year constitutes very unstable cases and 15% very stable cases. Table 4.1 shows the percentage occurrence of very unstable and very stable cases in the half hourly averaged data obtained at Howland during the period 1996 – 2001. For highly stable ($z/L > 0.5$) and unstable ($z/L < -1.0$) conditions, the analytical footprint solution is not expected to perform well and the present climatology analysis omits such cases.

4.4. Methods

The footprint climatology portion of the analysis is mainly based on Amiro (1998). The original analytical footprint model is modified to take into account the long-term climatology data. The footprint model was run for each half hourly mean of u_*, L and wind direction ($\bar{\theta}$),

calculating flux footprint for each upwind distance at an interval of 1 m up to 500 m. The flux footprint values are normalized by the integrated flux footprint to obtain the fractional contribution from each point upwind of the sensor. The fractional contribution or the cumulative flux footprint is further classified according to wind direction in 2-degree incremental bins and averaged within each bin.

Coordinates for each point are converted from radial to Cartesian system. The study area is divided into10 x 10 m^2 grids and the footprint flux values are averaged within each grid. The averaged value is then assigned to the mid point of the grid. No interpolation method was used either in the plotting or in the gridding process. The model was coded in Fortran-99 and run in Microsoft Developer Studio 97. Contour plots are made with Origin 6.1 by Origin Lab Corporation, MA, USA.

4.5. Data analysis

The orientation of footprint envelope depends on wind direction patterns. Recently, in their tracer flux experiment over a 9.8 m tall slash pine canopy, Leclerc et al. (2003a) reported the presence of non-local circulation and contribution of sources from areas well outside the footprint envelope. Their results show the transport of fluxes from hundreds of meters away from the footprint envelope when the wind flows over large inhomogeneous surfaces. In the light of this knowledge, the present data analysis determines the wind direction patterns over the Howland forest. The satellite image of the Howland site shows the presence of a bare ground area to the east of tower1 and the relative importance of sources located in this area can be investigated with the help of a wind climatology. Figure 4.2 shows the frequency distribution of wind direction and speed for different seasons in the year 2001. The length of each bar represents the percent occurrence of wind in each direction class among the total number of cases in the

season. The length of each small segment comprising of the main segment in a direction represents the percent occurrence of each wind speed class out of the total data in that season. In the case of wind direction, there is a strong bias existing in all four seasons as very few cases are observed from the east and the SE directions. During summer (June-July-August), SW and SSW wind directions are found to be very dominant. The wind is mostly uniform from all directions except from the east during wintertime. Some cases of high wind speed ($6 – 8 ms^{-1}$) are observed from the North, NW and NNE directions during March-April-May and September-October-November. This suggests, in general, that most of the time during the year 2001, the instrument senses the fluxes from the region to its SW and NW. Possibility of flux contributions from the clearcut is ruled out by the relatively less frequent easterly flow.

Figure 4.3 is similar to Figure 4.2 except that the wind speed is replaced by CO_2 concentration. The purpose of this analysis is to inspect any possible directional dependency in CO_2 concentration values. An examination of frequency distribution patterns for CO_2 concentration reveals that the high concentration values are associated with south and SW directions. On the other hand, virtually no high concentration values are seen when the wind blows from the north and NW directions, which is particularly evident during the period of March-April-May. It can be seen that NW and NNW directions are in general associated with low CO_2 concentrations. This shows the possible existence of a CO_2 deficient airflow form the NW and NNW and a CO_2 enriched flow from the SW and SSW. It is known that the measured CO_2 concentration is primarily a function of source/sink distributions around the tower, which in turn depends on species variability and canopy density. Howland forest is a mature coniferous forest, which possesses a high degree of species diversity. In order to further investigate the above mentioned feature a better understanding on the species composition, photosynthetic

activity are required. It is also important to study the terrain characteristics, such as ridges and valleys. However based on the satellite image, no major step changes are observed either in the SW or in the NW within a distance of 1 km and this rules out any possible influence of heterogeneity observed generally in the SW of the tower T1. So it can be concluded that the observed CO2 concentration is dependent on large-scale flow and a detailed analysis of the regional climatology is required.

The presence of a clear wind pattern and the directional dependency of CO_2 concentration data underline the importance of footprint analysis for this site.

4.6. Footprint climatology

Fig.4.4 shows wind roses for one day, one week, one month and one season in the year 2001 without any stability classification. The periods are chosen to be in summer as the CO_2 exchange between the air and the forest is expected to be most dynamic then. Corresponding footprint climatologies are shown on Fig.4.5 on which dark gray represents 50% of the source area, light gray 75% and lighter gray 90%. For a typical summer day the footprint extends to about 100 – 150m in the SW direction. The strong dependence of footprint on wind direction diminishes with averaging time. Isolated spikes to the east and NE are caused by the few number of observations from those wind directions. For summer season (3 months), 90% of the source area extends to about 300m to the west, SW, and south, while to the east it hardly reaches up to 200m. Upon examining Fig. 4.1 we see the main tower (T1) is situated in the middle of continuous softwood forest and does not encounter major step changes in its vicinity except for the small bare land to its right and small patches of hardwood in the North and SE. As the wind blows seldom from the East, the possibility of CO_2-enriched air being transported from the deforested area in the East is not significant. The footprint climatology for summer 2001 shows

the source area extending up to 200- 250 m towards this direction while the clearcut area is situated approximately 600m away from the tower.

To study the effect of stability on footprint distribution, we classified summer 2001 data into stable ($0.05 < z/L < 0.5$), unstable ($-1 < z/L \leq -0.05$) and near-neutral ($-0.05 < z/L \leq 0.05$) classes and plotted the footprint climatology for each class. Fig.4.6 shows the wind direction patterns for three stability classes. It can be seen that during stable cases the wind is frequent from the SW and SSW directions (12–16% of the total cases) while the flow from the east constitutes less than 2% of the total observations. Relatively most of the easterly flow (3-4%) is seen in the unstable class. As expected, the footprint envelope expands in the stable conditions and contracts in the unstable conditions. For instance, during unstable cases the footprint envelope is limited to an area as small as $0.2km^2$ while the total study area is $1km^2$.

To get a general understanding of the footprint envelope at the Howland site, we classified the half hourly mean data available for 1996-2001 into 4 seasons. The wind roses (Figure 4.7) show a similar pattern as in Fig. 4.2. Wind patterns can be considered uniform for Dec-Jan-Feb and Mar-Aprl-May. However, during the wintertime, the CO_2 exchange between the air and the forest will be minimum as the site experiences a snow pack of 2m depth. During summer, we see a strong southerly wind component. Due to the large number of data used in the analysis, the corresponding footprint climatologies do not show a clear difference between the seasons (Figure 4.8). A comparison between summer and winter suggests decrease in footprint extent in the east-west direction by approximately 50m. In general the footprint envelope is less than 400m in any direction at any time with the tower sensing less than 40% of the total $1km^2$ area.

The above analysis for the 6-year period shows the presence of a clear wind bias at the Howland site. Despite its dependence on wind direction, source area distributions shown here do not reflect the observed wind patterns, due to the large volume of data taken for the analysis. For example, the source area for the months Dec-Jan-Feb is nearly a circle around the sensor location. It is important to understand the wind distribution where the frequency of easterly winds is considerably lower. Even though we see a footprint envelope of 300 m toward the east during wintertime the occurrence of such cases is small when compared to the entire season.

4.7. Conclusions

Footprint climatology for the CO_2 flux measurements over the Howland forest site at Maine is developed. The wind direction classification shows a strong southerly component (14-16% of the total observations) during all seasons, while easterly flow is relatively weak constituting less than 4% of the total observations. The frequency distribution analysis of the CO_2 concentration data shows the presence of a CO_2-depleted flow from the NW and a CO_2-enriched air from the SW. This feature should be analyzed further with the help of regional climatology data. The presence of non-uniform wind pattern and wind direction dependent CO_2 concentration values emphasizes the importance of source area estimations at this site. The tower T1 senses about 40% of the total 1 km^2 area during stable conditions but only 20% in unstable conditions. The fetch is always less than 400 m in any direction. This climatology analysis gives guidance on the number of measuring points required for the 1 km^2 forest area. It is evident that the measurements from tower T1 are not representative of the whole study area.

Though the analysis is limited within the assumptions and simplifications of the original analytical footprint solution, improved results are expected by using RSL turbulent parameterizations. No actual source/sink distribution is known or used in this analysis. The

actual source/sink distribution data is important in further analysis and has to be incorporated in the footprint climatology studies.

References

Amiro, B.D., 1998. Footprint climatologies for evapotraspiration in a boreal catchment. Agric. For. Meteorol. 90, 195–201.

Aubinet, M., Grelle, A., Ibrom, A., Rannik, U., Moncrieff, J., Foken, Th., et al., 2000. Estimates of the annual net carbon and water exchanges of European forests: the EUROFLUX methodology. Adv. Ecol. Res. 30, 113–74.

Baldocchi, D.D., Hicks, B.B., Meyers, T.P., 1988. Measuring biosphere-atmosphere exchanges of biologically related gases with micrometeorological methods. Ecology. 69,1331–1340.

Baldocchi, D.D., Valentini, R., Running, S., Oechel, W., and Dahlman, R. 1996. Strategies for measuring and modelling carbon dioxide and water vapor fluxes over terrestrial ecosystems. Global Change Biology. 2,159-168.

Baldocchi, D.D., 1997. Flux footprints within and over forest canopies. Boundary-Layer Meteorol. 85, 273–292.

Baldocchi, D.D., Finnigan, J., Wilson, K., Paw, U.K.T., Falge, E., 2000. On measuring net ecosystem carbon exchange over tall vegetation on complex terrain. Boundary Layer Meteorol. 96, 257–291.

Cellier, P., Brunet, Y., 1992. Flux gradient relationships above tall plant canopies. Agric. For. Meteorol. 58, 93–117.

Chen, J., Chen, W., Liu, J., Cihlar, J., Gray, S., 2000. Annual carbon balance of Canada's forests during 1895–1996. Global Biogeochem. Cycles 14, 839–849

Cionco, R.M., 1965. A mathematical model for air flow in a vegetated canopy. J. Appl. Meteorol. 4, 517

Denmead, O.T., Bradley, E.F., 1985. Flux-gradient relationships in a forest canopy. in: B.A. Hutchison and B.B. Hicks (eds), The forest-atmosphere interaction. Reidel, Dordrecht, pp. 421–442.

Denmead, O.T., Bradley, E.F., 1987. On scalar transport in plant canopies. Irrig. Sci. 8, 131–149.

Denning, A.S., Random, D. A., Collatz, G. J., Sellers, P.J., 1996. Simulations of terrestrial carbon metabolism and atmospheric CO_2 in a general circulation model. Part 2: Simulated CO_2 concentrations. Tellus. 48B, 543–567.

Dyer, A.J., 1974. A review of flux-profile relationships. Boundary-Layer Meteorol. 7, 363–372.

Dyer, A.J., Hicks, B.B., 1970. Flux gradient relationships in the constant flux layer. Quart. J. Roy. Meteorol. Soc. 96, 715–721.

Falge, E., Baldocchi, D., Tenhunen, J., Aubinet, M., Bakwin, P., Berbigier, P., Bernhofer, C., Burba, G., Clement, R., Davis, K.J., Elbers, J.A., Goldstein, A.H., Grelle, A., Granier, A., Guðmundsson, J., Hollinger, D., Kowalski, A.S., Katul, G., Law, B.E., Malhi, Y., Meyers, T., Monson, R.K., Munger, J.W., Oechel, W., Paw U, K.T. Pilegaard, K., Rannik, Ü., Rebmann, C., Suyker, A., Valentini, R., Wilson, K., Wofsy, S., 2002. Seasonality of ecosystem respiration and gross primary production as derived from FLUXNET measurements. Agric. For. Meteorol. 113, 53–74.

Finn, D., Lamb, B., Leclerc, M.Y., Horst, T.W., 1996. Experimental evaluation of analytical and Lagrangian surface-layer flux footprint models. Boundary-Layer Meteorol., 80, 283–308.

Flesch, T., Wilson, J., 1992. A two-dimensional trajectory-Simulation model for non-Gaussian, inhomogeneous turbulence within plant canopies. Boundary-Layer Meteorol. 61, 349–374.

Flesch, T.K., 1996. The footprint for flux measurements, from backward lagrangian stochastic models. Boundary-Layer Meteorol. 78, 399–404.

Garratt, J.R., 1978. Flux profile relations above tall vegetation. Quart. J. Roy. Meteorol. Soc. 104, 199–211.

Gash, J.H.C., 1986. A note on estimating the effect of a limited fetch on micrometeorological evaporation measurements. Boundary-Layer Meteorol. 35, 409–413.

Griffis, T.J., Black, T.A., Morgenstern, K., Barr, A.G., Nesic, Z., Drewitt, G.B., Gaumint-Guay, D., McCaughey, J.H., 2003. Ecophysiological controls on the carbon balance of three southern boreal forests. Agric. For. Meteorol. 117, 53–71.

Hollinger, D.Y., Kelliher, F.M., Byers, J.N., Hunt, J.E., McSeveny, T.M., Weir, P.L., 1994. Carbon dioxide exchange between an undisturbed old-growth temperate forest and the atmosphere. Ecology 75, 134–150

Horst, T.W., Weil, J.C., 1992. Footprint estimation for scalar flux measurements in the atmospheric surface layer. Bounday-Layer Meteorol. 59, 279–296.

Horst, T.W., Weil, J.C., 1994. How far is far enough?: The fetch requirements for micrometeorological measurements of surface fluxes. J. Atmos. Ocean. Tech. 11, 1018–1026.
Horst, T.W., 1999. The footprint estimation of atmosphere-surface exchange fluxes by profile techniques. Boundary-Layer Meteorol. 90, 171–188.

Hsieh, C., Katul, G., Chi, T., 2000. An approximate analytical model for footprint estimation of scalar fluxes in thermally stratified atmospheric flows. Advances in Water Resources. 23, 765–772.

Kljun, N., Rotach, M.W., Schmid, H.P., 2002. A three-dimensional backward Lagrangian footprint model for a wide range of boundary-layer stratifications. Boundary-Layer Meteorol. 103**,** 205–226.

Leclerc, M.Y., Thurtell, G.W., 1990. Footprint prediction of scalar fluxes using a Markovian analysis. Boundary-Layer Meteorol. 52, 247–258.

Leclerc, M.Y., Shen, S., Lamb, B., 1997. Observations and large-eddy simulation modeling of footprints in the lower convective boundary layer. J. Geophys. Res.102, 9323–9334.

Leclerc, M.Y., Karipot, A., Prabha,T., Allwine, G., Lamb, B., Gholz, H.L., 2003a. Impact of non-local advection on flux footprints over a tall forest canopy: a tracer flux experiment. Agric. For. Meteorol. 115, 17–34.

Leclerc, M.Y., Meskhidze, N., Finn, D., 2003b. Comparison between measured tracer fluxes and footprint model predictions over a homogeneous canopy of intermediate roughness. Agric. For. Meteorol. 117, 145–158.

Nakamura, R., Mahrt, L., 2001. Similarity theory for local and spatially averaged momentum fluxes. Agric. For. Meteorol. 108, 265–279.

Oechel W.C., Vourlitis G.L., Brooks S., Crawford T.L., Dumas E., 1998. Inter-comparison among chamber, tower and aircraft net CO_2 and energy fluxes measured during the Artic System Science Land-Atmosphere-Ice Interactions (ARCSS_LAII) flux study. J. Geophy. Res. 103, 28,993–29,003.

Panofsky, H. A., Dutton, J. A., 1984. Atmospheric turbulence. John Wiley and Sons, USA, 397 pp.

Pasquill, F., 1972. Some aspects of boundary layer description. Quart. J. Roy. Meterol. Soc. 98, 469–494.

Paulson, C.A., 1970. The mathematical representation of wind speed and temperature profiles in the unstable atmospheric surface layer. J. Appl. Meteorol. 9, 857–861.

Rannik, U., Aubinet, M., Kurbanmuradov, O., Sabelfeld, K.K., Markkanen, T., Velsa, T., 2000. Footprint analysis for measurements over a heterogeneous forest. Boundary-Layer Meteorol. 97, 137–166.

Rannik, U., Markkanen, T., Raittila, J., Hari, P., Vesala, T., 2003. Turbulence statistics inside and over forest: Influence on footprint prediction. Boundary-Layer Meteorol. 109, 163–189.

Raupach, M.R., 1979. Anomalies in flux-gradient relationships over forest. Boundary-Layer Meteorol. 16, 467–486.

Schmid, H.P., Oke, T.R., 1990. A model to estimate the source area contributing to the turbulent exchange in the surface layer over patchy terrain. Q. J. R. Meteorol. Soc. 116, 965–988.

Schmid, H.P., Lloyd, C.R., 1999. Spatial representativeness and location bias of flux footprints over inhomogeneous areas. Agric. For. Meteorol. 93, 195–209.

Schuepp, P.H., Desjardins, R.L., MacPherson, J.I., Boisvert, J.B., Austin, L.B., 1987. Airborne determination of regional water use efficiency: Present capabilities and initial field tests. Agric. For. Meteorol. 41, 1–9.

Schuepp, P.H., Leclerc, M.Y., Macpherson, J.I., Desjardins, R.L., 1990. Footprint predictions for scalar fluxes from analytical solutions of the diffusion equation. Boundary-Layer Meterol. 50, 355–373.

Simpson, I.J., Thurtell, G.W., Neumann, H.H., Hartog, G.D., Edwards, G.C., 1998. The validity of similarity theory in the roughness sublayer above forests. Boundary-Layer Meteorol. 87, 69–99.

Soegaard, H., Jensen, N.O., Boegh, E., Hasager, C.B., Schelde, K., Thomsen, A., 2003. Carbon dioxide exchange over agricultural landscape using eddy correlation and footprint modeling. Agric. For. Meteorol. 114, 153–173.

Stoughton, T.E., Miller, D.R., Yang, X., Hendrey, G.M., 2000. Footprint climatology estimation of potential control ring contamination in the Duke Forests FACTS-1 experiment site. Agric. For. Meteorol. 100, 73–82.

Stull, R.B., 1997. An introduction to boundary layer meteorology. Kluwer Academic Publishers, Boston, 670 pp.

Thom, A.S., Stewart, J.B., Oliver, H.R., Gash, J.H.C., 1975. Comparison of aerodynamic and ennrgy budget estimates of fluxes over a pine forest. Quart. J. Roy. Meteorol. Soc. 101, 93–105.

Table. 4.1. Percentage occurrence of very unstable and very stable cases in the half hourly mean data observed at Howland forest during the period 1996–2001

Year	Very Unstable (%)	Very Stable (%)
1996	4.46	16.0
1997	4.5	16.5
1998	5.8	12.7
1999	3.9	13.5
2000	4.1	14.4
2001	3.9	15.7

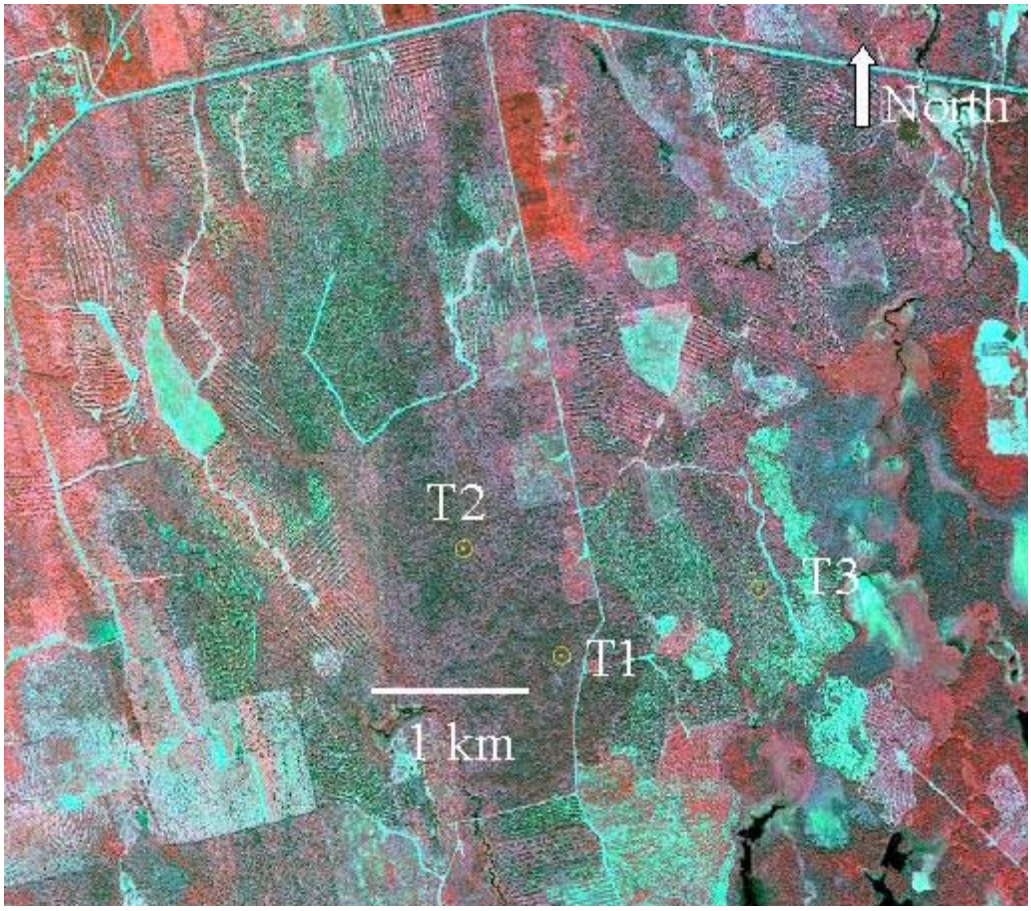

Figure 4.1. Satellite image of the Howland *Ameriflux* site. T1, T2 and T3 are eddy-flux sensor towers. This study uses the data obtained from tower T1. The bright red areas are generally hardwoods and the darker green areas are softwoods. Ground is seen in light green color. The long strips visible to the NW of T1 represent strip-cutting areas.

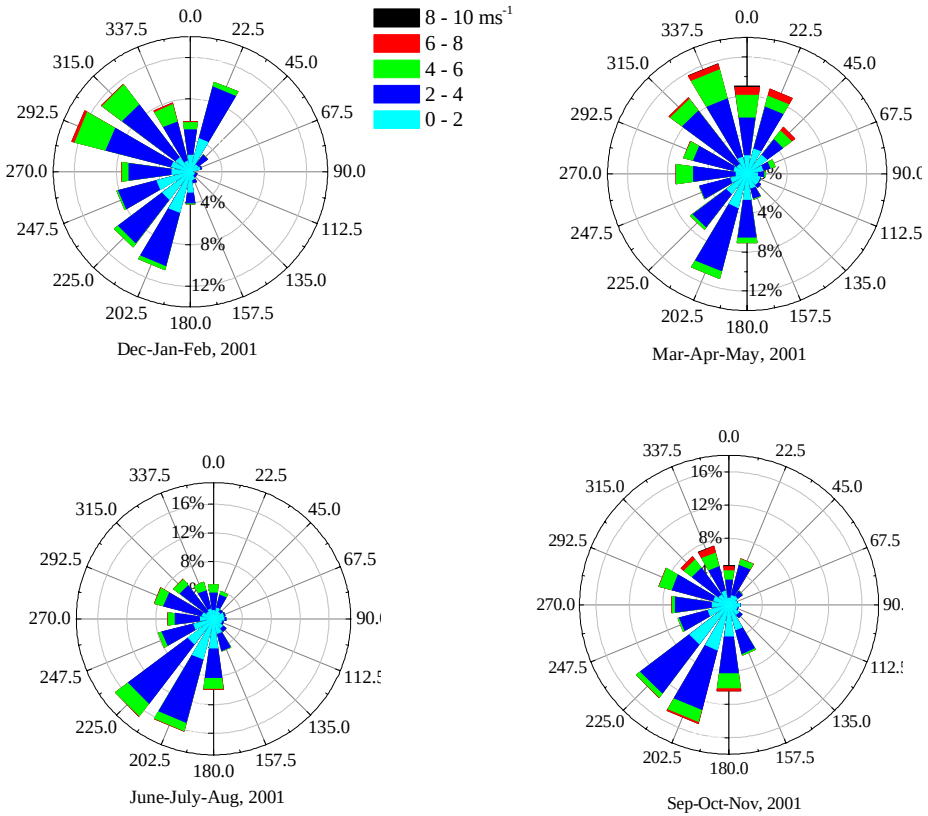

Figure 4.2. Frequency distribution of wind speed and direction at Howland forest in the year 2001.

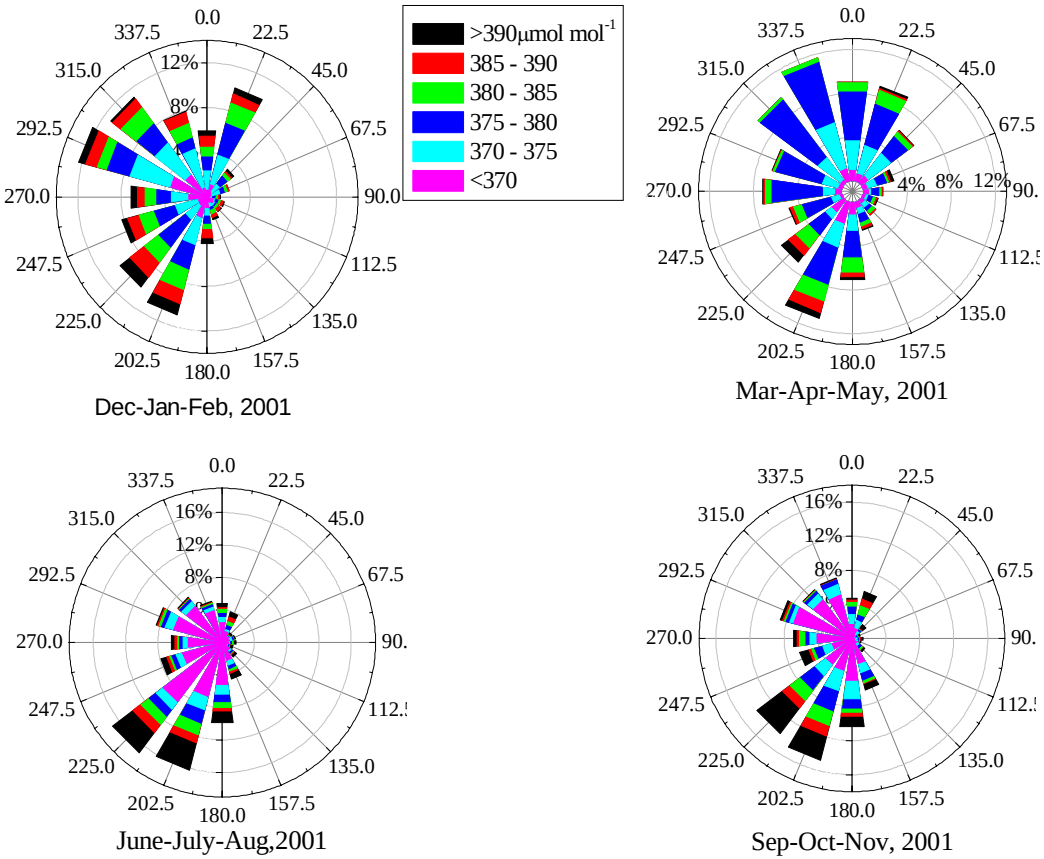

Figure 4.3. Frequency distribution of wind direction and CO_2 concentration at Howland forest in the year 2001.

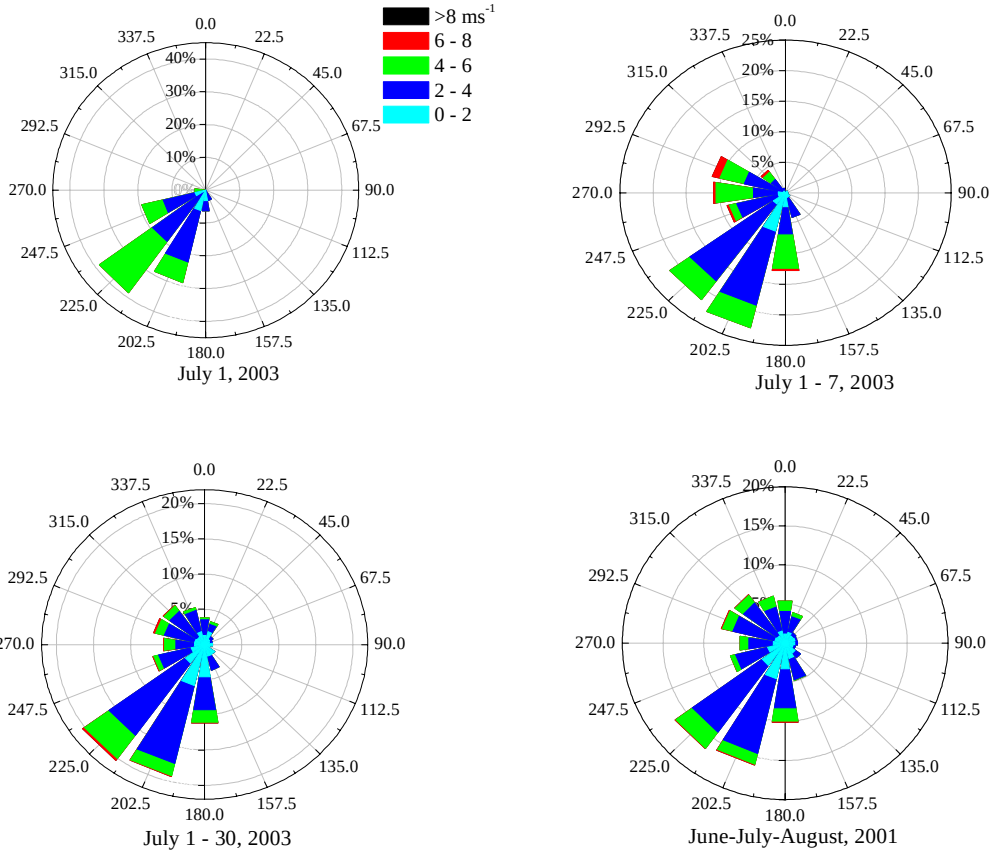

Figure 4.4. Frequency distribution of wind speed and direction at Howland forest for one day, one week, one month and one season in the year 2001.

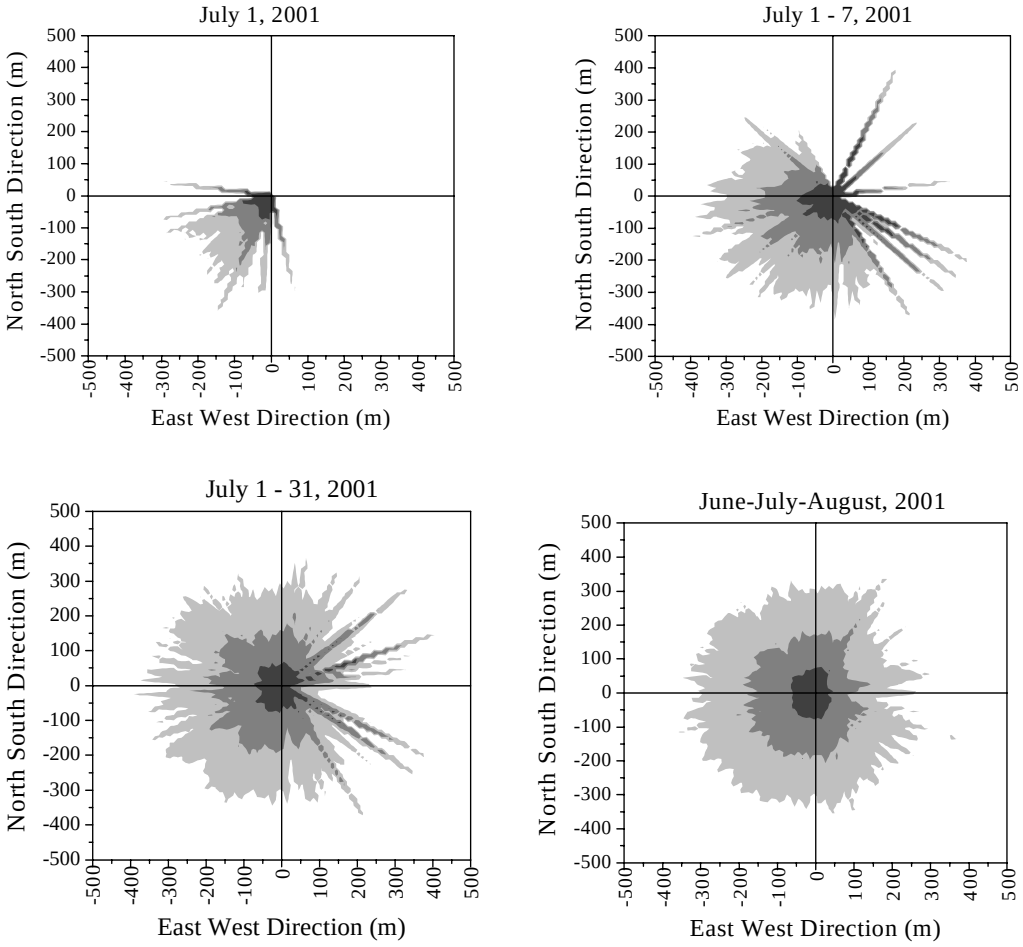

Figure 4.5. Footprint climatology at Howland forest for one day, one week, one month and one season in the year 2001.

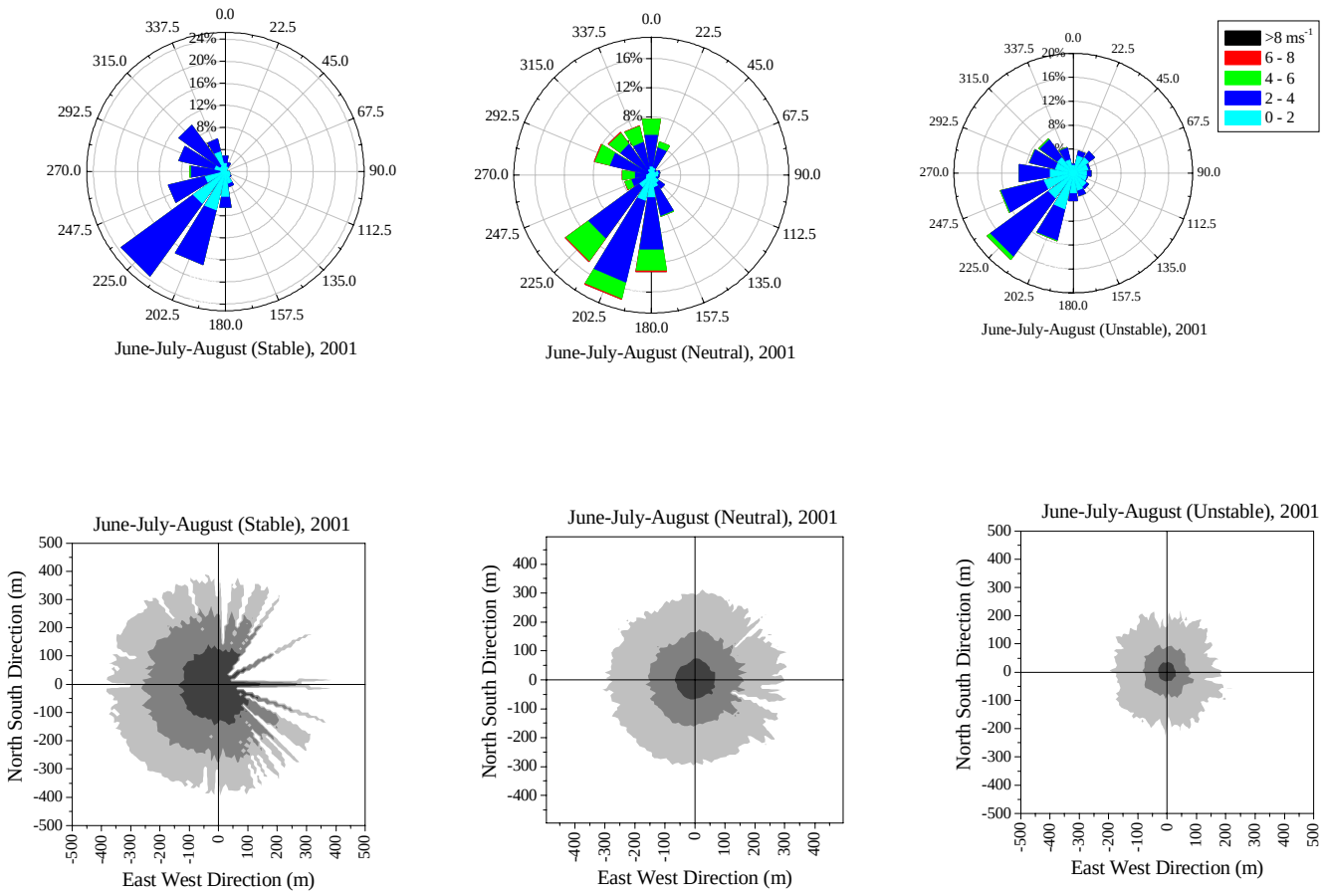

Figure 4.6. Frequency distribution of wind speed and direction at Howland forest for stable, neutral and unstable conditions (above) and corresponding footprint climatology distributions (below).

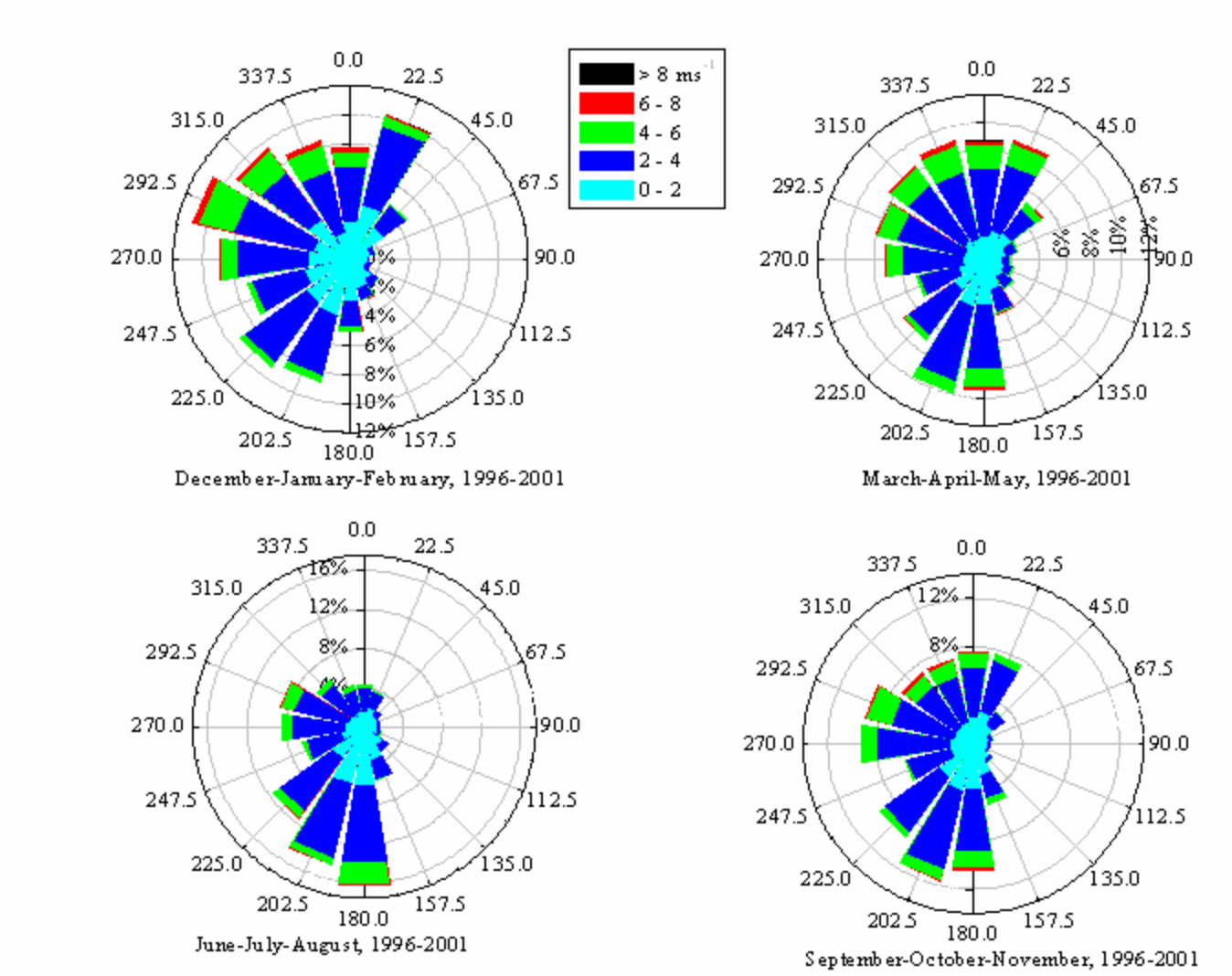

Figure 4.7. Frequency distribution of wind speed and direction at Howland forest for the period 1996–2001.

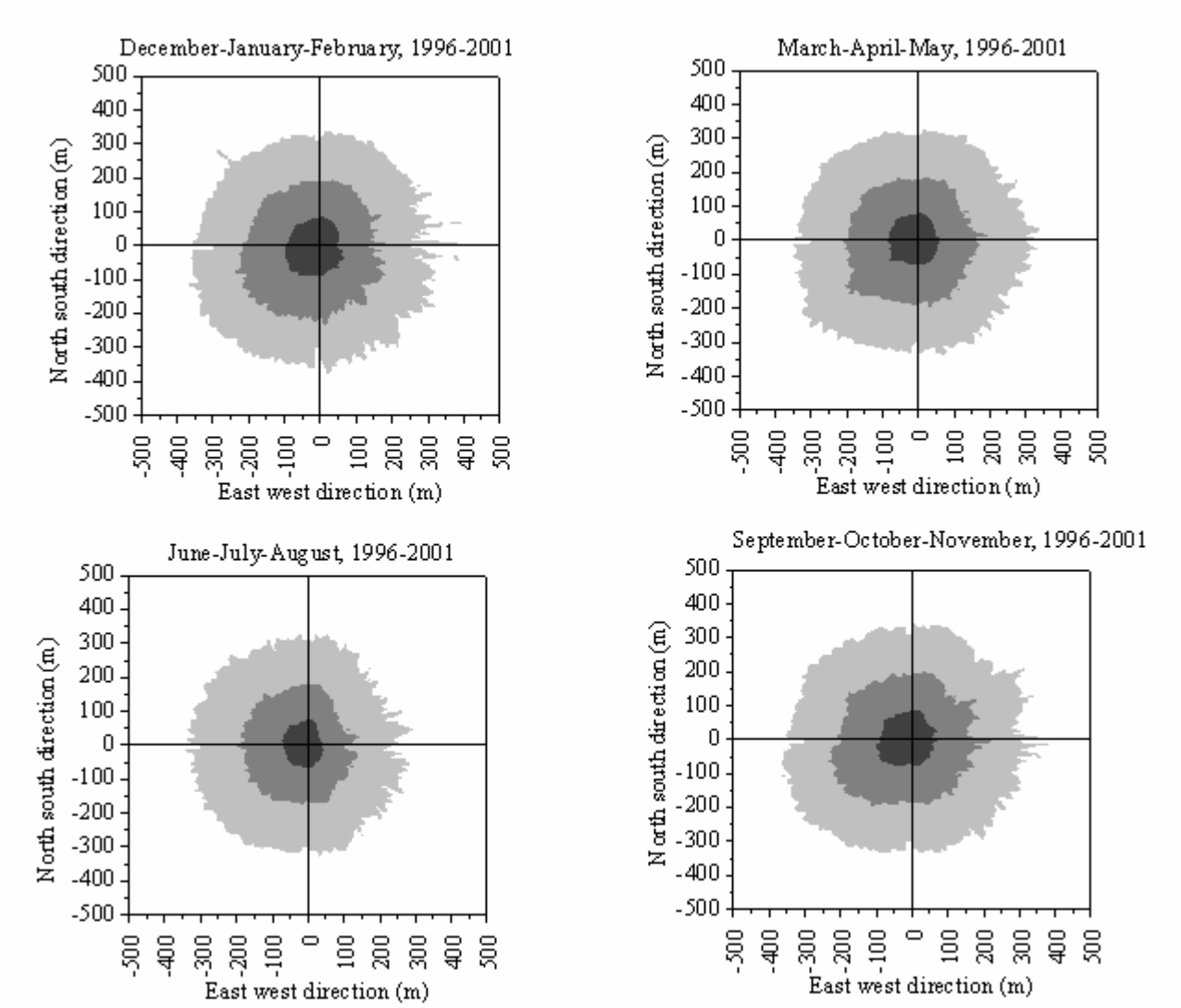

Figure 4.8. Footprint climatology at the Howland forest for the period 1996–2001.

CHAPTER 5

CONCLUSION

Continuous measurements of atmospheric constituents over the last 50 years show rising levels of greenhouse gases particularly CO_2. Rising level of atmospheric carbon can cause changes on the global environment such as increased global temperature, sea level rise and perturbations in precipitation and soil moisture patterns. This knowledge instigated a large number of studies on global carbon budget and carbon assimilation capacity of forest areas. The exchange of CO_2 between the vegetation and the air above is measured in terms of flux by using eddy-covariance systems. The eddy-covariance system measures the flux at a given point above the vegetation canopy. In order to understand the spatial context of the measurement, the surface area or the upwind fetch that contributes to the point measurement should be known. This area (or distance, in one dimensional case) that is representative of a point flux measurement is known as flux footprint. The concept of footprint thus enhances the accuracy of the point flux measurements.

Simple footprint models are based on analytical diffusion equations that are originally developed for turbulence over smooth surfaces. In this study, we modified a widely used analytical footprint solution for enhanced turbulence observed in the roughness sub layer (RSL) over forest canopies. The modified model uses a more realistic exponential wind profile in the crown space of the canopy and enhanced scalar eddy diffusivity. The flux footprint maximum decreases by using an increased wind speed from the exponential profile. However due to the enhanced eddy diffusivities the flux maximum increases and effect of wind speed is not observed

in the new model. Future work in this subject should address the use of two dimensional footprint models considering the spatial variability of sources/sinks over natural forest canopies. The parameterization of RSL turbulence requires accurate flux measurements over a wide range of canopies.

The modified analytical model is used for footprint climatology study for CO_2 flux measurements at Howland *Ameriflux* site. The frequency distribution analysis of the wind direction and CO_2 concentration data shows the presence of a CO_2-depleted flow from the NW and a CO_2-enriched air from the SW. Homogeneous softwood stretch extending up to more than 1km to the NW of the eddy-flux tower might act as potential sink for carbon. Patches of bare ground areas present approximately 800m away to the south and SW of the tower could cause CO_2-enriched flow from those directions. The eddy flux system senses about 40% of the total $1km^2$ area during stable conditions but only 20% in unstable conditions. The fetch is always less than 400m in any direction. Further efforts are required to incorporate the actual source/sink distributions in the footprint model.